National Bureau of Standards
Library, N.W. Bldg
MAY 17 1965

NBS

Technical Note

No. 306

STUDIES OF SOLAR FLARE EFFECTS AND OTHER IONOSPHERIC DISTURBANCES WITH A HIGH FREQUENCY DOPPLER TECHNIQUE

V. Agy, D. M. Baker, and R. M. Jones

U. S. DEPARTMENT OF COMMERCE
NATIONAL BUREAU OF STANDARDS

THE NATIONAL BUREAU OF STANDARDS

The National Bureau of Standards is a principal focal point in the Federal Government for assuring maximum application of the physical and engineering sciences to the advancement of technology in industry and commerce. Its responsibilities include development and maintenance of the national standards of measurement, and the provisions of means for making measurements consistent with those standards; determination of physical constants and properties of materials; development of methods for testing materials, mechanisms, and structures, and making such tests as may be necessary, particularly for government agencies; cooperation in the establishment of standard practices for incorporation in codes and specifications; advisory service to government agencies on scientific and technical problems; invention and development of devices to serve special needs of the Government; assistance to industry, business, and consumers in the development and acceptance of commercial standards and simplified trade practice recommendations; administration of programs in cooperation with United States business groups and standards organizations for the development of international standards of practice; and maintenance of a clearinghouse for the collection and dissemination of scientific, technical, and engineering information. The scope of the Bureau's activities is suggested in the following listing of its four Institutes and their organizational units.

Institute for Basic Standards. Electricity. Metrology. Heat. Radiation Physics. Mechanics. Applied Mathematics. Atomic Physics. Physical Chemistry. Laboratory Astrophysics.* Radio Standards Laboratory: Radio Standards Physics; Radio Standards Engineering.** Office of Standard Reference Data.

Institute for Materials Research. Analytical Chemistry. Polymers. Metallurgy. Inorganic Materials. Reactor Radiations. Cryogenics.** Office of Standard Reference Materials.

Central Radio Propagation Laboratory.** Ionosphere Research and Propagation. Troposphere and Space Telecommunications. Radio Systems. Upper Atmosphere and Space Physics.

Institute for Applied Technology. Textiles and Apparel Technology Center. Building Research. Industrial Equipment. Information Technology. Performance Test Development. Instrumentation. Transport Systems. Office of Technical Services. Office of Weights and Measures. Office of Engineering Standards. Office of Industrial Services.

---

* NBS Group, Joint Institute for Laboratory Astrophysics at the University of Colorado.
** Located at Boulder, Colorado.

NATIONAL BUREAU OF STANDARDS

Technical Note 306

Issued April 28, 1965

STUDIES OF SOLAR FLARE EFFECTS AND OTHER IONOSPHERIC DISTURBANCES WITH A HIGH FREQUENCY DOPPLER TECHNIQUE

V. Agy, D. M. Baker, and R. M. Jones
Central Radio Propagation Laboratory
National Bureau of Standards
Boulder, Colorado

NBS Technical Notes are designed to supplement the Bureau's regular publications program. They provide a means for making available scientific data that are of transient or limited interest. Technical Notes may be listed or referred to in the open literature.

For sale by the Superintendent of Documents, U. S. Government Printing Office
Washington, D.C. 20402
Price: 75 cents

Table of Contents

		Page
	List of Tables	v
	List of Figures	vii
	Nomenclature	ix
	Abstract	xi
1.	Introduction	1
2.	Theoretical Considerations	7
	2.1 An Equivalence Theorem for Doppler Shifts	9
	2.2 Changing Ionospheric Parameters	11
	2.3 Frequency Deviations due to Rate of Change of Electron Density as Function of Height	21
3.	Solar Flare Observations with the Doppler Technique	31
	3.1 Percentage of Solar Flares Detected	32
	3.2 Duration, Rise Time, and Delay Time of Frequency Deviation	37
	3.3 Path Length Dependence of Frequency Deviations	40
	3.4 Frequency Dependence of Frequency Deviations	44
4.	Selected Events Detected by Doppler Technique	47
	4.1 Solar Flares	47
	4.2 Geomagnetic Variations	55
5.	Discussion	60
6.	Acknowledgements	64
7.	References	65
8.	Appendix I: The Doppler Shift Written as an Integral	67
9.	Appendix II: Equivalence Theorem for Doppler Shifts	72
10.	Appendix III: Relationship Between Doppler Shift and Virtual Height	74

Table of Contents

Page

11. Appendix IV: Catalog of Sudden Frequency Deviations Observed from October 1960 through December 1962 78

List of Tables

		Page
1.1	Circuits over which Doppler measurements have been made by CRPL	4
2.1	Tabulation of data for flare effects of November 22, 1961 and April 17, 19, and 20, 1962	28
3.1	Percentage of flares reported from October 1, 1960 to December 31, 1962 which were accompanied by SFD's	32
11.1	Catalog of sudden frequency deviations observed from October 1960 through December 1962	85

List of Figures

		Page
2.1	Doppler shift, Δf, for vertical propagation with reflection in a changing parabolic F layer	14
2.2	Doppler shift, Δf, for oblique propagation with reflection in a changing parabolic F layer	15
2.3	Doppler shift, Δf, for vertical propagation with fixed mirror-like reflection above a changing parabolic E layer	17
2.4	Doppler shift, Δf, for vertical propagation through a valley of changing depth between parabolic E and F layers.	19
2.5	Doppler shift, Δf, for oblique propagation through a valley of changing depth between parabolic E and F layers.	20
2.6	Comparison of $f_v \Delta f$ vs f_v with ionogram for SFD at 2014 UT on November 22, 1961.	24
2.7	Comparison of $f_v \Delta f$ vs f_v with ionogram for SFD at 2252 UT on April 17, 1962	25
2.8	Comparison of $f_v \Delta f$ vs f_v with ionogram for SFD at 1935 UT on April 19, 1962	26
2.9	Comparison of $f_v \Delta f$ vs f_v with ionogram for SFD at 1959 UT on April 20, 1962	27
2.10	Relationship between maximum frequency deviations observed on 4 and 5 Mc/s at vertical incidence, Boulder, Colorado	30
3.1	Variations of the percentage of reported solar flares detected, mean solar flux at 2800 Mc/s, and mean Zürich sunspot number during the period October 1, 1960 through December 31, 1962. . .	34
3.2	Percentage of reported solar flares detected by the Doppler technique as a function of month, October 1960 through December 1962.	35
3.3	Percentage of reported solar flares detected by the Doppler technique as a function of time of day, October 1960 through December 1962.	36
3.4	Percentage of reported solar flares detected by the Doppler technique as a function of solar zenith angle at the midpoint of the WWV to Boulder path, October 1960 through December 1962 .	38
3.5	Durations of sudden frequency deviations observed from October 1960 through December 1962	39
3.6	Rise times of sudden frequency deviations observed from October 1960 through December 1962	41
3.7	Time difference between maximum positive frequency deviation and maximum phase of optical flare, October 1960 through December 1962	42

Page

3.8 Frequency deviation of WWV-10 Mc/s observed at Shickley, Nebraska (1780 km) versus that observed at Boulder, Colorado (2400 km). . 43

3.9 Frequency deviation of WWV-10 Mc/s versus that of WWV-20 Mc/s, both observed at Boulder, Colorado 45

3.10 Frequency deviation of WWV-10 Mc/s versus that of WWV-15 Mc/s, both observed at Boulder, Colorado 46

4.1 Sudden frequency deviation observed during importance 1 flare on September 4, 1961, WWV-10 Mc/s received at Boulder 48

4.2 Sudden frequency deviation observed during importance 3+ flare on November 12, 1960, WWV-20 Mc/s received at Boulder. 50

4.3 Sudden frequency deviation observed during importance 3 flare on September 28, 1961, WWV-10 and WWV-20 Mc/s received at Boulder. 51

4.4 Sudden frequency deviation observed during importance 2 flare on April 19, 1962, WWV-10 and WWV-15 Mc/s received at Boulder. . 53

4.5 Sudden frequency deviation observed during importance 2 flare on April 19, 1962. 4 and 5 Mc/s vertical incidence at Boulder . 54

4.6 Sudden commencement observed by the Doppler technique at 2108 UT on September 30, 1961. WWV-10 and WWV-20 Mc/s received at Boulder. 56

4.7 Sudden commencement observed by the Doppler technique at 0219 UT on February 22, 1962. WWV-10 Mc/s received at Shickley, Nebraska, and WWV-10 and WWV-15 Mc/s received at Boulder, Colorado 57

4.8 Correlation between frequency variations observed at both oblique and vertical incidence and changes in the magnetic field observed at Boulder 59

10.1 Comparison of theoretical $f\Delta f$ versus f with ionogram 77

11.1 Sample Doppler record illustrating the range in magnitude of the sudden frequency deviations detected 80

Nomenclature

ΔA	change in non-deviative absorption, nepers
b	thickness of slab of ionization in non-deviative region, km
c	speed of light in vacuum, km/s
D	great circle distance between transmitter and receiver, km
f	frequency
f_c	critical frequency of parabolic layer, Mc/s
f_E	critical frequency of parabolic E layer, Mc/s
f_F	critical frequency of parabolic F layer, Mc/s
f_H	gyrofrequency, Mc/s
f_N	electron plasma frequency, Mc/s
f_v	$f \cos\phi_o$, equivalent vertical-incidence frequency, Mc/s
f_V	plasma frequency of valley between two parabolic layers, Mc/s
Δf	Doppler shift, c/s
h	reflection height, km
h'	virtual height, km
h_m	height of maximum electron density of parabolic layer, km
h_{mE}	height of maximum electron density of parabolic E layer, km
h_{mF}	height of maximum electron density of parabolic F layer, km
h_o	height of bottom of parabolic layer, km, or a height in non-deviative region below which dN/dt can be considered to be zero.
h_{oE}	height of bottom of parabolic E layer, km
h_{oF}	height of bottom of parabolic F layer, km
k	$\frac{f_N^2}{N}$, 8.05×10^{-11} $(Mc/s)^2$ m^3
N	electron density, m^{-3}

P	phase path, km
s	path length
t	time
X	$\frac{f_N^2}{f^2}$
y_m	$h_m - h_o$, semithickness of parabolic layer
Y	f_H/f
Y_L	$Y \cos\theta$
Y_T	$Y \sin\theta$
z	height as variable of integration
μ	phase refractive index
μ'	group refractive index
μ_o	phase refractive index at transmitter
ν	electron collision frequency
ρ	f_V/f_E
ϕ	angle between wave normal and vertical
ϕ_o	angle between wave normal and vertical at transmitter
θ	angle between wave normal and magnetic field

Abstract

This report presents some results of work done with a Doppler technique for studying ionospheric disturbances. The theoretical results include a calculation of the frequency shifts to be expected from changes in the parameters of a parabolic model ionosphere and a method of determining the height variation of the time rate of change of electron density during ionospheric disturbances. It is shown that the frequency shift, with oblique propagation, is the same as that with vertical propagation on the equivalent vertical-incidence frequency. The experimental results include a comprehensive catalog of all flare effects observed from 1 October 1960 through 31 December 1962, a statistical study of these flare effects, and the Doppler records of some solar flare effects detected during this period. A model in which the time rate of change of electron density is zero below the bottom of the E layer, and constant above that height, explains the frequency dependence of the maximum Doppler shifts observed during some solar flares.

STUDIES OF SOLAR FLARE EFFECTS AND OTHER IONOSPHERIC DISTURBANCES WITH A HIGH FREQUENCY DOPPLER TECHNIQUE

V. Agy, D. M. Baker, and R. M. Jones
Central Radio Propagation Laboratory

1. Introduction

The "Doppler technique" developed and described by Watts and Davies [1960] appears to be a powerful tool for probing the ionosphere, especially during times of rapid change. It has been shown to be effective, for example, in the study of solar-flare effects and of variations occurring at the time of a magnetic sudden commencement [Davies, 1962b]. The term "sudden frequency deviation", abbreviated to SFD (initially suggested by Chan and Villard [1963]), has been adopted to refer to solar-flare induced variations in the received frequency of a high frequency, ionospherically propagated radio signal.

In effect, the frequency f of the received signal from a highly stable CW transmitter is monitored continuously. If the phase path P changes with time, a shift in the received frequency is produced which may be written [Davies, 1962a]:

$$\Delta f = - \frac{f}{c} \frac{dP}{dt} \tag{1.1}$$

where c is the speed of light in vacuum. (This may be written

$$\Delta f = - \frac{f}{c} \frac{d}{dt} \int \mu \, ds \tag{1.2}$$

if the anisotropy of the ionosphere is neglected.)

The present monitoring technique involves recording, at a speed of .02 ips on magnetic tape, the beat between the received signal and that of a stable local oscillator. The beat frequency is set initially at a few cycles per second. If the tape is played back at 30 ips, this beat frequency is readily analyzed on a standard audio frequency analyzer and changes in the original frequency of one tenth of a cycle per second or more can easily be observed and measured. The transmitted and reference frequencies must be stable to within a few parts in 10^9 per day.

A simple theory, consisting of two special cases, for determining the layers affected during an ionospheric disturbance has been described by Davies [1962a] and by Davies, Watts, and Zacharisen [1962]. One case shows that for several probing frequencies propagating in the same mode (i.e., same ground path length, same number of hops, reflected from same layer) the Doppler shift varies inversely with carrier frequency ($\Delta f \propto 1/f$) when the change in phase path is due solely to changes in ionization in the non-deviative portion of the ionosphere. In the other case the frequency deviation varies directly with frequency ($\Delta f \propto f$) if the phase path change is due entirely to a vertical movement of the height of reflection.

Davies [1963] has suggested that in the non-deviative region the height determination can be improved by comparing the phase path change (ΔP) to the absorption suffered by the radio wave. An atmospheric model specifying electron collision frequency (ν) as a function of height can then be used to locate the "slab" of ionization assumed responsible for both effects. Similar work has been carried out by Kanellakos, Chan, and Villard [1962]. These studies have helped to establish the fact that

solar-flare effects are relatively frequent at heights above the D region of the ionosphere.

Davies [1962c] has also shown that the Doppler technique can be used for study of ionospheric drifts.

Those circuits over which Doppler measurements have been made by CRPL are given in table 1.1. Related techniques involving the direct measurement of phase change are also in use. The increasing use of these techniques and the high precision of the actual measurements (both of Doppler shift and of phase change) suggest that attention be given to further development of the theory so that the approach may be exploited to the fullest extent.

This paper presents work done with the Doppler technique by the Ionosphere Research Section of the Ionosphere Research and Propagation Division of CRPL. The theoretical treatment develops two methods of determining the heights at which ionospheric disturbances occur. Both approaches neglect the earth's magnetic field and the curvature of the ionosphere.

The first method approximates the ionosphere by one or two parabolic profiles and then determines the frequency dependence of the Doppler shift produced by the rate of change of the parameters (i.e., critical frequency, minimum height, height of maximum electron density, thickness of layer, and valley depth) defining the ionospheric model. If, then, the Doppler shifts are known for a number of frequencies at vertical and/or oblique incidence during a disturbance, it is possible to determine the time rate of change of the parameters which could have produced the observed Doppler shifts. This method is not difficult to apply since the

Table 1.1

Circuits over which Doppler measurements have been made by CRPL

Transmitter	Receiver	Path Length (km)	Freq. Mc/s	Period of Operation
Beltsville, Md. (WWV)	Boulder, Colorado	2430	5	02/09/63-07/15/63
"	"		10	12/15/60-12/20/60, 01/11/61-- (1)
"	"		15	12/21/60-01/10/61, 01/17/62-- (1)
"	"		20	10/02/60-06/02/61 09/08/61-01/17/62
"	Shickley, Nebraska	1780	10	08/12/61-04/18/62
Maui, Hawaii (WWVH)	Anchorage, Alaska	4480	15	06/08/62-12/03/62
"	Midway Island (3)	2200	5	05/31/62-07/10/62 (2) 10/25/62-11/06/62 (night)
"	"		10	05/31/62-07/10/62 (2) 10/25/62-11/06/62
"	"		15	05/31/62-07/10/62 (2) 10/25/62-11/06/62 (day)
"	Wake Island (3)	3900	10	05/26/62-07/29/62
"	"		15	05/28/62-07/29/62

Maui, Hawaii (WWVH)	Makupuu Pt., Oahu, Hawaii (4)	140	5	11/10/62-08/29/63
Pt. Barrow, Alaska	Anchorage, Alaska	1160	9.9475	02/23/62-12/03/62
Tripoli, Libya	Accra, Ghana	3300	19.904	09/11/61-10/14/61
Monrovia, Liberia	"	1180	10.1018	10/19/62-- (1)
"	"		20.2036	10/22/62-- (1)
"	Natal, Brazil	2990	10.1018	11/30/62-- (1)
"	"		20.2036	11/14/62-- (1)
Sunset (Boulder), Colorado	Boulder, Colo.	25	2.100	06/02/61-09/08/61
"	"		4.000	08/04/61-- (1)
"	"		5.054	07/30/61-- (1)
"	Ft. Collins, Colo.	75	4.000	02/01/62-03/01/62
Erie, Colorado	Boulder, Colorado	15	2.100	02/25/63-06/21/63

(1) Circuit in operation as of July 1964

(2) Either 5 and 10 or 10 and 15 Mc/s in operation during this period

(3) Subject to interference from JJY, Tokyo

(4) Hawaiian records obtained by Dr. Walter Steiger of the University of Hawaii

layer parameters are easily determined from the ionogram and the solution for the time rate of change involves solving only a few simultaneous linear equations.

The second approach gives a solution for the time rate of change of electron density as a function of height when the Doppler shift as a function of the equivalent vertical-incidence frequency can be given. It can be applied to any monotonic ionospheric profile, but the accuracy of the solution depends on the amount of data available.

Most solar flare effects in the ionosphere produce characteristic effects on the Doppler records. The early recognition of this fact led to the suggestion that the Doppler technique be used for flare patrol work. Much of the record analysis and the experimental effort has dealt with flare effects--specifically with the percentage of flares detected, the time characteristics of the frequency deviations, and the magnitude of the effects relative to probing frequency, path length, and solar zenith angle. The section of the report dealing with the observations gives the empirical results derived to date and a catalog of solar flare effects as observed on the CRPL Doppler records from 1 October 1960 through 31 December 1962. A few sets of observations are treated according to the methods described in the theoretical section.

2. Theoretical Considerations

In order for the Doppler technique to be of value as a tool for ionospheric research, a theory is needed which adequately relates the observed frequency variations to the ionospheric changes producing them. A simple theory for vertical incidence (neglecting the earth's magnetic field) has been developed by Davies [1962a, 1962b]. According to this theory, if changes take place in a non-deviative slab of thickness b in which the rate of change of ionization can be considered constant with height, then

$$\Delta f = \frac{kb}{cf} \frac{dN}{dt} . \tag{2.1}$$

In this case the observed frequency deviation is inversely proportional to the operating frequency. However, if the only change is a vertical movement of the height at reflection, then

$$\Delta f = - 2 \frac{f}{c} \frac{dh}{dt} \tag{2.2}$$

and the frequency deviation is directly proportional to the operating frequency. These equations can be applied to oblique incidence if b is replaced by $b/\cos \phi_o$ and dh/dt is replaced by $dh/dt \cos \phi_o$, where ϕ_o is the angle of incidence on the ionosphere.

If both types of change occur at the same time (i.e., if the change in height of reflection and a change in the non-deviative region occur simultaneously but independently) then

$$\Delta f = \frac{kb}{cf} \frac{dN}{dt} - 2 \frac{f}{c} \frac{dh}{dt} . \tag{2.3}$$

If such independent changes did occur and measurements of Δf were made on two different frequencies, then $b\, dN/dt$ and dh/dt could be determined from

(2.3) [Davies, 1962d].

Davies [1963] has further shown that for a thin, non-deviative slab in which the collision frequency is $\nu(\ll \omega)$

$$\frac{\Delta A}{\Delta P} = - \frac{\nu}{c} , \tag{2.4}$$

where ΔA is the change in non-deviative absorption in nepers and ΔP is the change in phase path given by

$$\Delta P(t) = - \frac{c}{f} \int_{t_o}^{t} \Delta f \, dt . \tag{2.5}$$

Hence, if both $\Delta A(t)$ and $\Delta f(t)$ are measured, it is possible to determine $\nu(t)$ from (2.4) and (2.5). If the collision frequency profile $\nu(h)$ is known, then the average height $h(t)$ at which the additional electron density is produced can be found. However, even where this method is applicable it is rather insensitive due to the lack of knowledge of the variation of collision frequency with height.

The simple theory has not explained all the frequency deviations observed. The theoretical work covered in this report is a beginning in the development of a theory which will explain the Doppler observations at both vertical and oblique incidence. The major aim has been to develop a method of determining the height variation of dN/dt from the Doppler observations. A knowledge of dN/dt as a function of height during a solar flare would be helpful in determining which wave length bands are enhanced during the flare. A knowledge of the enhancement of radiation during a flare should help in gaining an understanding of the processes taking place in the sun.

2.1. An Equivalence Theorem for Doppler Shifts

For oblique propagation relations similar to (2.1) and (2.2) can be derived if the earth's magnetic field and the curvature of the ionosphere are neglected. The resulting relations are:

$$\Delta f = \frac{kb}{cf \cos \phi_o} \frac{dN}{dt} \tag{2.6}$$

for a change of ionization in a non-deviative slab, and

$$\Delta f = - 2 \frac{f \cos \phi_o}{c} \frac{dh}{dt} \tag{2.7}$$

for a vertical movement of the height of reflection. In these equations ϕ_o is the angle of incidence on the ionosphere. These two equations can be written as

$$\Delta f = \frac{kb}{f_v c} \frac{dN}{dt} \tag{2.8}$$

and

$$\Delta f = - 2 \frac{f_v}{c} \frac{dh}{dt} \tag{2.9}$$

where $f_v = f \cos \phi_o$. A comparison of (2.8) and (2.9) with (2.1) and (2.2) reveals that, in these simple cases, the Doppler shift observed on a wave frequency f, incident on the ionosphere at an angle ϕ_o, would be the same as that observed on a frequency f_v incident vertically on the ionosphere. This "equivalence" between the Doppler shifts observed for vertical and oblique propagation is easily seen for these simple cases. In Appendix II it is shown that such an equivalence holds in the general case, if the earth's magnetic field and the curvature of the ionosphere are neglected. Hence, an equivalence theorem for Doppler shifts can be stated as follows:

$$\Delta f(f, \phi_o) = \Delta f(f \cos \phi_o, 0) \tag{2.10}$$

where $\Delta f(f, \phi_o)$ is the Doppler shift, on a frequency f, incident on the ionosphere at an angle ϕ_o. The frequency f_v is called the equivalent vertical-incidence frequency.

As derived, this equivalence relation applies only for no magnetic field. However, it is probably a good approximation even with the magnetic field for frequencies which are large compared to the gyrofrequency. Therefore, rather than attempting to treat vertical-incidence and oblique-incidence data separately, it seems more advantageous to use the equivalence theorem to reduce the oblique-incidence data to equivalent vertical-incidence data, and to apply a single theory to the combined data. In this connection it may be noted that with oblique-incidence observations the amount of useful data may exceed the number of probing frequencies used. At oblique incidence more than one propagation mode is often possible (e.g., E and F layer propagation, one- and two-hop propagation, etc.), and the Doppler shifts observed on the different modes may be quite different. In such a case, if the propagation modes can be identified, the Doppler shift observed on each gives an independent piece of data.

This equivalence theorem should be very useful in analyses of Doppler data obtained on different paths and from different parts of the world, and it will provide a convenient means whereby various observers can exchange their data. Of course, before data from different paths or different regions can be meaningfully compared certain corrections, such as corrections for the number of hops or the differences in solar zenith angle, may have to be applied to the observed frequency deviations.

2.2. Frequency Deviations Due to Changing Ionospheric Parameters

Although in many cases the ionosphere can be described adequately only by specifying the height distribution of electron density, it is often convenient to represent the ionosphere by a suitable model (e.g., parabolic). If the distribution does not change in character (if, for example, a parabolic distribution remains parabolic) it is possible to find Δf as a function of the time derivatives of the parameters defining the distribution. Primarily for illustrative purposes and for comparison with the first order theory [Davies, 1962a], the algebra and the computations have been carried out for several model ionospheres. Both vertical and oblique propagation are considered. The earth's magnetic field and the curvature of the earth and ionosphere are neglected.

For vertical propagation of a wave, the phase path P is given by

$$P = 2 \int_o^h \mu \, dz \, , \tag{2.11}$$

where h is the reflection height. For oblique propagation, the phase path is given by

$$P = \int_s \mu \, ds \, , \tag{2.12}$$

where s is the path length.

If the ionospheric profile consists of parabolic layers, then the plasma frequency f_N in each layer is given by

$$f_N^2 = f_c^2 \left[2 \left(\frac{z - h_o}{h_m - h_o} \right) - \left(\frac{z - h_o}{h_m - h_o} \right)^2 \right], \tag{2.13}$$

for $h_o \leq z \leq 2\ h_m - h_o$. In each layer, the phase refractive index μ for a wave of frequency f is given by

$$\mu = \sqrt{1 - \frac{f_N^2}{f^2}} = \sqrt{1 - \frac{f_c^2}{f^2}\left(2\left[\frac{z - h_o}{h_m - h_o}\right] - \left[\frac{z - h_o}{h_m - h_o}\right]^2\right)}. \qquad (2.14)$$

For vertical propagation this expression for the refractive index may be used in (2.11) to find the phase path in terms of the parameters defining the model ionosphere. The time derivative of P may then be found in terms of the time derivatives of the layer parameters, and the Doppler shift, Δf, is then given by (1.1). Similarly the Doppler shift for oblique propagation could be found from (2.14), (2.12), and (1.1) using the fact that the transmission distance is constant (i.e., the transmitter and receiver are fixed). However, because of the equivalence theorem presented in section 2.1, the calculations need be performed only for vertical propagation. The Doppler shift for oblique propagation can then be found by substituting f cos ϕ_o for f in the equations for vertical propagation. Indeed, the equivalence theorem was discovered while working with changing parabolic layers.

Three models considered will now be discussed separately.

Model 1: reflection in a changing parabolic layer (figure 2.1a). For this case

$$\Delta f = -\frac{f}{c}\frac{\partial P}{\partial h_o}\frac{dh_o}{dt} - \frac{f}{c}\frac{\partial P}{\partial h_m}\frac{dh_m}{dt} - \frac{f}{c}\frac{\partial P}{\partial f_c}\frac{df_c}{dt} \qquad (2.15)$$

where

$$-\frac{f}{c}\frac{\partial P}{\partial h_o} = \frac{f_c}{c}\left[-x - \frac{1 - x^2}{2}\,\ell n\,\frac{1 + x}{1 - x}\right]$$

$$-\frac{f}{c}\frac{\partial P}{\partial h_m} = \frac{f_c}{c}\left[-x + \frac{1 - x^2}{2}\,\ell n\,\frac{1 + x}{1 - x}\right] \qquad (2.16)$$

$$-\frac{f}{c}\frac{\partial P}{\partial f_c} = \frac{y_m}{c}\left[-x + \frac{1 + x^2}{2}\,\ell n\,\frac{1 + x}{1 - x}\right]$$

and

$$x = \frac{f}{f_c} \qquad (2.17)$$

for vertical propagation, or

$$x = \frac{f \cos \phi_o}{f_c} \qquad (2.18)$$

$$\tan \phi_o = \frac{D}{\left(2h_o + x y_m\,\ell n\,\frac{1 + x}{1 - x}\right)} \qquad (2.19)$$

for oblique propagation. Plots of the coefficients in (2.15) $[-f/c\ \partial P/\partial h_o,\ -f/c\ \partial P/\partial h_m,\ -f/c\ \partial P/\partial f_c]$ versus f, for specific values of the parameters h_o, h_m, and f_c, are given in figure 2.1 for vertical propagation. Similar curves are shown in figure 2.2 for oblique propagation over paths of 200, 1000, and 2400 km. For a layer defined by values of h_o, h_m, and f_c different from those chosen, figures 2.1 and 2.2 can still be applied by using equation (2.16) to scale the curves.

For the special case $dh_o/dt = dh_m/dt = dh/dt$ and $df_c/dt = 0$, (2.15) reduces to (2.2), the expression for the Doppler shift caused by vertical movement of the ionosphere (or of the height of reflection).

Doppler shift, Δf, for vertical propagation with reflection in a changing parabolic F layer

$$f_c = 10 \text{ Mc/s}, \quad h_o = 200 \text{ km}, \quad h_m = 300 \text{ km}$$

$$\Delta f = -\frac{f}{c}\frac{\partial P}{\partial h_o}\frac{dh_o}{dt} - \frac{f}{c}\frac{\partial P}{\partial h_m}\frac{dh_m}{dt} - \frac{f}{c}\frac{\partial P}{\partial f_c}\frac{df_c}{dt}$$

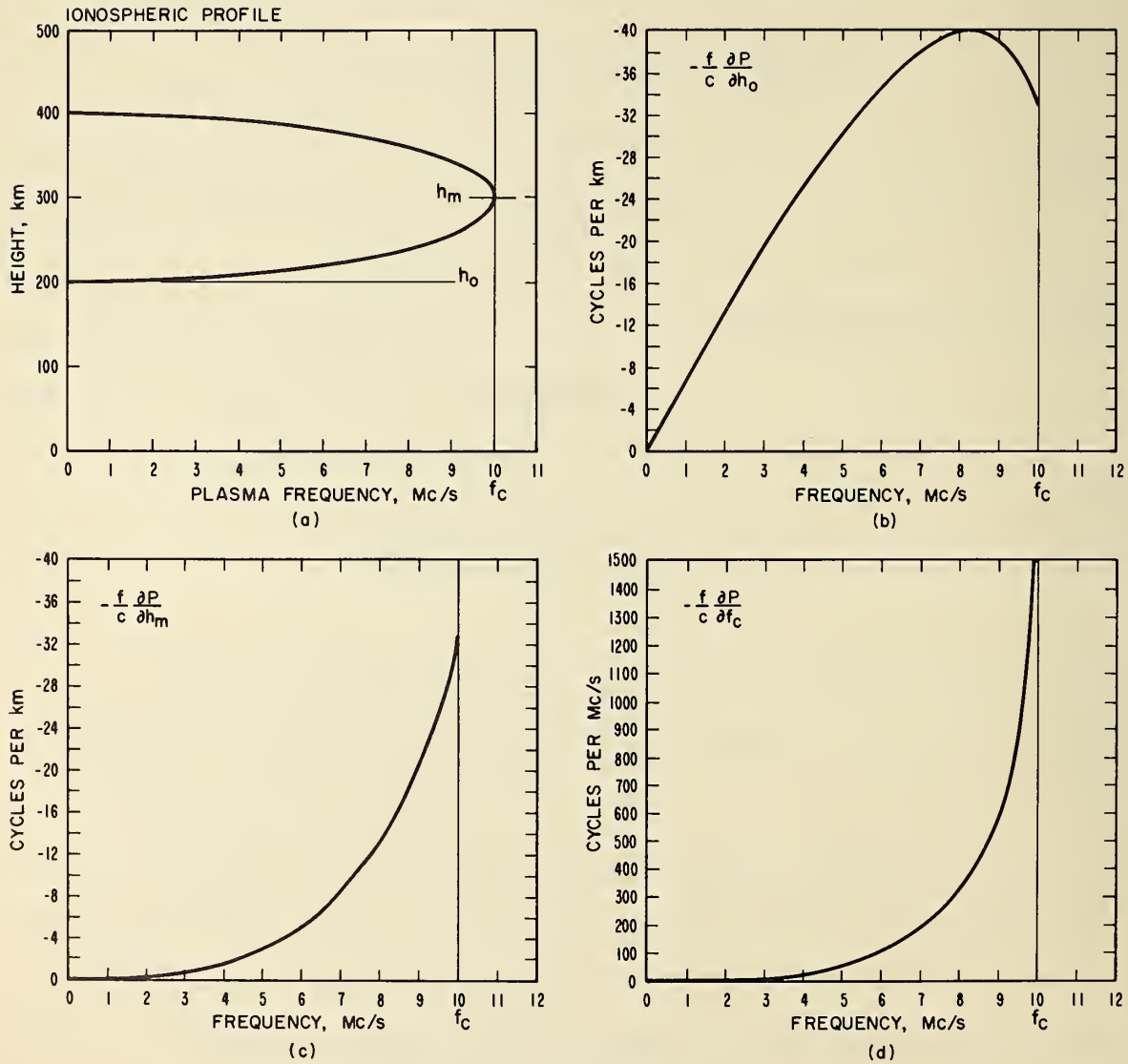

Figure 2.1

Doppler shift, Δf, for oblique propagation with reflection in a changing parabolic F layer

$$f_c = 10 \text{ Mc/s}, \quad h_o = 200 \text{ km}, \quad h_m = 300 \text{ km}$$

$$\Delta f = -\frac{f}{c}\frac{\partial P}{\partial h_o}\frac{dh_o}{dt} - \frac{f}{c}\frac{\partial P}{\partial h_m}\frac{dh_m}{dt} - \frac{f}{c}\frac{\partial P}{\partial f_c}\frac{df_c}{dt}$$

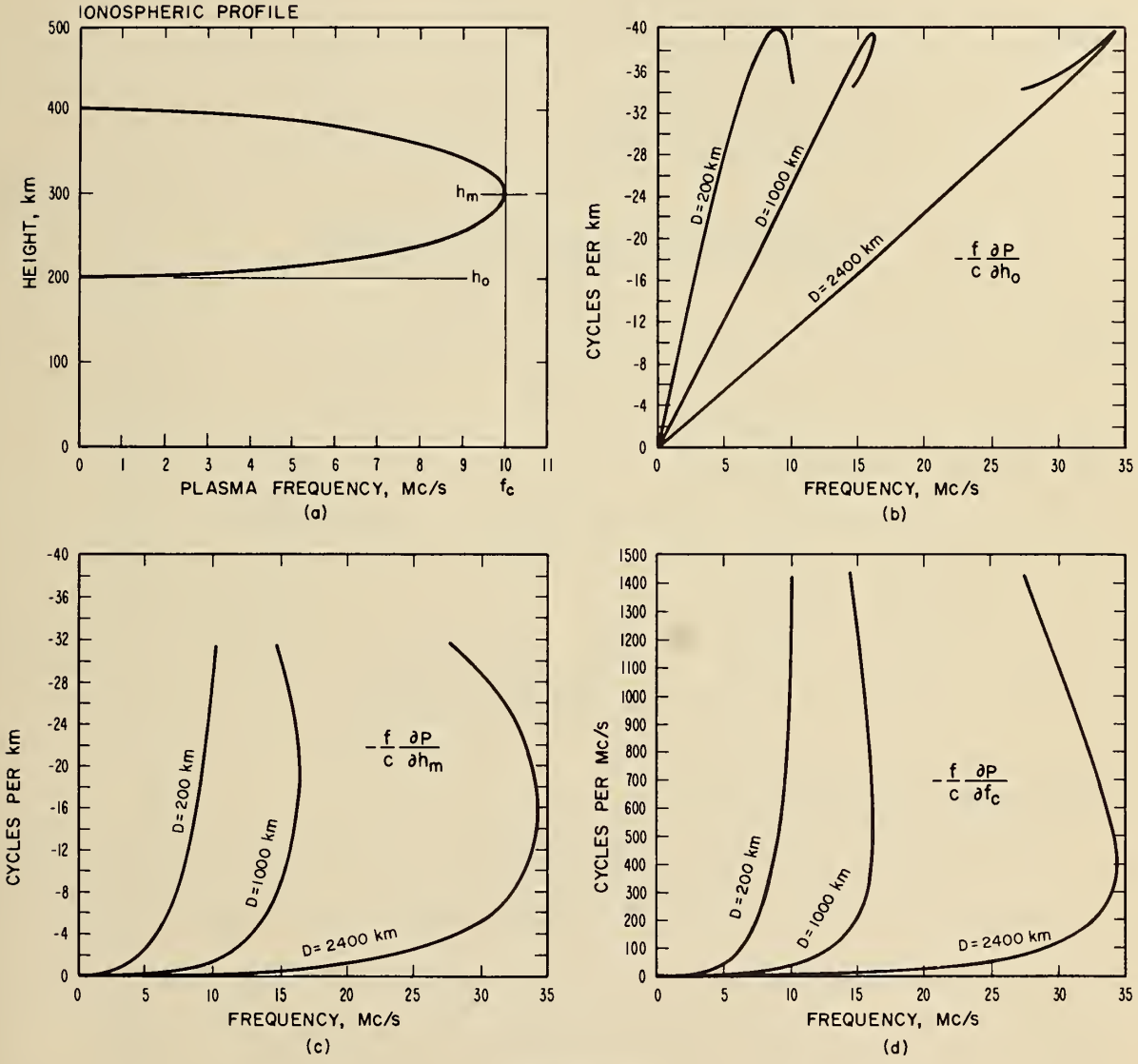

Figure 2.2

Model 2: propagation through a changing parabolic layer with reflection from a mirror reflector (figure 2.3a). In this case

$$\Delta f = - \frac{f}{c} \frac{\partial P}{\partial f_c} \frac{df_c}{dt} - \frac{f}{c} \frac{\partial P}{\partial y_m} \frac{dy_m}{dt} \tag{2.20}$$

where

$$- \frac{f}{c} \frac{\partial P}{\partial f_c} = \frac{y_m}{c} \left[-2x + (1 + x^2) \ln \frac{x + 1}{x - 1} \right]$$

$$- \frac{f}{c} \frac{\partial P}{\partial y_m} = \frac{f_c}{c} \left[2x + (1 - x^2) \ln \frac{x + 1}{x - 1} \right] \tag{2.21}$$

and

$$x = \frac{f}{f_c} \qquad \text{(eq. 2.17)}$$

for vertical propagation, or

$$x = \frac{f \cos \phi_o}{f_c} \qquad \text{(eq. 2.18)}$$

$$\tan \phi_o = \frac{D}{\left(2h_o + 2 \, x \, y_m \ln \frac{x + 1}{x - 1} \right)} \tag{2.22}$$

for oblique propagation.

For vertical propagation with specific values of f_c and y_m the coefficients $- f/c \, \partial P/\partial f_c$ and $-f/c \, \partial P/\partial y_m$ are shown as functions of frequency in figure 2.3. The dashed curves in this figure show what the behavior would be if Δf were inversely proportional to frequency. For frequencies much greater than the critical frequency of the parabolic layer (i.e., when the parabolic layer can be considered non-deviative) the Doppler shift clearly exhibits an inverse frequency dependence as is predicted by (2.1).

Doppler shift, Δf, for vertical propagation with fixed mirror-like reflection above a changing parabolic E layer

$f_c = 3$ Mc/s, $y_m = 20$ km

$$\Delta f = -\frac{f}{c}\frac{\partial P}{\partial f_c}\frac{df_c}{dt} - \frac{f}{c}\frac{\partial P}{\partial y_m}\frac{dy_m}{dt}$$

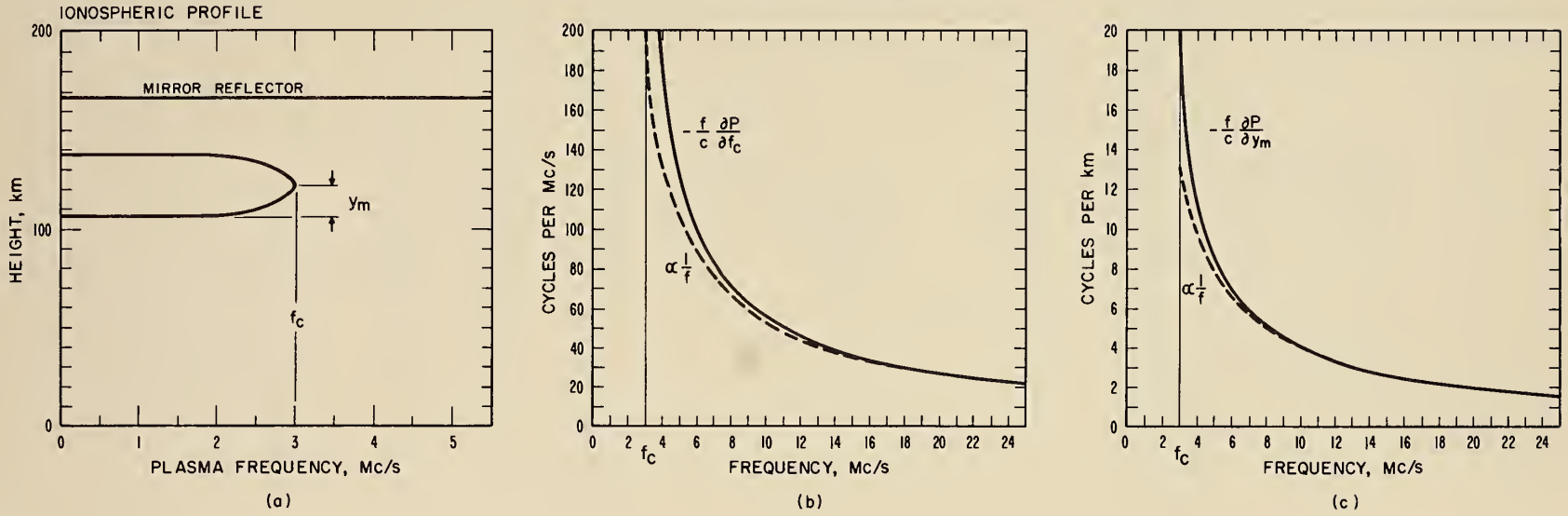

Figure 2.3

Model 3: propagation through one parabolic layer and a valley of changing depth with reflection in a second parabolic layer (figure 2.4a). For this model

$$\Delta f = - \frac{f}{c} \frac{\partial P}{\partial \rho} \frac{d\rho}{dt} \tag{2.23}$$

where

$$- \frac{f}{c} \frac{\partial P}{\partial \rho} = \frac{2 f_E}{c} \frac{h_{mF} - h_{mE} - y_F \sqrt{1 - \left(\frac{f_V}{f_E} \right)} - y_E \sqrt{1 - \left(\frac{f_V}{f_E} \right)^2}}{\sqrt{x^2 - 1}} \tag{2.24}$$

$$\rho = \frac{f_V}{f_E} \tag{2.25}$$

$$\frac{d\rho}{dt} = \frac{1}{f_E} \frac{df_V}{dt} \tag{2.26}$$

and

$$x = \frac{f}{f_V} \tag{2.27}$$

for vertical propagation, or

$$x = \frac{f \cos \phi_o}{f_V} \tag{2.28}$$

for oblique propagation. The formula for $\tan \phi_o$ is not given because of its complexity.

The frequency dependence of $-f/c \; \partial P/\partial \rho$ for $\rho = 0.05$ and 0.95 is shown in figure 2.4b and 2.4c for vertical propagation and figure 2.5b and 2.5c for oblique propagation. The dashed curves vary as $1/f$. For vertical propagation through a changing non-deviative valley ($\rho = 0.05$ or

Doppler shift, Δf, for vertical propagation through a valley of changing depth between parabolic E and F layers

$f_E = 3$ Mc/s, $f_V = \rho \cdot f_E$, $f_F = 10$ Mc/s

$h_{oE} = 100$ km, $h_{mE} = 120$ km, $h_{oF} = 200$ km, $h_{mF} = 300$ km

$$\Delta f = -\frac{f}{c}\frac{\partial P}{\partial \rho}\frac{d\rho}{dt}$$

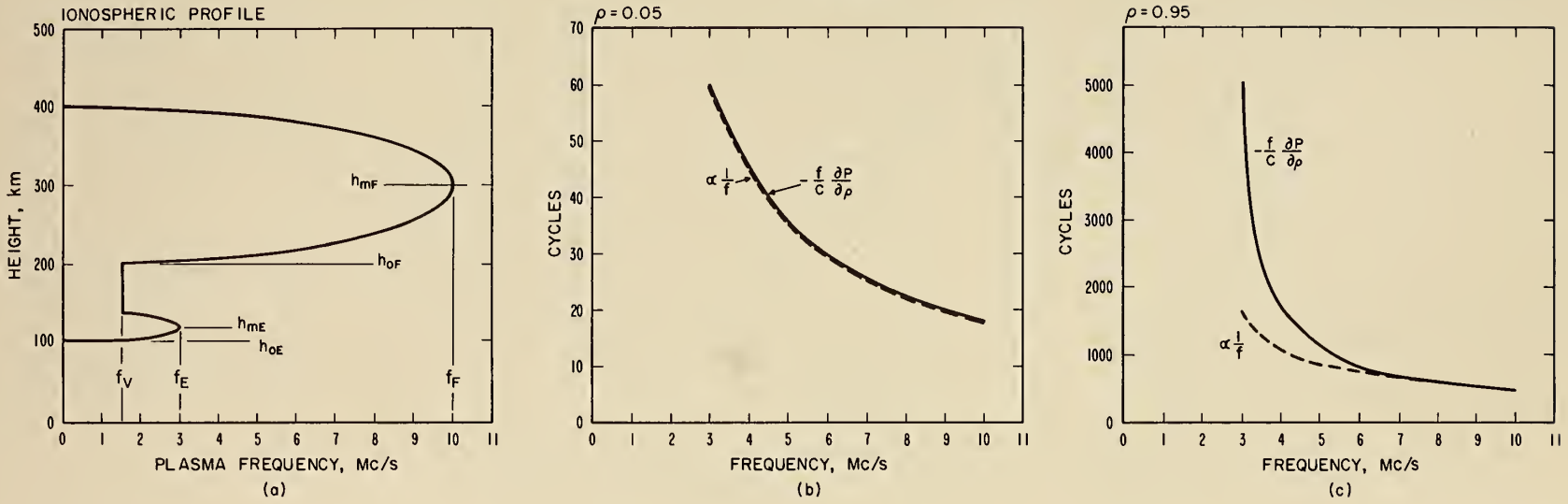

Figure 2.4

Doppler shift, Δf, for oblique propagation through a valley of changing depth between parabolic E and F layers

$f_E = 3$ Mc/s, $f_V = \rho \cdot f_E$, $f_F = 10$ Mc/s

$h_{oE} = 100$ km, $h_{mE} = 120$ km, $h_{oF} = 200$ km, $h_{mF} = 300$ km, $D = 1500$ km

$$\Delta f = -\frac{f}{c}\frac{\partial P}{\partial \rho}\frac{d\rho}{dt}$$

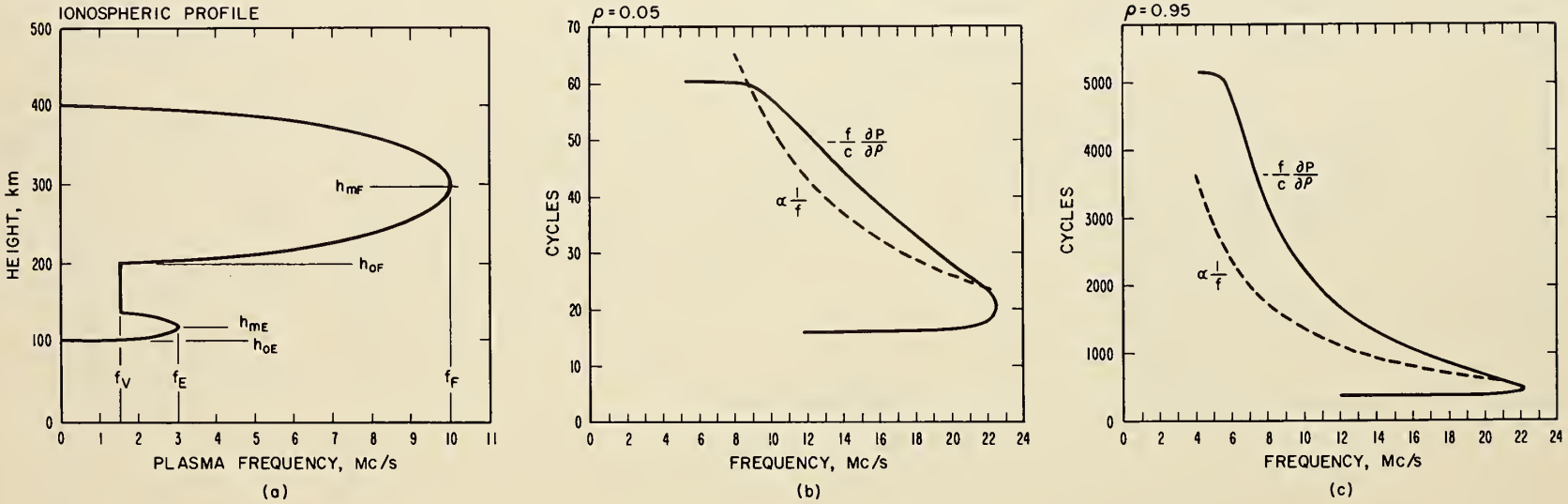

Figure 2.5

for higher frequencies when $\rho = 0.95$) the Doppler shift is inversely proportional to frequency as shown in figure 2.4b and 2.4c. However, at oblique incidence when the valley is non-deviative the Doppler shift does not show a 1/f dependence, as shown in figure 2.5b and 2.5c. This is due to the frequency dependence of the angle of incidence ϕ_o.

As shown in figures 2.2 and 2.5 for high frequencies at oblique incidence ($f > f_c$) two values of the Doppler shift become possible. In each case one possible Doppler shift would be observed on the low-angle ray and the other on the high-angle ray.

2.3. Rate of Change of Electron Density as a Function of Height

Although the methods developed in the preceding section may be useful in some cases, their usefulness is limited by the necessity of approximating the ionospheric profile by parabolic layers. This section presents a method for determining the rate of change of electron density as a function of height using the true height profile directly.

It is shown in Appendix I that the Doppler shift can be written as an integral over the ray path. For vertical propagation

$$\Delta f = -2 \frac{f}{c} \int_o^h \frac{\partial \mu}{\partial t} \, dz \tag{2.29}$$

Neglecting the earth's magnetic field this becomes

$$\Delta f = \frac{k}{fc} \int_o^h \frac{\partial N/\partial t \, dz}{\sqrt{1 - kN/f^2}} \tag{2.30}$$

If the true height profile, N(h) is known and if Δf is known as a function of frequency, then (2.30) can be inverted to give $\partial N/\partial t$ as a function of height. If N(h) is monotonic (2.30) reduces to Abel's equation, the solution of which is

$$\frac{\partial N}{\partial t}(f_N) = \frac{c}{k}\frac{2}{\pi}\frac{df_N}{dh}\frac{d}{df_N}\int_0^{f_N}\frac{f\,\Delta f\,df}{\sqrt{f_N^2 - f^2}} \qquad (2.31)$$

[Whitaker and Watson, 1952]. If $f_N(h)$ is known, then $\partial N/\partial t(h)$ can be found from $\partial N/\partial t(f_N)$. If a valley exists so that N(h) is not monotonic, then $\partial N/\partial t$ cannot be determined uniquely in or above the valley.

If the magnetic field is not neglected and if it is assumed that the Doppler shift due to changes in the magnetic field itself are negligible, then (2.29) can be solved by numerical methods to give a unique solution for $\partial N/\partial t(h)$ for a monotonic true height profile. A computer program has been written which will perform this calculation if N(h) and $\Delta f(f)$ are known. The method is analogous to that used in true height reduction from ionograms [Budden, 1955]. Unfortunately, the data available for any particular event have not determined the frequency dependence of Δf sufficiently well to warrant application of this technique.

An interesting special case arises when $\partial N/\partial t$ is zero below a height h_o (below the deviative regions) and constant above h_o. The Doppler shift for this case has been calculated in Appendix III. The result, which is exact if the effect of the earth's magnetic field is neglected, but only approximate otherwise, is

$$\Delta f = \frac{k}{fc}\frac{\partial N}{\partial t}(h' - h_o)\ , \qquad (2.32)$$

where h' is the virtual height of reflection for the frequency f. According to the equivalence theorem for Doppler shifts, (2.32) should also be approximately true for oblique propagation if f is replaced by f_v.

Several of the measurements made at Boulder of the maximum Δf observed during solar flares agree with (2.32). This indicates that these measurements can be explained by $\partial N/\partial t$ that is zero below the E layer and constant with height in the E and F regions. The agreement of the data with (2.32) is illustrated in two ways.

First, (2.32) indicates that a plot of $f\Delta f$ versus f should look approximately like the appropriate ionogram. The agreement is shown for four specific events in figures 2.6, 2.7, 2.8, and 2.9, where plots of $f_v\Delta f$ versus f_v have been superimposed on tracings of the ionograms obtained at the end points of the path shortly before the flares.

The scale used to plot $f_v\Delta f$ was adjusted so that the 4 Mc/s value and one E-layer value (except for 22 November 1961, where, due to lack of E-layer data, h_o was chosen to be at the bottom of the E-layer) would coincide with the Boulder ionogram. The adjustment of the scale in this manner determines h_o and $\partial N/\partial t$ in (2.32).

The data for these four events are given in table 2.1, along with the value of $\partial N/\partial t$ determined. For the oblique paths, the equivalent vertical-incidence frequencies were determined by using transmission curves [Smith, 1939; Davies, 1965] on the ionograms, and the observed frequency deviations have been divided by the number of hops.

Second, if measurements are made on two frequencies (4 and 5 Mc/s in

Comparison of $f_v \Delta f$ vs f_v with ionogram for SFD
at 2014 UT on November 22, 1961

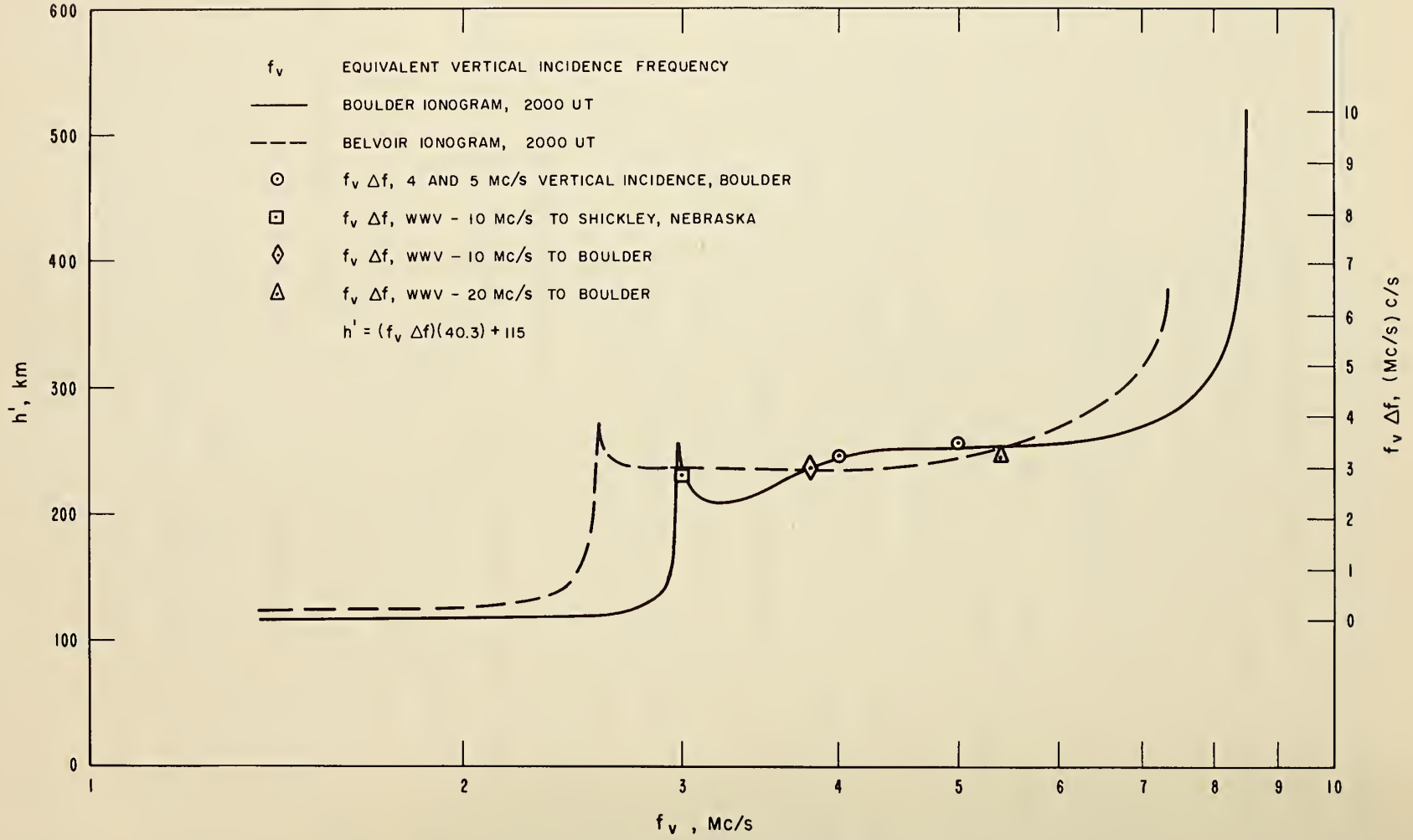

Figure 2.6

Comparison of $f_v \Delta f$ vs f_v with ionogram for SFD
at 2252 UT on April 17, 1962

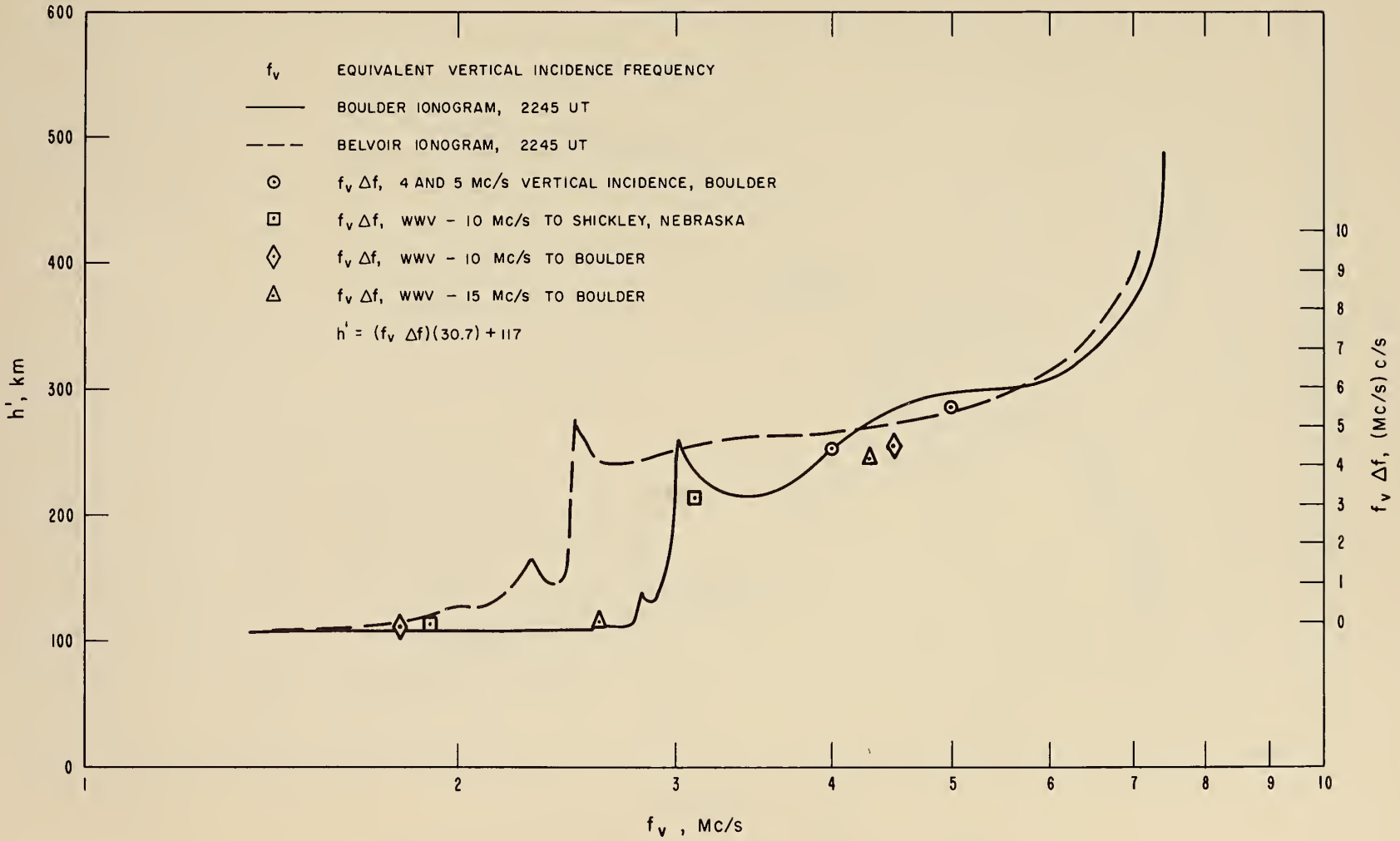
f_v EQUIVALENT VERTICAL INCIDENCE FREQUENCY
BOULDER IONOGRAM, 2245 UT
BELVOIR IONOGRAM, 2245 UT
$f_v \Delta f$, 4 AND 5 Mc/s VERTICAL INCIDENCE, BOULDER
$f_v \Delta f$, WWV - 10 Mc/s TO SHICKLEY, NEBRASKA
$f_v \Delta f$, WWV - 10 Mc/s TO BOULDER
$f_v \Delta f$, WWV - 15 Mc/s TO BOULDER
$h' = (f_v \Delta f)(30.7) + 117$
h', km
f_v , Mc/s
$f_v \Delta f$, (Mc/s) c/s

Figure 2.7

Comparison of $f_v \Delta f$ vs f_v with ionogram for SFD
at 1935 UT on April 19, 1962

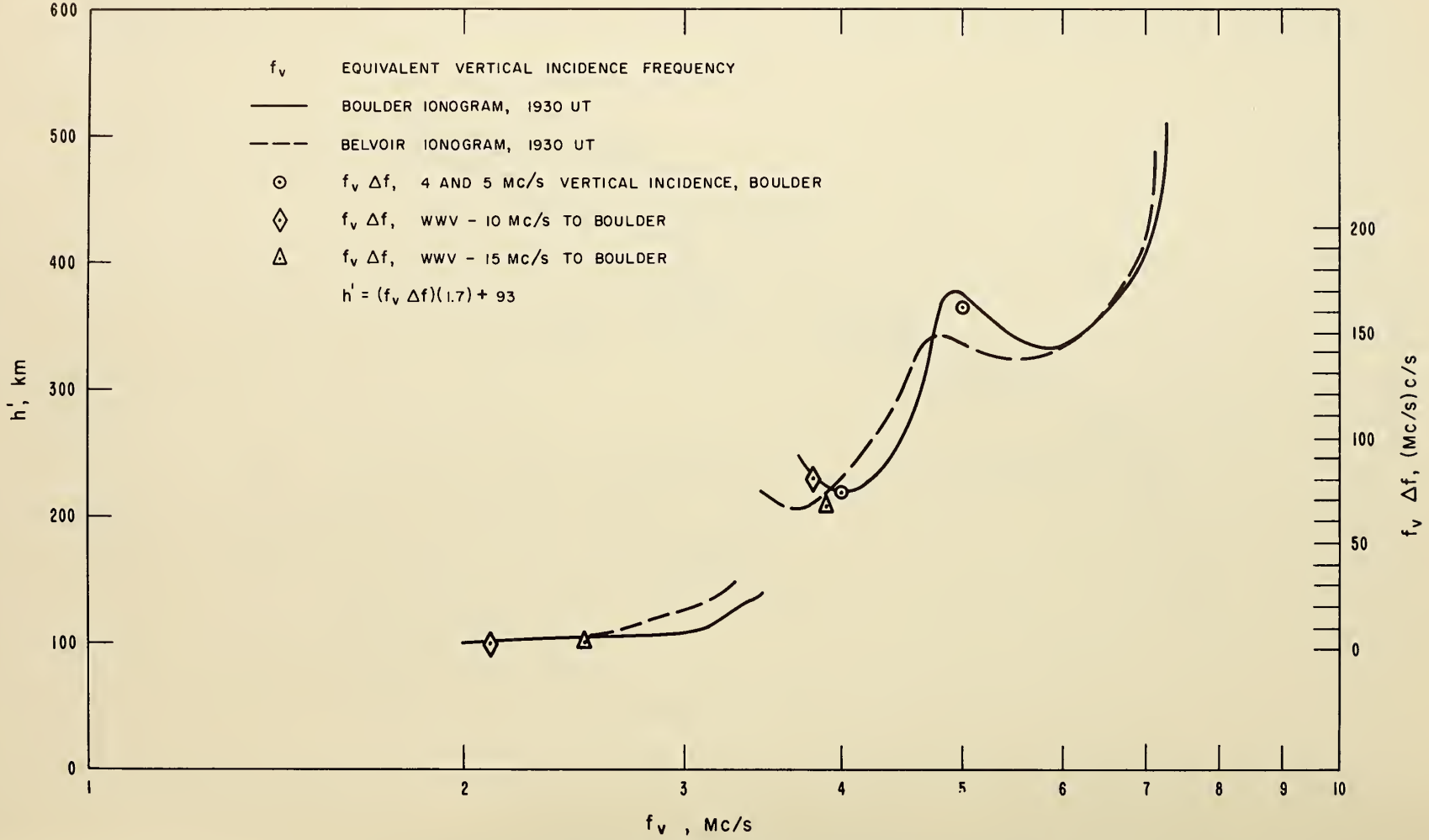

Figure 2.8

Comparison of $f_v \Delta f$ vs f_v with ionogram for SFD
at 1959 UT on April 20, 1962

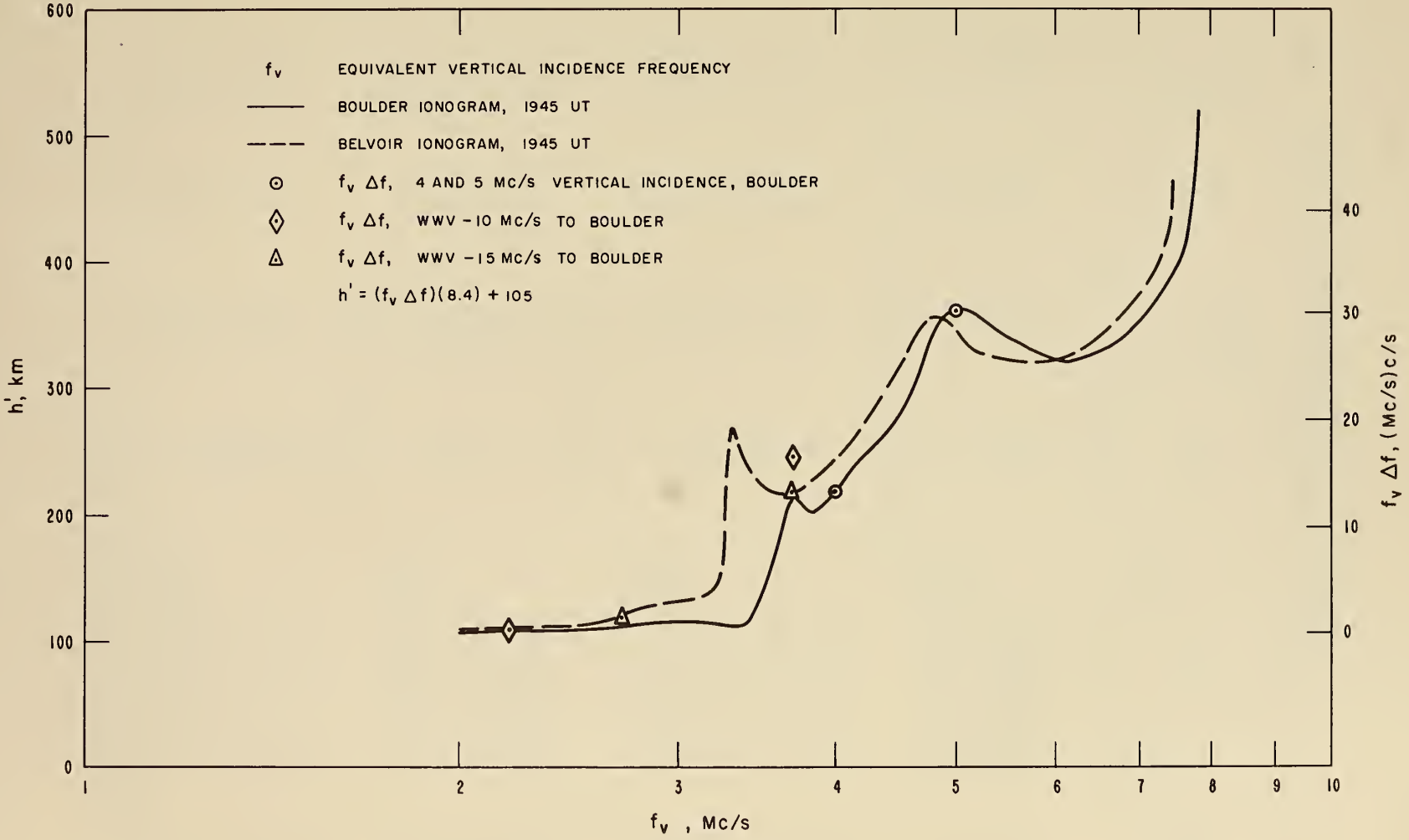

Figure 2.9

Table 2.1

Tabulation of data for flare effects of November 22, 1961, and April 17, 19, and 20, 1962

f Mc/s	Path	Mode	Maximum Observed Δf c/s	f_v Mc/s	$f_v \Delta f$* Mc/s · c/s	$\partial N/\partial t$ cm^{-3} sec^{-1}
			November 22, 1961			
20	WWV-Boulder	F	0.6	5.4	3.2	92
10	WWV-Boulder	F-F	1.6	3.8	3.0	
10	WWV-Shickley	F	0.95	3.0	2.8	
5	Vert inc Boulder	F	0.7	5.0	3.5	
4	Vert inc Boulder	F	0.8	4.0	3.2	
			April 17, 1962			
15	WWV-Boulder	E	0.0	2.6	0.0	120
		F	1.0	4.3	4.3	
10	WWV-Boulder	E	0.0	1.8	0.0	
		F-F	1.9	4.7	4.5	
10	WWV-Shickley	E	0.0	1.9	0.0	
		F	1.0	3.1	3.1	
5	Vert inc Boulder	F	1.1	5.0	5.5	
4	Vert inc Boulder	F	1.1	4.0	4.4	
			April 19, 1962			
15	WWV-Boulder	E	2.0	2.5	5.0	2200
		F	18.0	3.9	70.2	
10	WWV-Boulder	E	2.0	2.1	4.2	
		F-F	43.0	3.8	81.7	
5	Vert inc Boulder	F	32.0	5.0	160.0	
4	Vert inc Boulder	F	19.0	4.0	76.0	
			April 20, 1962			
15	WWV-Boulder	E-E	1.2	2.7	1.6	450
		F	3.8	3.7	14.0	
10	WWV-Boulder	E-E	0.7	2.2	0.8	
		F-F	9.0	3.7	16.7	
5	Vert inc Boulder	F	6.0	5.0	30.0	
4	Vert inc Boulder	F	3.4	4.0	13.6	

* Δf corrected for number of hops

this case) at vertical incidence, then (2.32) predicts that

$$\Delta f_5 = \frac{4}{5} \frac{h'_5 - h_o}{h'_4 - h_o} \Delta f_4 \qquad (2.33)$$

where Δf_4, Δf_5, h'_4, and h'_5 are the frequency deviations and virtual heights of reflection for 4 and 5 Mc/s. The agreement of the data with (2.33) is shown in figure 2.10b. In each case h_o was taken to be the bottom of the E layer. Figure 2.10a shows Δf_4 versus Δf_5.

The preceding analyses show that a $\partial N/\partial t$ which is zero below the E layer and constant in the E and F regions will explain the maximum Doppler shifts measured during several solar flares.

Relationship between maximum frequency deviations observed on 4 and 5 Mc/s at vertical incidence, Boulder, Colorado

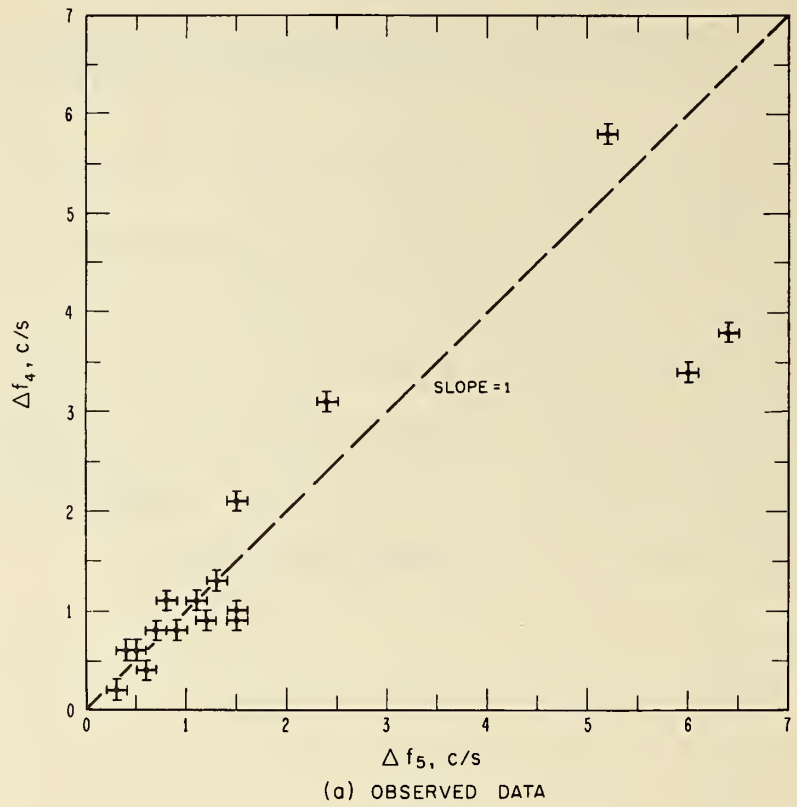

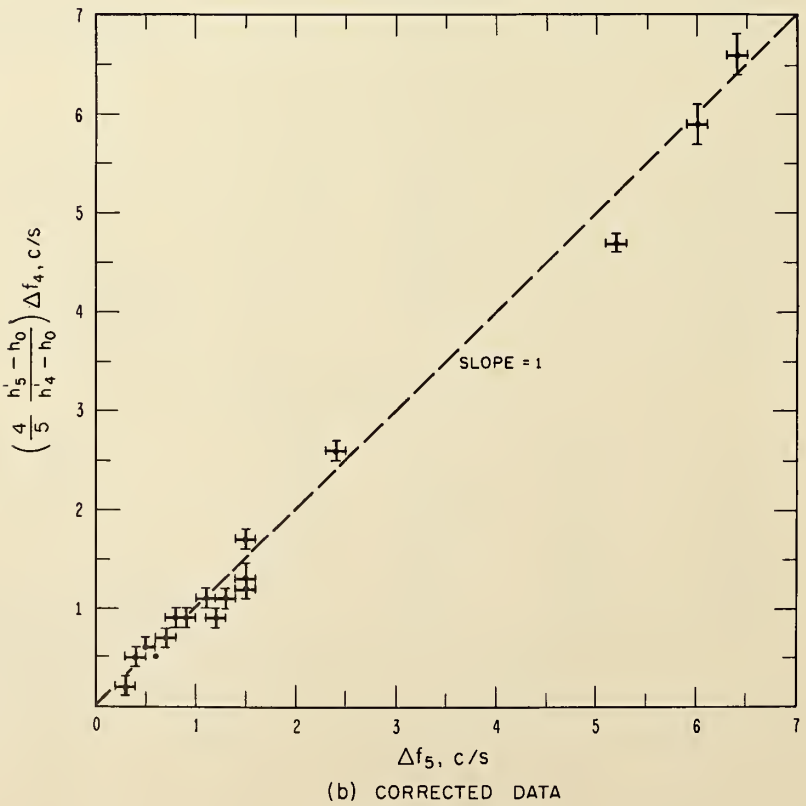

Figure 2.10

3. Solar Flare Observations with the Doppler Technique

The following discussion of flare effects deals with the sudden frequency deviations observed between October 1, 1960 and December 31, 1962 on the following frequencies and propagation paths: (1) WWV-10, -15 and -20 Mc/s, Beltsville, Maryland to Boulder, Colorado; (2) WWV-10 Mc/s, Beltsville, Maryland to Shickley, Nebraska; (3) 4.000 and 5.054 Mc/s, Sunset, Colorado to Boulder, Colorado. Table 1.1 gives the periods during which these paths and frequencies were in use.

The analysis in this section has been restricted to those sudden frequency deviations which could be correlated with solar flares reported in the CRPL-F Series, Part B, Solar-Geophysical Data. A list of all sudden frequency deviations observed between October 1, 1960 and December 31, 1962, whether they could be correlated with a known solar flare or not, is given in Appendix IV.

The shape, duration, and magnitude of sudden frequency deviations vary considerably from flare to flare. However, the general characteristics of an SFD, as illustrated in figure 4.1, are a rapid positive frequency deviation followed by a smaller negative frequency shift and a gradual recovery to the pre-flare conditions. The negative frequency deviation is sometimes absent. The maximum frequency deviation varies from a few tenths of a cycle per second to tens of cycles per second, and the duration may vary from less than a minute to ten minutes or more. The specific events, to be discussed in Section 4, illustrate the variability of the sudden frequency deviations observed.

3.1. Percentage of Solar Flares Detected by Doppler Technique

The percentages of the reported flares which can be correlated with sudden frequency deviations are given in table 3.1 as a function of flare importance. In computing these percentages, and all the percentages to follow in this section, care was taken to exclude any reported flares which occurred during periods of unusable records for the WWV to Boulder path. Also, only flares reported during conditions of ground sunlight at the midpoint of the WWV to Boulder path were included.

Table 3.1

Percentage of flares reported from October 1, 1960, to December 31, 1962, which were accompanied by SFD's

Flare H_α Importance	Number of Flares Reported	Percentage with SFD
1-	2994	10
1	648	21
2	55	49
3	10	80
1,2,3	713	24
All	3707	13

Although no simple relationship exists between the optical (H_α) importance of a flare and its associated effect on the ionosphere, it can be stated that the greater the optical importance of a flare the greater the probability that it will cause a sudden frequency deviation.

These percentages which have been calculated as a function of flare

importance are naturally dependent upon the importance assigned to each flare. Unfortunately there is often disagreement among various observatories as to the importance of a given flare. Consequently, in many cases the flare importance used is somewhat arbitrary. In the present analysis, whenever the importance of a flare could not be assigned by a consideration of the most frequently reported importance and/or the reported observing conditions at each observatory, preference has usually been given to the smaller reported importance.

The percentages of the flares which were accompanied by sudden frequency deviations, for each month from October 1960 through December 1962, are shown in figure 3.1a. The number at the bottom of each column gives the number of flares upon which the percentage is based. The variations in the mean solar flux at 2800 Mc/s and the mean Zurich sunspot number for the same period are shown in figures 3.1b and 3.1c respectively. The percentage of flares detected shows neither a systematic seasonal dependence nor any well-defined variation with the mean level of solar activity. The lack of a systematic seasonal variation in the percentage of the flares detected is shown more clearly by figure 3.2 in which all data for a given month are combined.

Figure 3.3 shows the percentage of the flares accompanied by sudden frequency deviations as a function of the time of day at the midpoint of the WWV to Boulder path. A diurnal variation is evident in 3.3a, 3.3c, and 3.3d. The lack of diurnal variation in the data for flares of optical importances 2 and 3 can be attributed to the small number of such flares during the period. Again the number at the bottom of each column

VARIATIONS OF THE PERCENTAGE OF REPORTED SOLAR FLARES DETECTED, MEAN SOLAR FLUX AT 2800 Mc/s, AND MEAN ZURICH SUNSPOT NUMBER DURING THE PERIOD OCTOBER 1, 1960 THROUGH DECEMBER 31, 1962

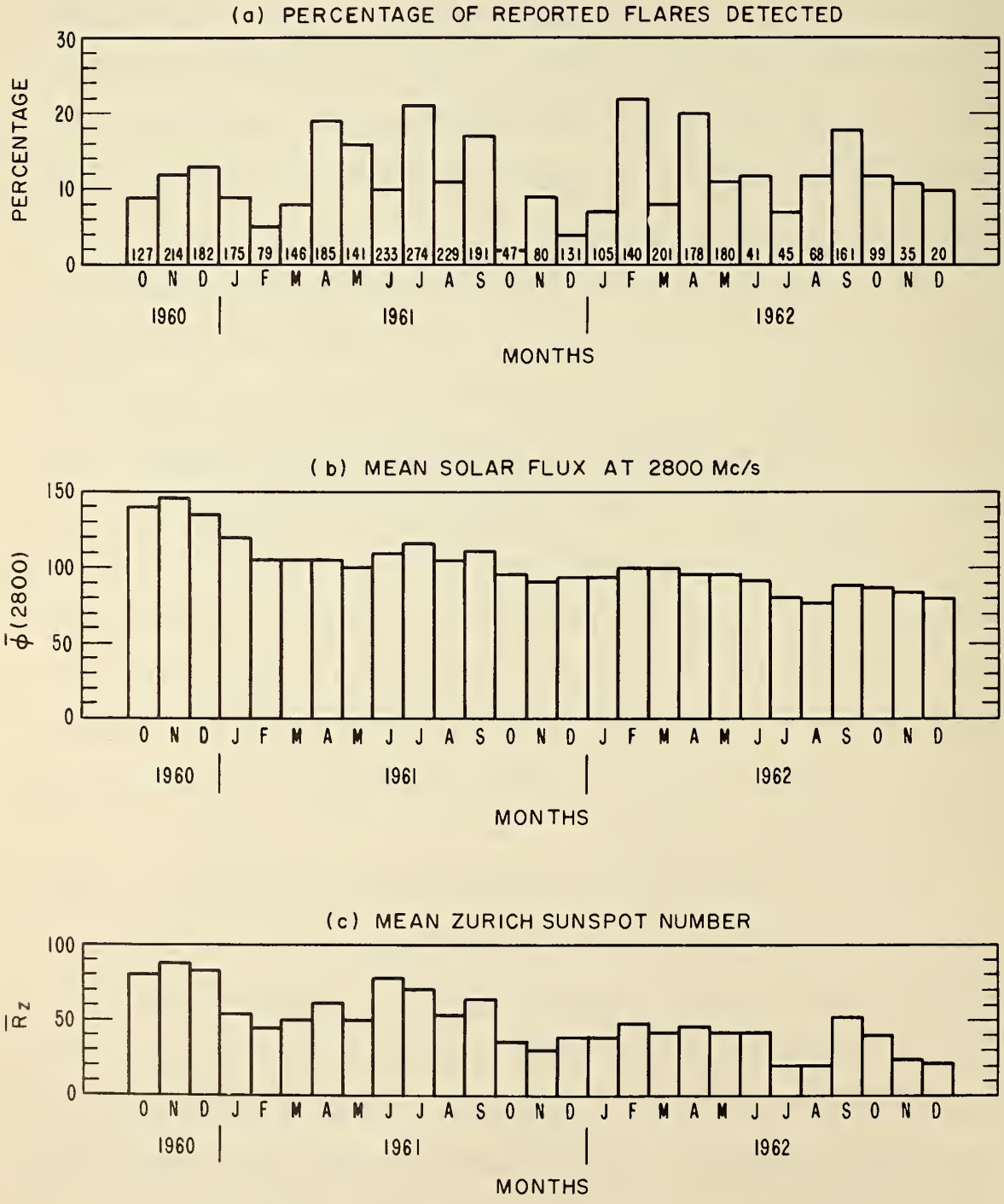
(a) PERCENTAGE OF REPORTED FLARES DETECTED
PERCENTAGE
30
20
10
0
127 214 182 175 79 146 185 141 233 274 229 191 47 80 131 105 140 201 178 180 41 45 68 161 99 35 20
O N D J F M A M J J A S O N D J F M A M J J A S O N D
1960
1961
1962
MONTHS
(b) MEAN SOLAR FLUX AT 2800 Mc/s
$\bar{\phi}$(2800)
150
100
50
0
O N D J F M A M J J A S O N D J F M A M J J A S O N D
1960
1961
1962
MONTHS
(c) MEAN ZURICH SUNSPOT NUMBER
$\bar{R}_Z$
100
50
0
O N D J F M A M J J A S O N D J F M A M J J A S O N D
1960
1961
1962
MONTHS

Figure 3.1

PERCENTAGE OF REPORTED SOLAR FLARES DETECTED BY THE DOPPLER TECHNIQUE AS A FUNCTION OF MONTH
OCTOBER 1, 1960 THROUGH DECEMBER 31, 1962

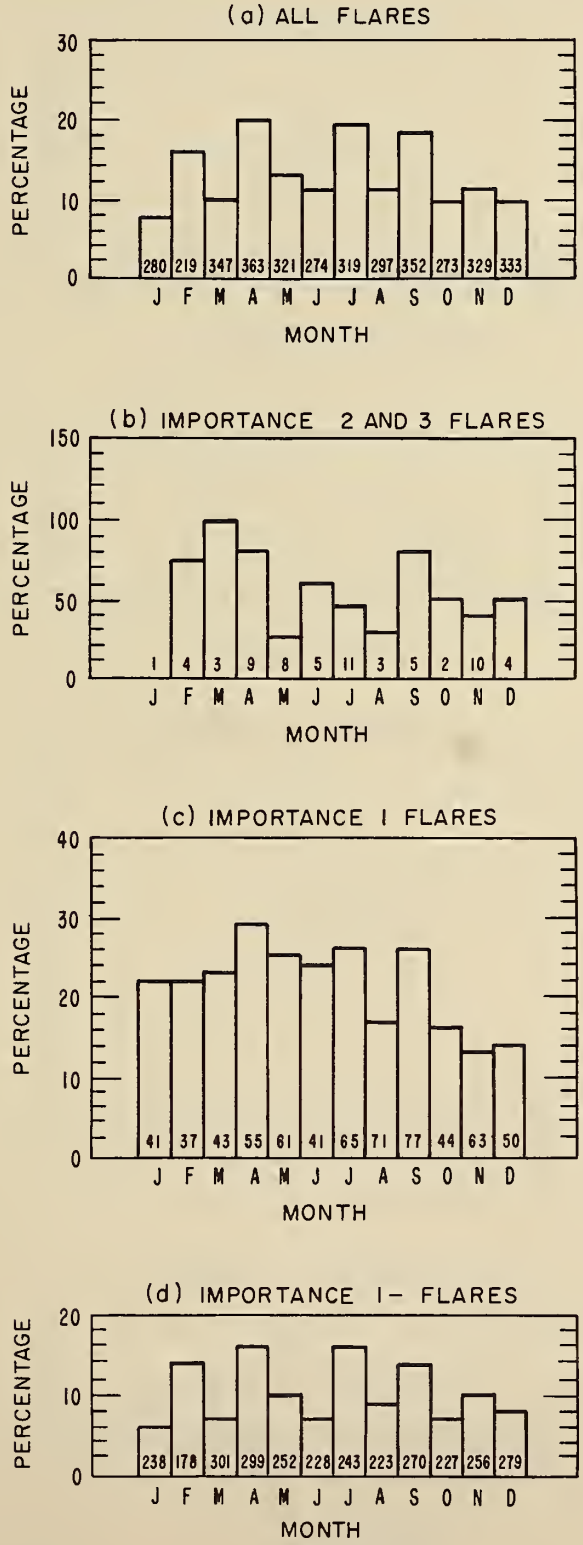

Figure 3.2

PERCENTAGE OF REPORTED SOLAR FLARES
DETECTED BY THE DOPPLER TECHNIQUE AS A
FUNCTION OF TIME OF DAY
OCTOBER 1, 1960 THROUGH DECEMBER 31, 1962

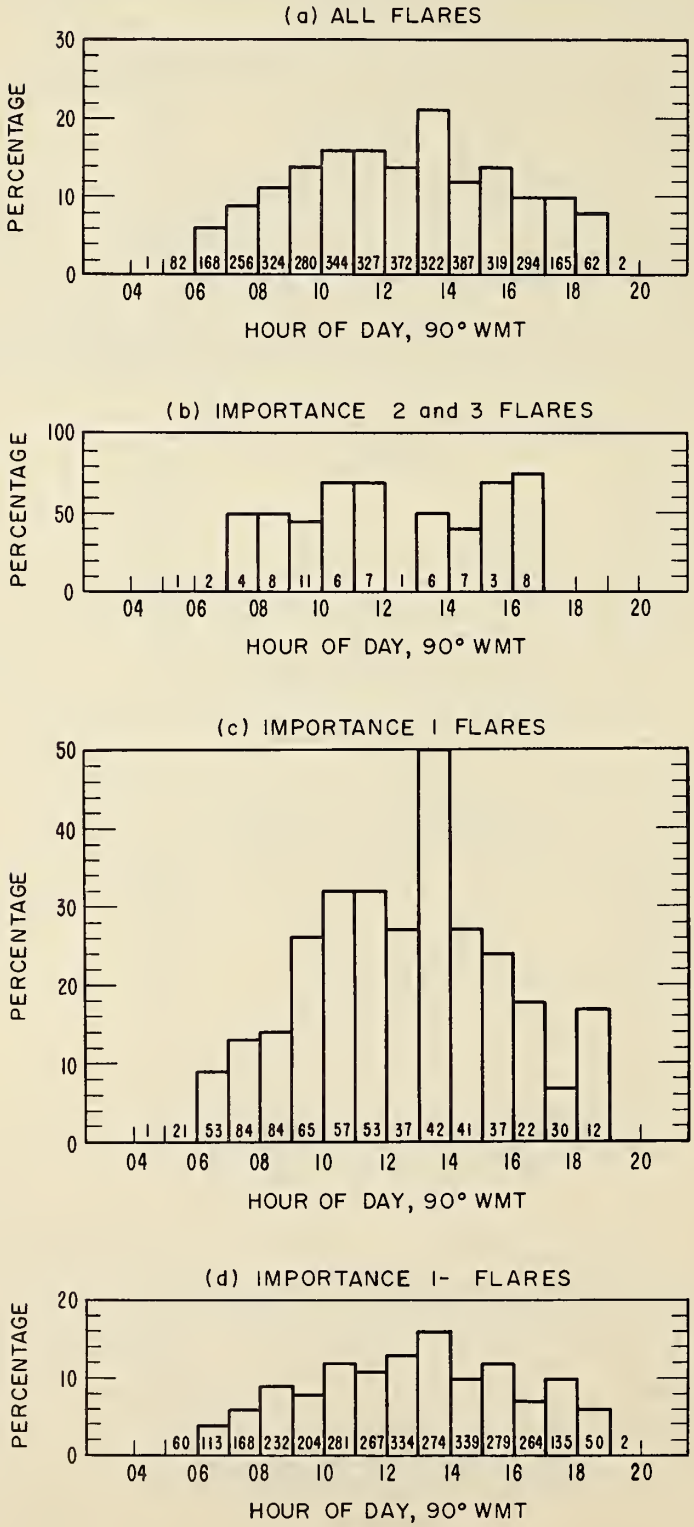

Figure 3.3

gives the number of flares on which the percentage is based.

The solar-zenith-angle dependence of the percentage of flares detected is shown explicitly in figure 3.4. In this figure the percentage of flares detected is shown as a function of the solar zenith angle at the midpoint of the WWV to Boulder path. In figures 3.4a and 3.4d there is a peak for zenith angles of 30 to 40 degrees. The decrease in the percentage detected as the zenith angle increases is to be expected; however, the decrease for zenith angles less than 30 degrees is surprising and may be due to sampling errors.

In summary, the data presented in this section indicate that the percentage of solar flares which are accompanied by sudden frequency deviations tends to increase with increasing optical importance, shows no pronounced seasonal variation, but does exhibit a marked diurnal and solar zenith angle variation with a maximum near local noon. A final conclusion regarding the apparent lack of correlation between the percentage of flares detected and the general level of solar activity will require observation over a greater portion of the solar activity cycle.

3.2. Duration, Rise Time, and Delay Time of Sudden Frequency Deviations

The general time characteristics of sudden frequency deviations are presented in this section. The number of sudden frequency deviations with a given duration is shown in figure 3.5. The duration has been taken to be the time elapsed between the beginning of the positive frequency deviation and the return to the preflare conditions. Often the duration defined in this way cannot be measured precisely due to the

PERCENTAGE OF REPORTED SOLAR FLARES DETECTED BY THE DOPPLER TECHNIQUE AS A FUNCTION OF SOLAR ZENITH ANGLE AT MIDPOINT OF WWV TO BOULDER PATH, OCTOBER 1, 1960 THROUGH DECEMBER 31, 1962

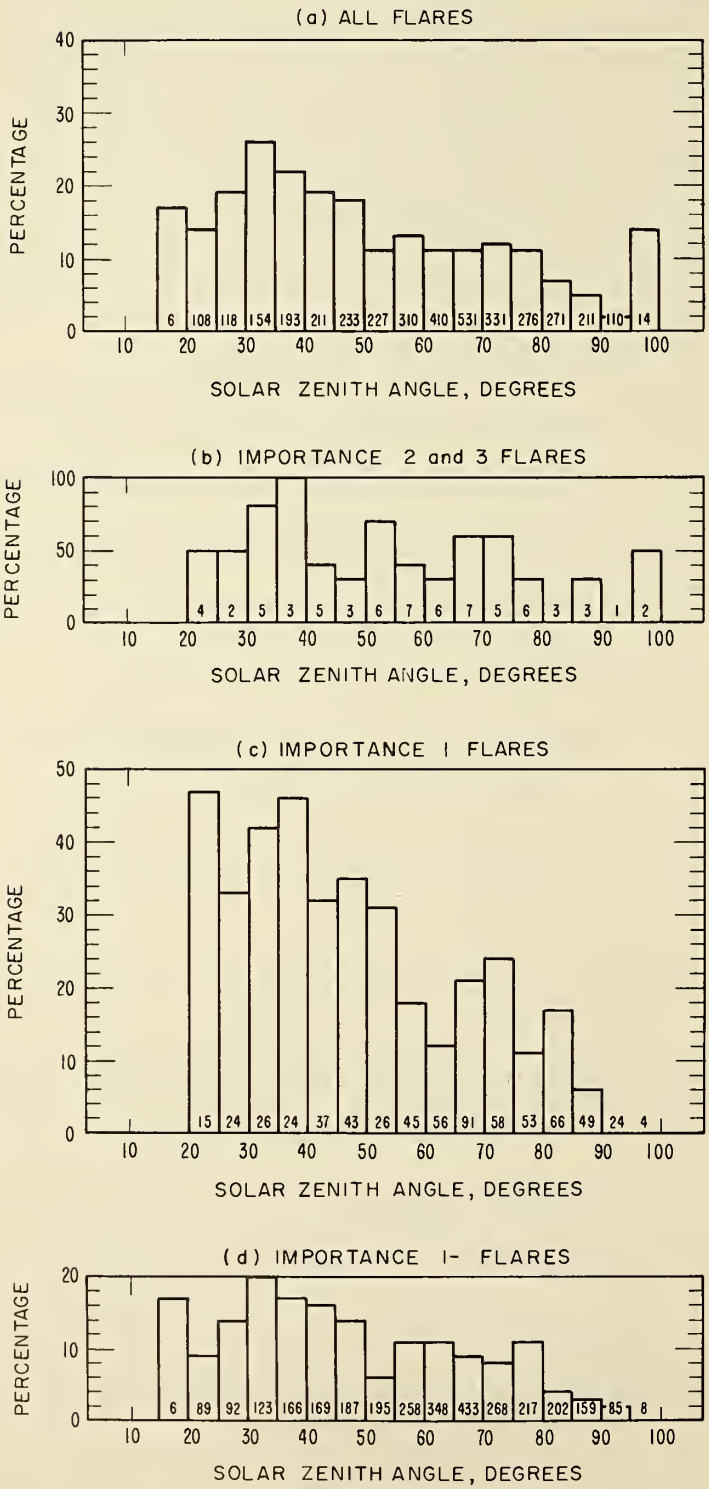

Figure 3.4

DURATIONS OF SUDDEN FREQUENCY DEVIATIONS
OBSERVED FROM
OCTOBER 1, 1960 TO DECEMBER 31, 1962
DURATION = $t_{end} - t_{beg}$

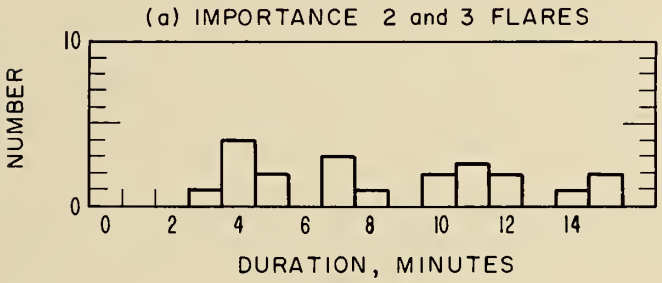

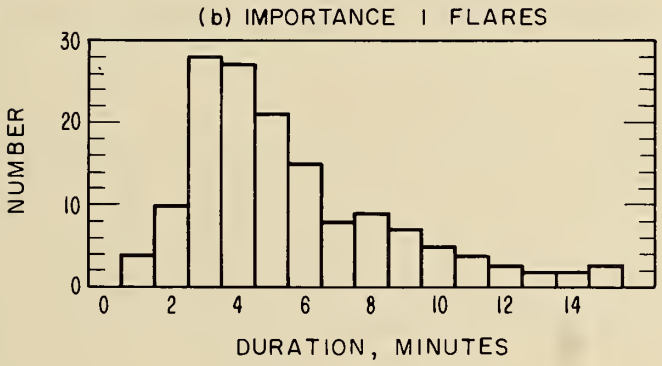

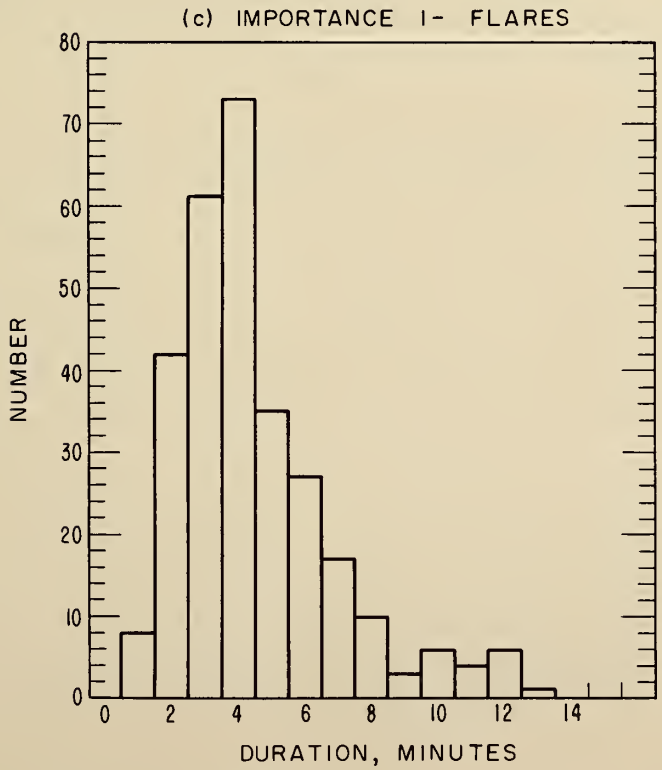

Figure 3.5

difficulty in determining the exact time at which the flare-related frequency deviation ends; however, figure 3.5 does serve to give a general idea of the durations of the flare effects observed by the Doppler technique. The observed durations range from one minute to more than fifteen minutes with the most common durations being from two to five minutes.

Figure 3.6 shows that the most common "rise time", the time from the beginning of the sudden frequency deviation to the maximum positive deviation, is one or two minutes. Very few sudden frequency deviations have rise times greater than three minutes.

The time relationship between the maximum positive frequency deviations of sudden frequency deviations and the maximum phase of the corresponding solar flares is shown in figure 3.7. The maxima of most sudden frequency deviations occur one to four minutes before the flare maxima. In very few cases does the maximum frequency deviation occur after the maximum of the solar flare.

3.3. Path Length Dependence of Frequency Deviations

Figure 3.8 shows the solar flare induced frequency deviations of WWV-10 Mc/s received at Shickley, Nebraska (1780 km), plotted against those of WWV-10 Mc/s received at Boulder, Colorado (2400 km). The slope of the broken line is given by the ratio of the ground path lengths. This figure indicates that the frequency deviations for a fixed frequency vary directly with the path length for paths in the neighborhood of 2000 km. Kanellakos, Chan, and Villard [1962] have found that the flare induced frequency deviations on 15 and 18 Mc/s vary approximately directly

RISE TIMES OF SUDDEN FREQUENCY DEVIATIONS
OBSERVED FROM OCTOBER 1, 1960
TO DECEMBER 31, 1962

RISE TIME = $t_{max} - t_{beg}$

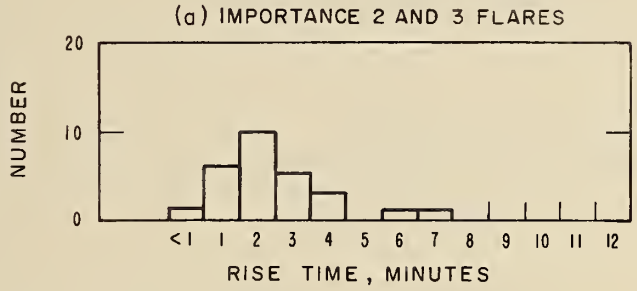

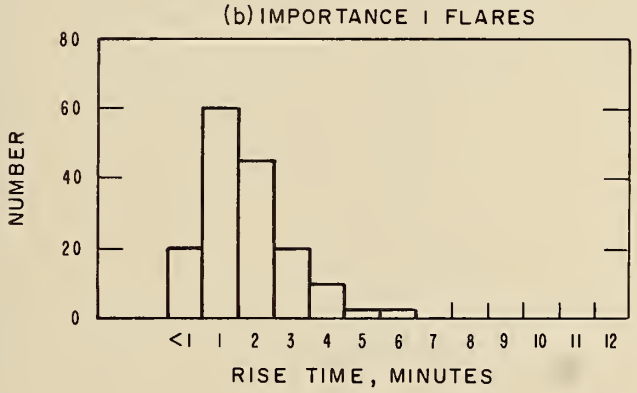

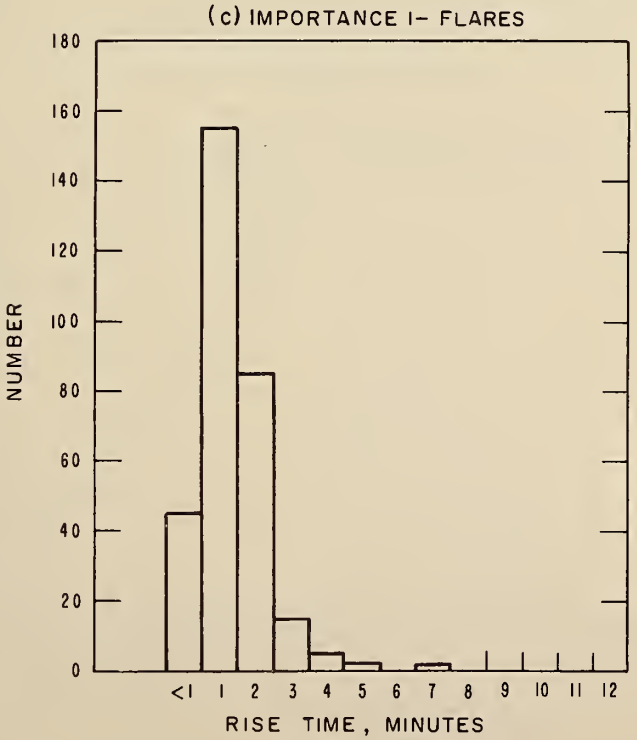

Figure 3.6

TIME DIFFERENCE, ΔT_{max}, BETWEEN MAXIMUM POSITIVE FREQUENCY DEVIATION AND MAXIMUM PHASE OF SOLAR FLARE
OCTOBER 1, 1960 THROUGH DECEMBER 31, 1962
$\Delta T_{max} = t_{max}$ (SFD) $- t_{max}$ (FLARE)

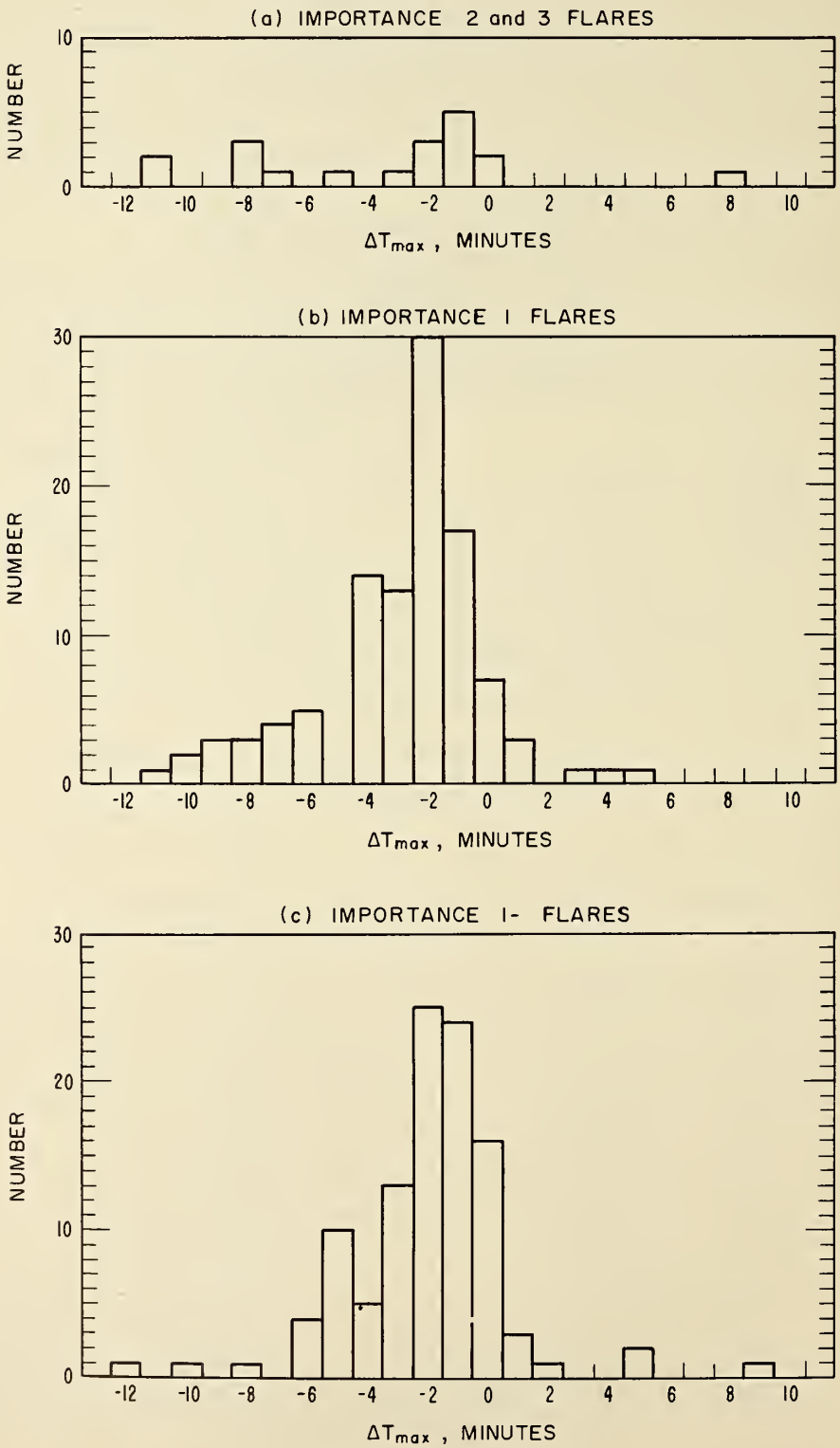

Figure 3.7

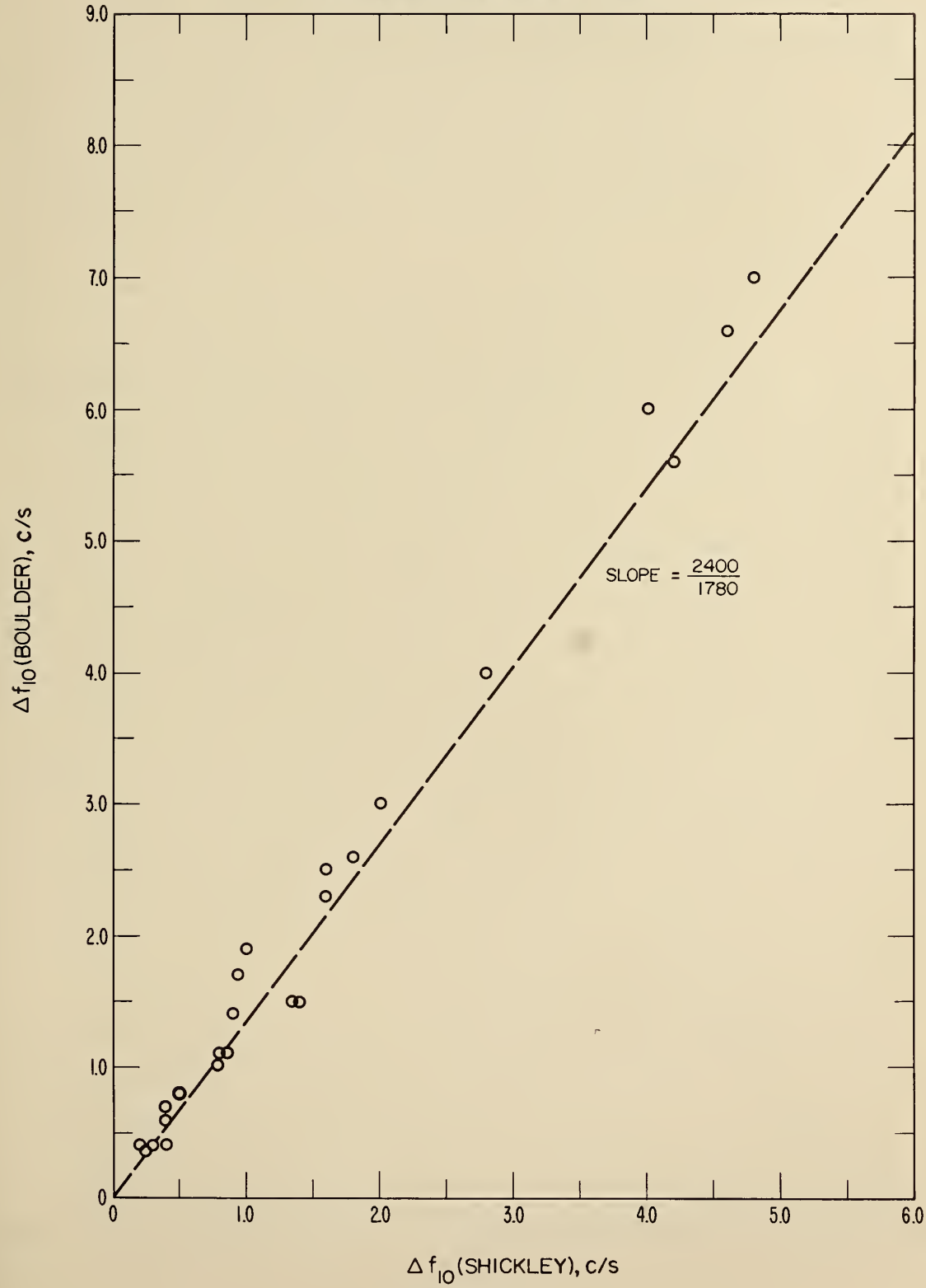
FREQUENCY DEVIATION OF WWV – 10 Mc/s OBSERVED AT SHICKLEY, NEBRASKA (1780 km) VERSUS THAT OBSERVED AT BOULDER, COLORADO (2400 km)
9.0
8.0
7.0
6.0
5.0
4.0
3.0
2.0
1.0
0
1.0
2.0
3.0
4.0
5.0
6.0
SLOPE = 2400/1780
Δ f10 (BOULDER), c/s
Δ f10 (SHICKLEY), c/s

Figure 3.8

with path length for paths of 2450 and 5650 km. Therefore, it appears that for oblique paths, the effect of solar flares on the frequency of ionospherically propagated signals varies directly with the ground path length. It is to be expected that this direct path length dependence will hold only for paths which are of such length that the ratio of the ground path lengths is approximately the same as the ratio of the path lengths in the ionosphere.

3.4. Frequency Dependence of Frequency Deviations

Figure 3.9 shows the maximum positive frequency deviation observed on WWV-20 Mc/s versus that observed on WWV-10 Mc/s, both frequencies being received at Boulder (2400 km); similarly, figure 3.10 shows the relationship between the deviations observed on WWV-15 and WWV-10 Mc/s. In each case the dashed line indicates the behavior expected if the frequency deviation were inversely proportional to the operating frequency. The deviations observed on these oblique paths tend to vary inversely with the operating frequency, although there are some significant departures from an inverse dependence. These two figures show only the observed data. Due to the difficulty in determining the propagation modes for this long path, the data have not been analyzed in terms of equivalent vertical-incidence frequency.

The relationship between the maximum positive frequency deviations observed on 4 and 5 Mc/s at near vertical incidence at Boulder has been shown in figure 2.10. A plot of the observed data, figure 2.10a, shows no systematic frequency dependence. However, as shown by figure 2.10b, the frequency deviations agree well with the behavior predicted by (2.33).

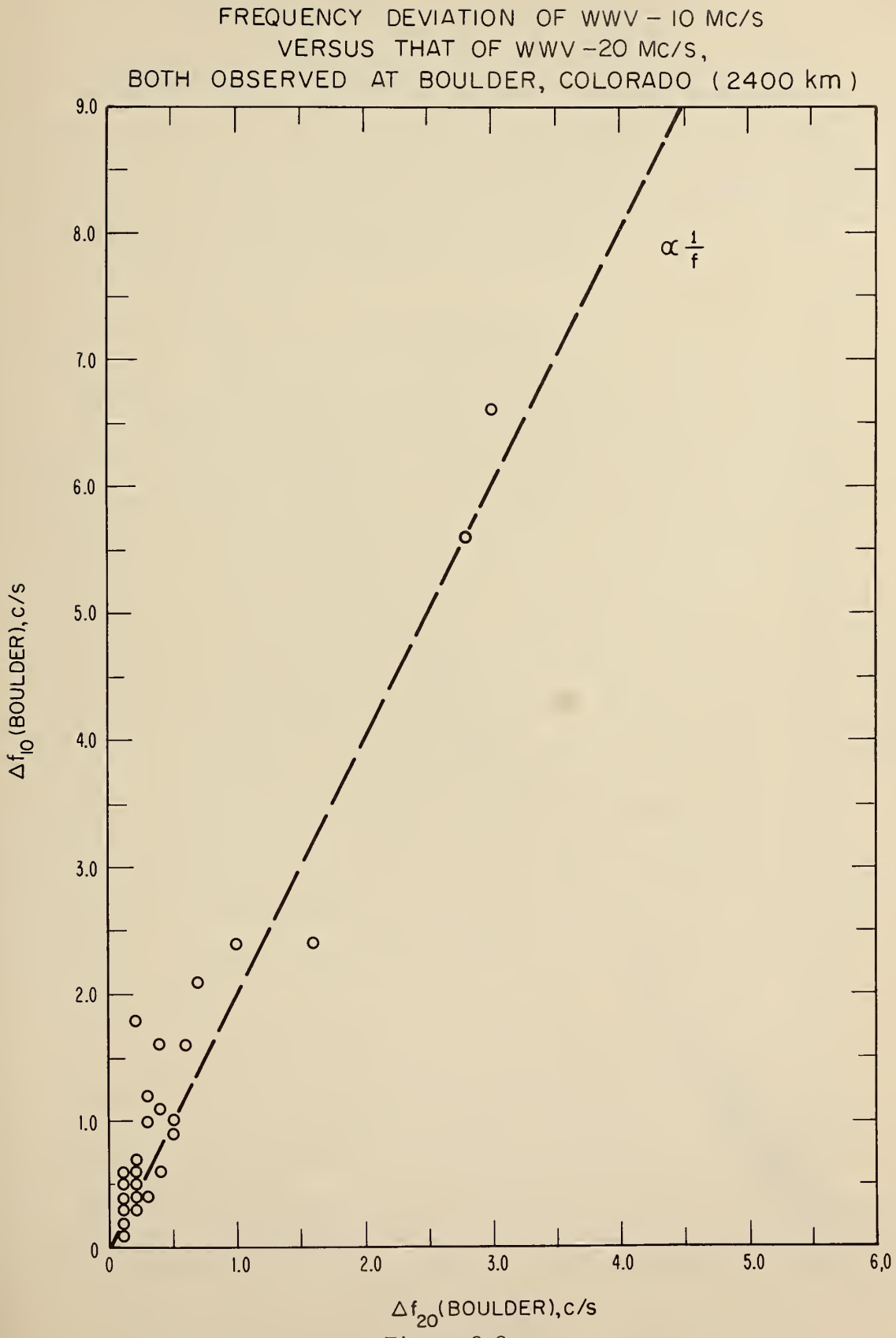
FREQUENCY DEVIATION OF WWV – 10 Mc/s
VERSUS THAT OF WWV –20 Mc/s,
BOTH OBSERVED AT BOULDER, COLORADO (2400 km)
$\alpha \frac{1}{f}$
Δf_{10} (BOULDER), c/s
Δf_{20} (BOULDER), c/s
0
1.0
2.0
3.0
4.0
5.0
6.0
7.0
8.0
9.0

Figure 3.9

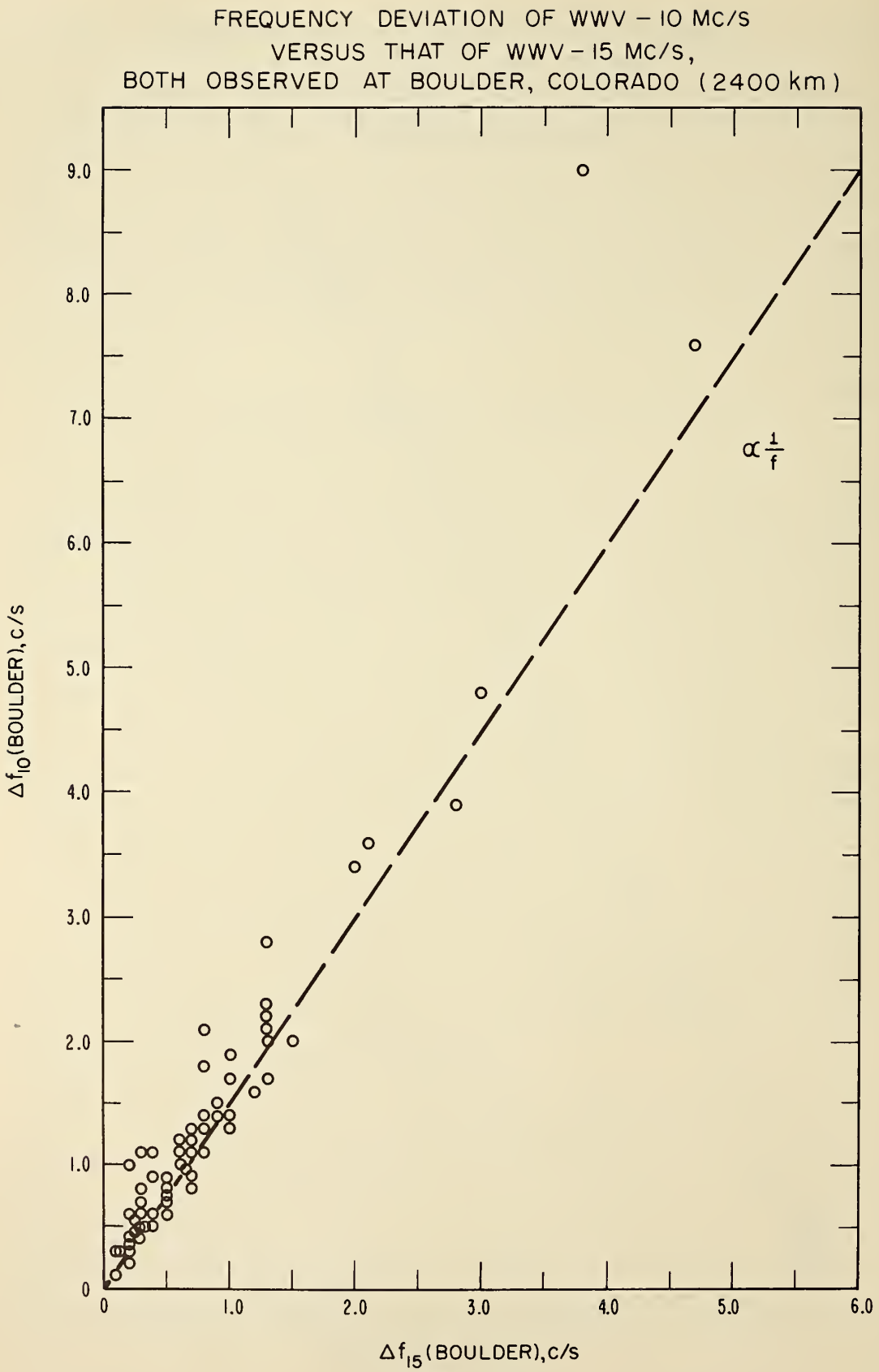
FREQUENCY DEVIATION OF WWV – 10 Mc/s
VERSUS THAT OF WWV – 15 Mc/s,
BOTH OBSERVED AT BOULDER, COLORADO (2400 km)
Δf_{10} (BOULDER), c/s
Δf_{15} (BOULDER), c/s
$\propto \frac{1}{f}$
0
1.0
2.0
3.0
4.0
5.0
6.0
7.0
8.0
9.0

Figure 3.10

4. Selected Events Detected by the Doppler Technique

In this section are included examples of the events detected by the Doppler technique. The types of frequency deviation illustrated include those associated with solar flares, with geomagnetic sudden commencements, and with certain other geomagnetic variations.

4.1. Solar Flares

Frequency deviations accompanying solar flares (SFD's) can be observed only in the sunlit hemisphere. They show great variation in magnitude, shape, and duration, but always begin with an increase in the received frequency. The initial positive phase may or may not be followed by a negative deviation. A typical sudden frequency deviation is of much shorter duration than the optical flare and tends to occur between the beginning and maximum phase of the Hα flare. Those flares which produce significant increases in the electron density in the lower regions of the ionosphere cause increased absorption of the HF signals used in the Doppler technique; however, no change in absorption has been detected during most of the sudden frequency deviations observed. A detailed study must be made on the relationships between SFD's and other flare associated effects.

A "classical" sudden frequency deviation is shown in figure 4.1. This effect was observed during a flare, of optical importance 1, on 4 September 1961. The times of the optical flare were reported as 1424-1435-1512 UT (beginning-maximum-end). The sudden frequency deviation is very simple in this case: a rapid rise to a sharp peak, a negative

Sudden frequency deviation observed during importance 1 flare on
September 4, 1961, WWV-10 Mc/s received at Boulder

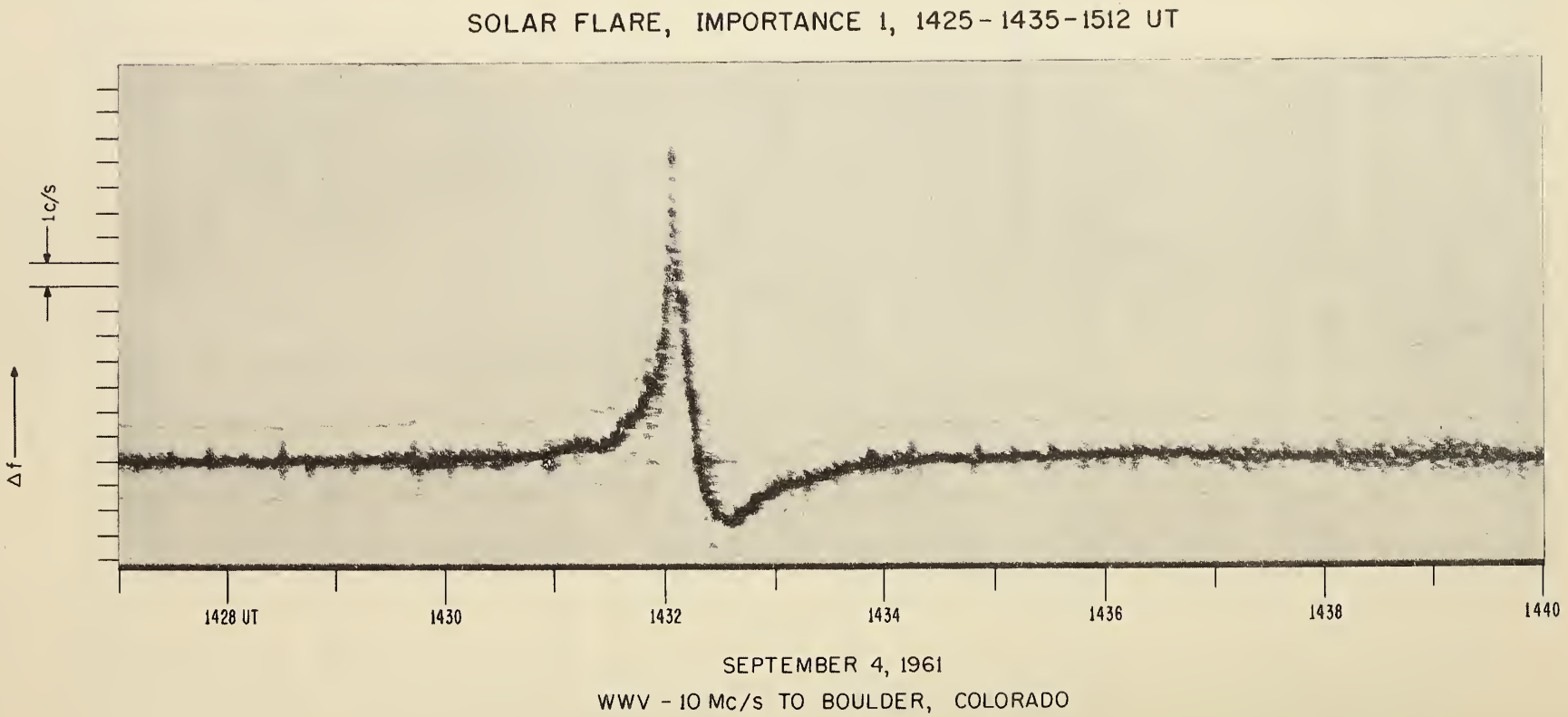

Figure 4.1

deviation, and a recovery to the pre-flare conditions. The entire effect takes place between the beginning and maximum phase of the optical flare. The maximum positive deviation is considerably larger than the negative deviation. Such "classical" sudden frequency deviations are rarely observed.

An unusually complex sudden frequency deviation is shown in figure 4.2. This effect was observed during a flare on 12 November 1960 (1315-1330-1425D, importance 3+) which was accompanied by a sea-level cosmic ray increase. The time variations of this frequency deviation indicate that the x-ray flux causing the ionospheric changes must have undergone rapid and complex variations with time. The duration of this event is greater than is usually observed; nevertheless, the major frequency variations are over before the optical flare reaches its maximum phase. This event has been discussed by Knecht and Davies [1961a, 1961b]; Munro [1961]; Davies, Watts, and Zacharisen [1962]; and Davies [1963].

Figure 4.3 shows a sudden frequency deviation observed on WWV-10 Mc/s and WWV-20 Mc/s received at Boulder on 28 September 1961 (optical flare 2202-2224-2530 UT, importance 3). This event illustrates a feature often observed on oblique-incidence Doppler records; namely, a splitting of the traces due to E- and F-layer propagation. These traces are labeled in figure 4.3a; the F-layer trace shows a large deviation while the E-layer trace shows only a small shift. Moreover, the E-layer trace lacks the oscillations of the F-layer trace. The small frequency shift suffered by the E-layer propagation mode during this event indicates that the major portion of the changes detected by this technique occurred above the height of reflection in the E layer. This event has been discussed

Sudden frequency deviation observed during importance 3+ flare on November 12, 1960, WWV-20 Mc/s received at Boulder

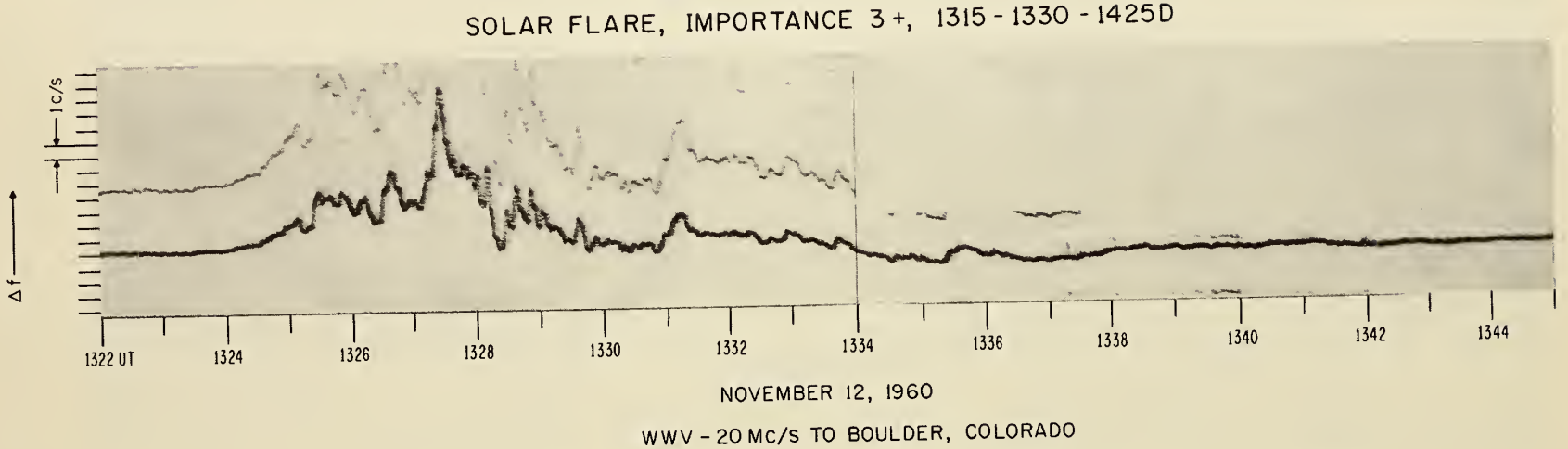

Figure 4.2

Sudden frequency deviation observed during importance 3 flare on September 28, 1961, WWV-10 and WWV-20 Mc/s received at Boulder

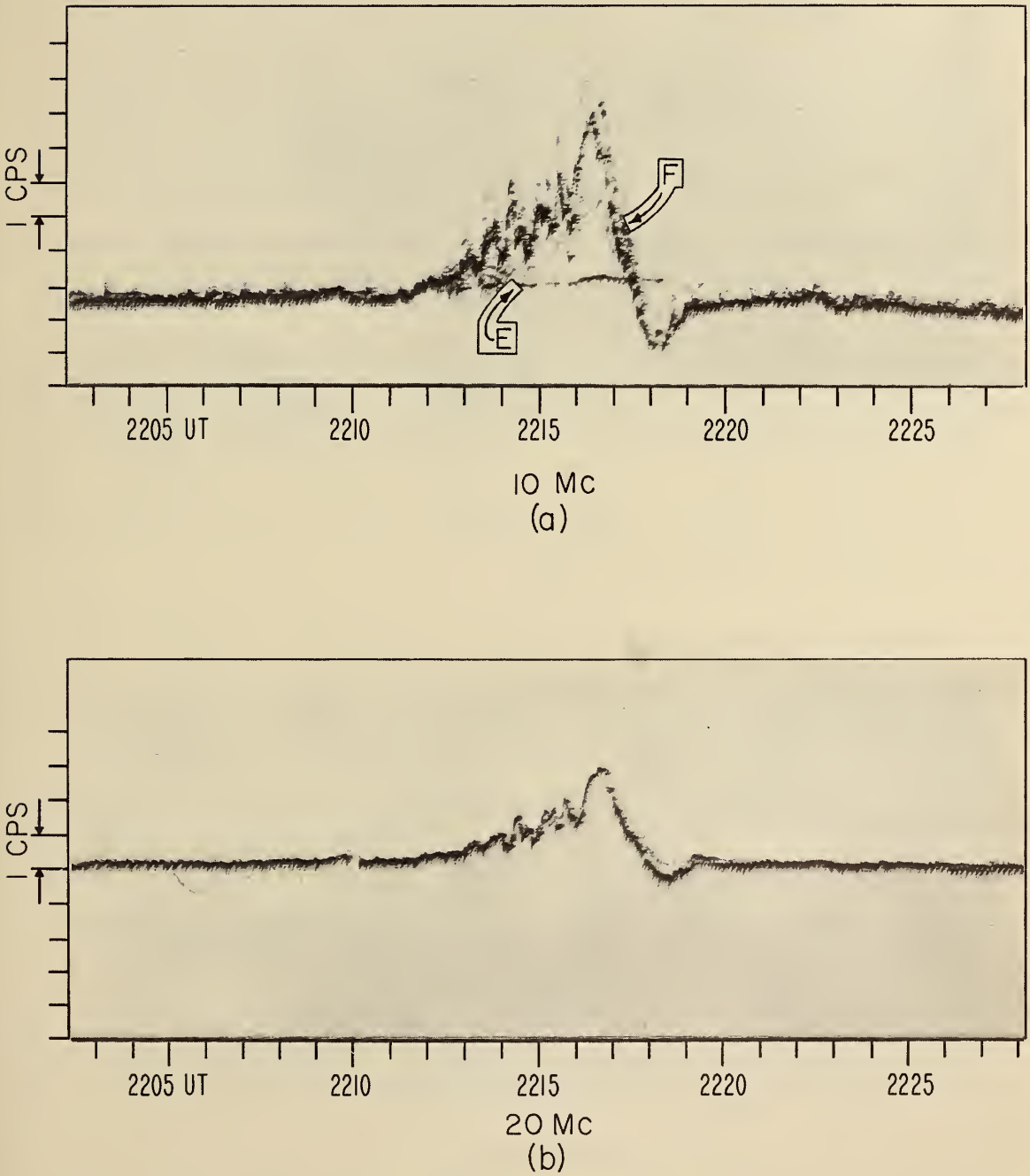

Figure 4.3

by Davies [1962b] and by Kanellakos and Villard [1962].

The largest sudden frequency deviation yet observed at Boulder is shown in figures 4.4 and 4.5. This effect accompanied a flare of optical importance 2 (1935-1937-2031) on 19 April 1962. The maximum frequency deviation on WWV-10 Mc/s received at Boulder (figure 4.4a) exceeded 40 cycles per second. The positive phase of the effect lasted less than a minute; the overall duration of the event was about 3 minutes. Since the Doppler technique detects the rate of change of electron density, the great magnitude of this event indicates only that this flare caused an extremely rapid change in electron density; the change in the total electron content of the ionosphere need not have been very great. The rate of change of electron density caused by this flare has been investigated in section 2.3 of this report.

The size of the deviation observed on WWV-10 Mc/s (figure 4.4a) relative to that on WWV-15 Mc/s (figure 4.4b) is partly due to WWV-10 Mc/s being two-hop propagation to Boulder while one-hop propagation was possible on WWV-15 Mc/s. The equivalent vertical-incidence frequencies for F-layer propagation of WWV-10 and -15 Mc/s to Boulder were approximately the same, and, as shown in section 2.1, the frequency deviation per hop depends upon the equivalent vertical-incidence frequency. The deviations observed at near vertical incidence at Boulder on 4 and 5 Mc/s are shown in figure 4.5. The great difference in the magnitudes of the effects observed on 4 and 5 Mc/s is explained by the fact that 5 Mc/s was very close to the critical frequency of the F1 layer as shown in figure 2.8.

Sudden frequency deviation observed during importance 2 flare on April 19, 1962, WWV-10 and WWV-15 Mc/s received at Boulder

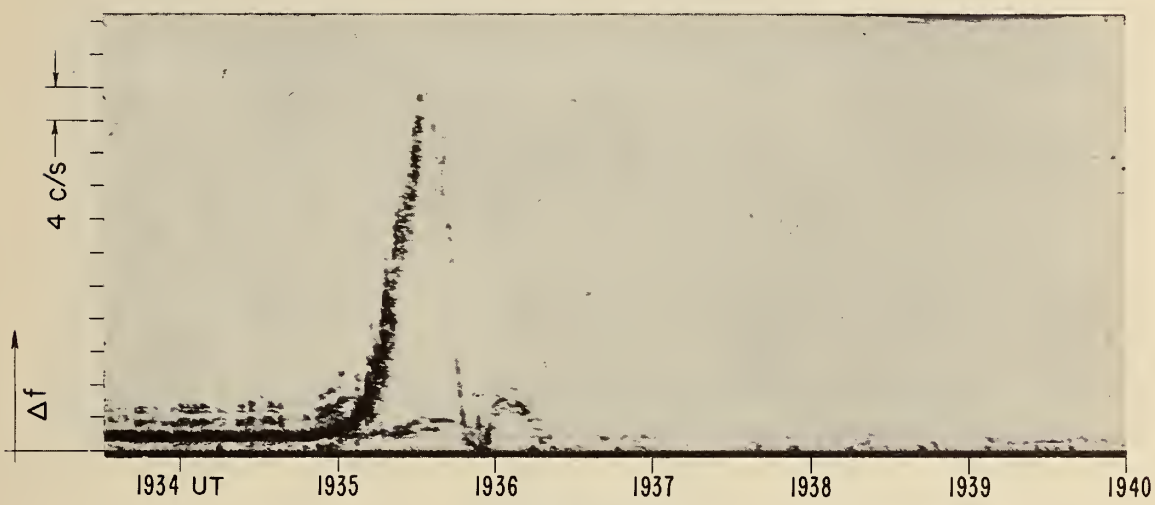

Figure 4.4

Sudden frequency deviation observed during importance 2 flare on April 19, 1962. 4 and 5 Mc/s vertical incidence at Boulder

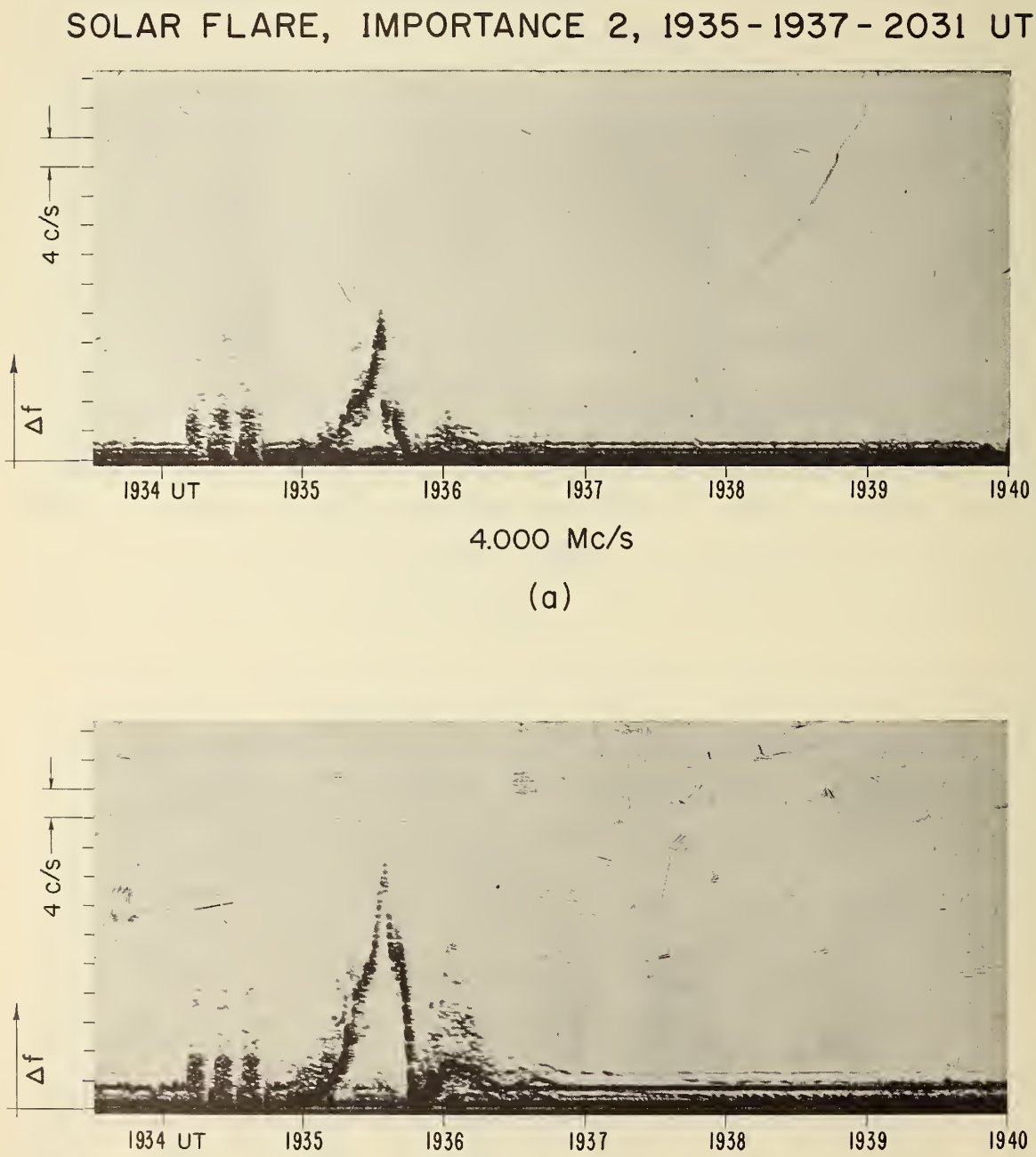

Figure 4.5

Like the event of 28 September 1961 (figure 4.3), the oblique-incidence records of the 19 April 1962 flare (figure 4.4) show both E- and F-layer traces, the E-layer trace being only slightly deviated. The existence of separate traces for different propagation modes is very helpful in analyzing these events.

4.2. Geomagnetic Variations

The frequency variations observed during geomagnetic sudden commencements are often very similar to solar flare effects. However, with a little experience, it is usually not difficult to separate the two phenomena. Like solar flare effects, sudden commencement effects show great variation from one event to another. Unlike flare effects, sudden commencement effects can be observed during the night as well as the day.

A lack of data has delayed a statistical study of sudden commencement effects. However, a preliminary investigation indicates that about 47 percent of the sudden commencements reported in the Journal of Geophysical Research (J. Virginia Lincoln, "Geomagnetic and Solar Data") have been accompanied by frequency deviations.

Sudden commencement effects detected by the Doppler technique have been previously discussed by Davies [1962b]; Kanellakos and Villard [1962]; and Chan, Kanellakos, and Villard [1962].

Two examples of frequency deviations related to sudden commencements are shown in figures 4.6 and 4.7. The event of 30 September 1961 (figure 4.6) is characterized by an initial small negative deviation, a

Sudden commencement observed by the Doppler technique at 2108 UT on September 30, 1961. WWV-10 and WWV-20 Mc/s received at Boulder

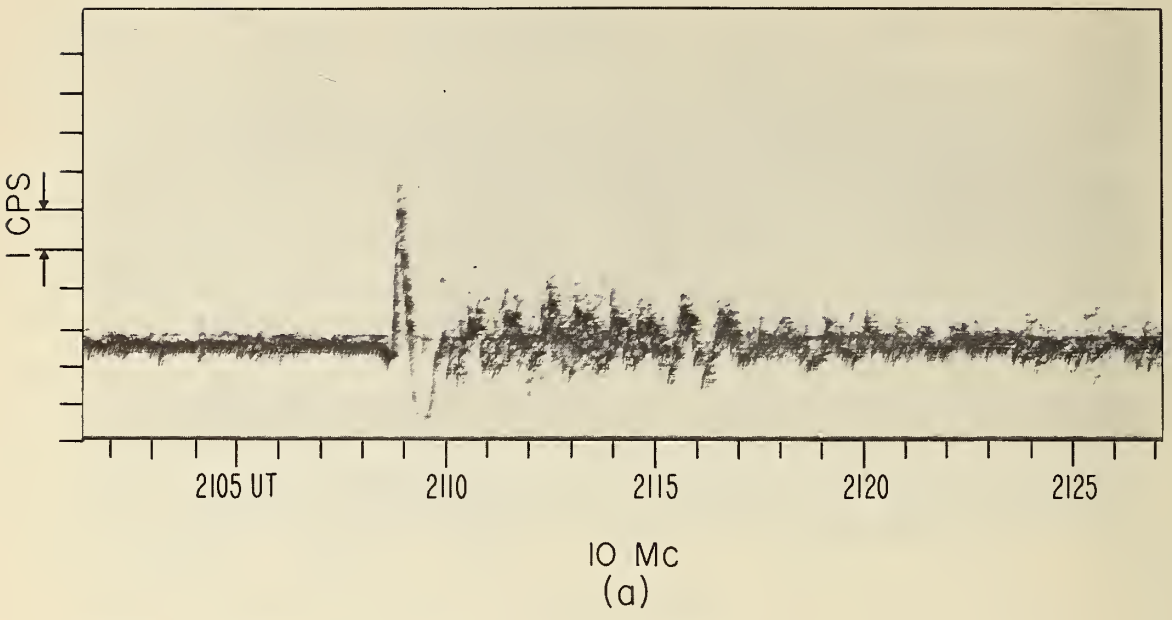

10 Mc
(a)

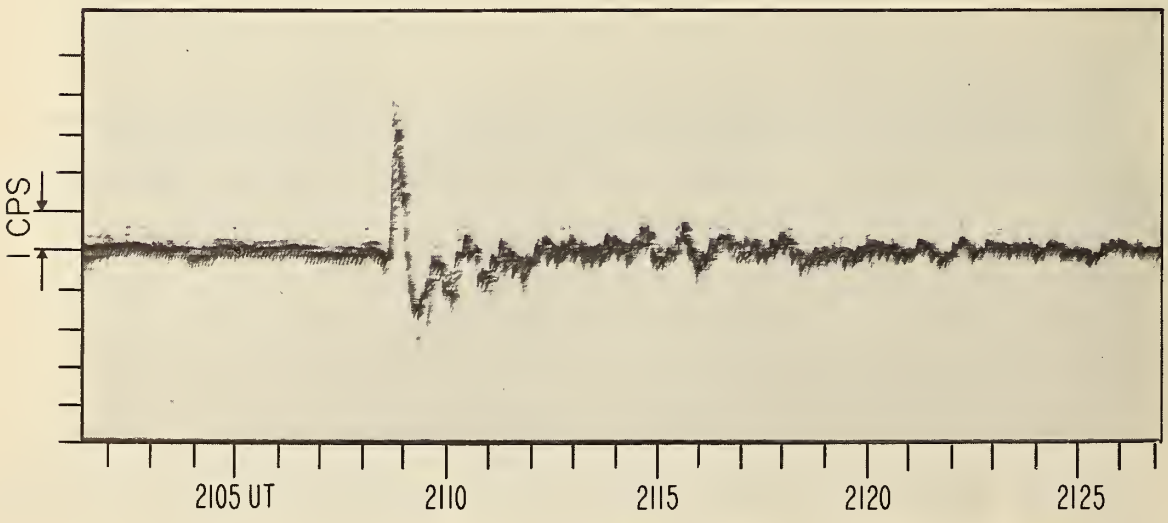

20 Mc
(b)

SEPTEMBER 30, 1961
WWV

Figure 4.6

Sudden commencement observed by the Doppler technique at 0219 UT on February 22, 1962. WWV-10 Mc/s received at Shickley, Nebraska, and WWV-10 and WWV-15 Mc/s received at Boulder, Colorado

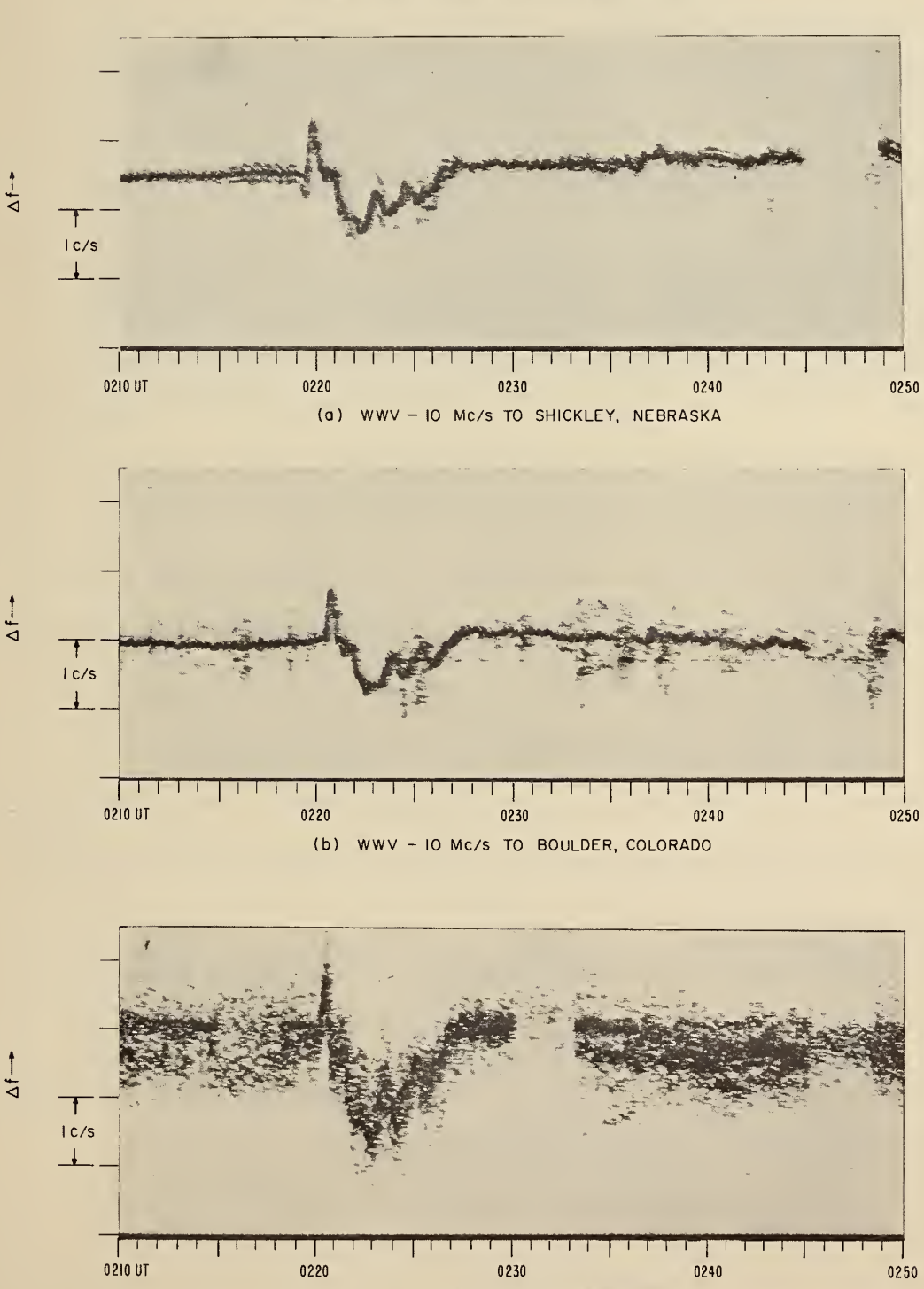

Figure 4.7

sharp positive spike, and a fifteen minute period of small amplitude oscillations. The sudden commencement at 0220 UT on 22 February 1962 (figure 4.7) was accompanied by a positive deviation of one minute duration followed by a negative frequency shift which lasted about seven minutes. Both of these effects are easily distinguishable from the flare effects shown in figures 4.1 through 4.5: the first by the initial negative shift and the oscillations following the peak and the second by the nature and magnitude of the negative phase relative to the positive phase.

Figure 4.8a shows the Doppler records of WWV-15 and 5.054 Mc/s received at Boulder for a period of about one hour on 26 February 1962 during which three sudden impulses were reported (1533, 1552, and 1611 UT). A tracing of the corresponding portion of the Boulder magnetogram is shown in figure 4.8b. The correlation between the frequency deviations and the variations of the magnetic declination (D trace) is good. The simultaneous frequency variations observed on 5 Mc/s (near vertical incidence) and WWV-15 Mc/s indicate that the disturbances causing these variations occurred simultaneously over a relatively large area. The frequency variations occurring at the times of the reported sudden impulses are very similar to one another.

A brief survey has indicated that approximately 25 percent of the sudden impulses in the geomagnetic field reported in the Journal of Geophysical Research (J. Virginia Lincoln, "Geomagnetic and Solar Data") have been detected by the Doppler technique.

Correlation between frequency variations observed at both oblique and vertical incidence and changes in the magnetic field observed at Boulder

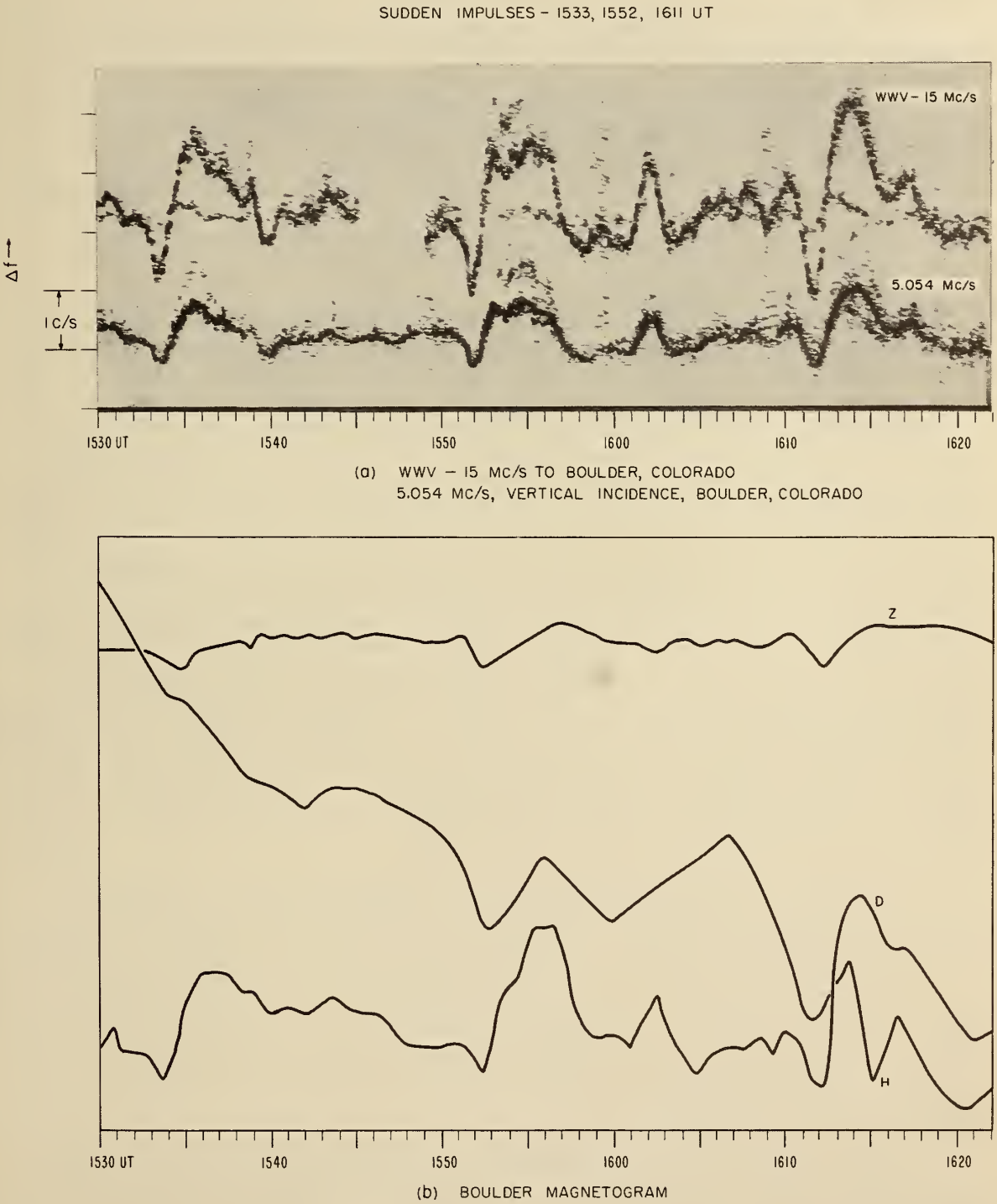

FEBRUARY 26, 1962

Figure 4.8

5. Discussion

This report has presented some results of ionospheric research done at CRPL with the Doppler technique developed by Watts and Davies [1960]. This technique has proven to be a sensitive method of detecting the effects of solar flares in the E and F regions of the ionosphere, and the major portion of this report has been devoted to these flare effects (sudden frequency deviations).

Theoretically, it has been shown that the Doppler shift, observed on a given frequency propagated over a given path, depends only on the equivalent vertical-incidence frequency. An equivalence theorem has been derived which relates the frequency deviation observed on an oblique path to that which would have been observed with vertical propagation at the equivalent vertical-incidence frequency (neglecting the earth's magnetic field, electronic collisions, and curvature of the ionosphere). This equivalence relation will be useful in comparing Doppler data obtained from different paths or from different parts of the world, and it will provide a convenient means of data interchange.

Two theoretical approaches have been undertaken in an attempt to better understand the Doppler observations. The first approach consists of the calculation of the frequency dependence of the Doppler shifts to be expected from changes in the parameters defining various parabolic layer models of the ionosphere.

The second theoretical treatment has suggested a method for determining the height variation of the time rate of change of electron density during an ionospheric disturbance from a knowledge of the Doppler

shift as a function of frequency. The frequency dependence of Δf during a specific disturbance has not yet been sufficiently well determined to warrant applying this method. However, it has been shown that the frequency deviations observed during several solar flares could have been produced by a $\partial N/\partial t$ which was zero below the E region and constant in the E and F regions.

Statistically it has been found that 13 percent of all the optical flares and subflares reported from October 1960 through December 1962 caused sudden frequency deviations. The percentage of flares detected increases with the optical importance of the flare, shows no pronounced seasonal variation, but does exhibit a diurnal variation with a peak near local noon.

Most sudden frequency deviations have durations of from 2 to 4 minutes; this is much shorter than the duration of the typical optical flare. The sudden frequency deviation almost always occurs between the beginning and maximum phase of the optical flare, with the maximum frequency deviation usually occurring 1 to 2 minutes before the maximum phase of the H_α flare.

For long paths, the observed frequency deviations tend to vary directly with the ground path length and inversely with operating frequency. For vertical propagation the observed frequency deviations show no systematic frequency dependence; however, it has been shown that the vertical-incidence data are consistent with the theory which assumes that the time rate of change of ionization during the flare is independent of height.

The CRPL is presently making Doppler measurements over both oblique- and vertical-incidence paths in the United States and oblique paths near the magnetic equator in Africa. In addition, the Battelle Institute of Frankfurt, Germany, supplies oblique-incidence records of MSF (Rugby, England) received at Frankfurt, and workers in England, Hawaii, India, and Japan have shown interest in using the technique. For the immediate future these paths will provide broader coverage for a continuing flare patrol and will be used to study the solar zenith angle and latitude dependences of the ionospheric effects of solar flares.

However, a more sophisticated network of paths is highly desirable if the technique is to be used to best advantage. Although, in principle, the equivalence theorem can be used to assist in the comparison of data obtained from different paths, in practice it becomes difficult to determine the propagation modes for long paths and, hence, it is difficult to apply the equivalence theorem to such paths. On the other hand, vertical propagation emphasizes the local ionospheric variations. Hence it seems that relatively short paths should be the best for study of widespread ionospheric disturbances, such as those caused by solar flares. A worldwide network of such paths is needed in order to conduct a definitive study of the solar zenith angle and latitude dependence of solar flare effects. Such a network would also provide a worldwide monitoring system for flare and geomagnetic disturbance effects. In order to adequately study the height variation of ionospheric disturbances, it will be necessary to use several frequencies over a single path.

So far major attention has been given to the maximum positive frequency deviations induced by solar flares. Some attention should be given to the other characteristics of flare effects (negative phases and recovery rates) to determine whether these can be of assistance in studying the ionospheric response to solar flare radiation. In addition, the effects accompanying geomagnetic disturbances need to be investigated and the mechanism causing them discovered.

Further study should also be made of the relationship between the different ionospheric effects (SWF, SEA, SPA, SFD, etc.) and the various solar phenomena, such as the different types of radio emissions, which accompany visible flares. Such a study would be of assistance in determining the time characteristics and enhancements of the various radiation bands causing the ionospheric disturbances. Another objective of such a study should be to investigate the possibility of predicting the occurrence of solar disturbances which will significantly affect the earth's environment.

The Doppler technique should be capable of detecting any type of rapid ionospheric variation which occurs at heights no greater than the reflection levels for the frequencies used. It should be useful for studying ionospheric effects associated with geomagnetic disturbances as well as those associated with solar flares. In addition, the technique should aid in the study of ionospheric oscillations and the motions of ionospheric irregularities. To be used to best advantage, the Doppler measurements should be made in conjunction with other ionospheric observations (e.g., ionograms, field strength records).

6. Acknowledgments

Partial support for the final stages of preparation of this report was received from the Advanced Research Projects Agency, Nuclear Test Detection Office under Contract No. 183.

7. References

Budden, K. G. (1955), A method for determining the variation of electron density with height from curves of equivalent height against frequency, Proceedings of the Cambridge Conference on Physics of the Ionosphere, Physical Society, 332.

Chan, K. L., D. P. Kanellakos, and O. G. Villard, Jr. (1962), Correlation of short-period fluctuations of the earth's magnetic field and instantaneous frequency measurements, J. Geophys. Res. 67, No. 5, 2066-2072.

Chan, K. L. and O. G. Villard, Jr. (1963), Sudden frequency deviations induced by solar flares, J. Geophys. Res. 68, No. 10, 3197-3224.

Davies, K. (1962a), Doppler studies of the ionosphere with vertical incidence, Proc. IRE 50, No. 1, 94-95.

Davies, K. (1962b), Ionospheric effects associated with the solar flare of September 28, 1961, Nature 193, No. 4817, 763-764.

Davies, K. (1962c), The measurement of ionospheric drifts by means of the Doppler technique, J. Geophys. Res. 67, No. 12, 4909-4913.

Davies, K. (1962d), Correction to "Doppler studies of the ionosphere with vertical incidence," Proc. IRE 50, No. 6, 1544.

Davies, K. (1963), Doppler studies of the ionospheric effects of solar flares, Proceedings of the International Conference on the Ionosphere, London, 1962, Institute of Physics and Physical Society.

Davies, K. (1965), Ionospheric Radio Propagation, NBS Monograph 80, Chapter 4, Section 4.3.1.

Davies, K., J. M. Watts, and D. H. Zacharisen (1962), A study in F2 layer effects as observed with a Doppler technique, J. Geophys. Res. 67, No. 2, 601-609.

Kanellakos, D. P., K. L. Chan, and O. G. Villard, Jr. (1962), On the altitude at which some solar flare induced ionization is released, J. Geophys. Res. 67, No. 5, 1795-1804.

Kanellakos, D. P., and O. G. Villard, Jr. (1962), Ionospheric disturbances associated with the solar flare of September 28, 1961, J. Geophys. Res. 67, No. 6, 2265-2277.

Knecht, R. W., and K. Davies (1961a), Solar flare effects in the F region of the ionosphere, Nature 190, No. 4778, 797-798.

Knecht, R. W., and K. Davies (1961b), Nature 192, No. 4800, 348.

Munro, G. H. (1961), Possible solar flare effects in the F region of the ionosphere, Nature 192, No. 4800, 347.

Smith, N. (1939), The relation of radio sky-wave transmission to ionosphere measurements, Proc. IRE 27, 332-346.

Watts, J. M., and K. Davies (1960), Rapid frequency analysis of fading radio signals, J. Geophys. Res. 65, No. 8, 2295-2301.

Whittaker, F. C., and T. N. Watson (1952), A Course of Modern Analysis, 4th ed., Cambridge University Press, p. 229.

8. Appendix I - The Doppler Shift Written as an Integral

To show:

The Doppler shift is given by

$$\Delta f = - \frac{f}{c} \int_{path} \frac{\partial \mu}{\partial t} \, ds \tag{8.1}$$

for propagation at any angle and by

$$\Delta f = -2 \frac{f}{c} \int_{o}^{h} \frac{\partial \mu}{\partial t} \, dz \tag{8.2}$$

for vertical propagation.

Restrictions:

(1) The ionosphere is assumed concentric.

(2) The effect of the earth's magnetic field is neglected except for vertical propagation.

Proof:

The Doppler shift is given by [Davies, 1962a]

$$\Delta f = - \frac{f}{c} \frac{dP}{dt} \, . \tag{8.3}$$

In order to calculate the Doppler shift, the time derivative of the phase path must be found. Assuming the ionosphere is horizontally uniform, the time derivative of the phase path is given by:

$$\frac{dP}{dt} = \frac{d}{dt} \int_{path} \mu ds \ . \tag{8.4}$$

Substituting $ds = dz/\cos\phi$ in (8.4),

$$\frac{dP}{dt} = \lim_{z \to h} \frac{d}{dt} 2 \int_{o}^{z} \frac{\mu dz}{\cos\phi} \ . \tag{8.5}$$

Performing the indicated differentiation of the integral in (8.5),

$$\frac{dP}{dt} = \lim_{z \to h} 2 \int_{o}^{z} \frac{\partial \mu}{\partial t} \frac{dz}{\cos\phi} + \lim_{z \to h} \left[2 \int_{o}^{z} \frac{\mu \sin\phi \frac{\partial \phi}{\partial t}}{\cos^2\phi} dz + 2 \frac{\mu}{\cos\phi} \Big|_z \frac{dz}{dt} \right] . \tag{8.6}$$

Using $ds = dz/\cos\phi$ to take the limit of the left term and using Snell's law for curved earth $(a + z)\ \mu \sin \phi = a\ \mu_o \sin \phi_o$

$$\frac{dP}{dt} = \int_{path} \frac{\partial \mu}{\partial t} ds + \lim_{z \to h} 2\ \mu_o \sin\phi_o \left[\int_{o}^{z} \frac{a}{a + z} \frac{\frac{\partial \phi}{\partial t} dz}{\cos^2\phi} \right.$$

$$\left. + \frac{a}{(a + z) \sin\phi \cos\phi} \Big|_z \frac{dz}{dt} \right] . \tag{8.7}$$

The term in brackets can be calculated using the criterion that the distance between the transmitter and receiver is constant. Neglecting the effect of the earth's magnetic field,

$$\frac{dD}{dt} = 0 = \lim_{z \to h} \frac{d}{dt} 2a \int_{o}^{z} \frac{\tan\phi}{a + z} dz \ . \tag{8.8}$$

Performing the differentiation indicated in (8.8),

$$0 = \lim_{z \to h} \left[2a \int_0^z \frac{\sec^2\phi}{a+z} \frac{\partial\phi}{\partial t}\, dz + 2a \frac{\tan\phi}{a+z} \Big|_z \frac{dz}{dt} \right] . \qquad (8.9)$$

Subtracting $\mu_o \sin\phi_o$ times (8.9) from (8.7),

$$\frac{dP}{dt} = \int_{path} \frac{\partial\mu}{\partial t}\, ds + \lim_{z \to h} \frac{2a\mu_o \sin\phi_o}{a+z} \left[-\frac{\sin\phi}{\cos\phi} \Big|_z \frac{dz}{dt} + \frac{1}{\sin\phi \cos\phi} \Big|_z \frac{dz}{dt} \right] . \qquad (8.10)$$

The expression in brackets can be manipulated to give

$$\frac{dP}{dt} = \int_{path} \frac{\partial\mu}{\partial t}\, ds + \lim_{z \to h} \frac{2a\mu_o \sin\phi_o}{a+z} \left[\frac{\cos\phi}{\sin\phi} \Big|_z \frac{dz}{dt} \right] . \qquad (8.11)$$

Again using Snell's law,

$$\frac{dP}{dt} = \int_{path} \frac{\partial\mu}{\partial t}\, ds + \lim_{z \to h} \left[2 \mu \cos\phi \Big|_z \frac{dz}{dt} \right] \qquad (8.12)$$

The quantity in the brackets is zero when evaluated at the limit, since $\cos\phi$ is zero at reflection for oblique propagation, and μ is zero at reflection for vertical propagation. Therefore, from (8.12)

$$\frac{dP}{dt} = \int_{path} \frac{\partial\mu}{\partial t}\, ds . \qquad (8.13)$$

Substituting (8.13) into (8.3),

$$\Delta f = -\frac{f}{c} \int_{path} \frac{\partial\mu}{\partial t}\, ds . \qquad (8.14)$$

It is necessary to neglect the earth's magnetic field because the

proof assumes that the ray direction and the wave normal direction are the same, which is generally not the case when the effects of the magnetic field are included. The step from (8.6) to (8.7) assumes that the angle ϕ gives the wave normal direction, while (8.8) assumes that the angle ϕ gives the ray direction.

If the propagation is vertical, this restriction is not necessary, since equation (8.8) is not necessary for the proof. Combining (8.3) and (8.5), the Doppler shift for vertical propagation is given by

$$\Delta f = -2 \frac{f}{c} \frac{d}{dt} \int_o^h \mu \, dz \quad . \tag{8.15}$$

Performing the differentiation indicated in (8.15),

$$\Delta f = -2 \frac{f}{c} \int_o^h \frac{\partial \mu}{\partial t} \, dz - 2 \frac{f}{c} \mu \Big|_h \frac{dh}{dt} \quad . \tag{8.16}$$

The term $-2 \frac{f}{c} \mu \Big|_h \frac{dh}{dt}$ is zero, since the index of refraction is zero at reflection for vertical propagation. Therefore, from (8.16)

$$\Delta f = -2 \frac{f}{c} \int_o^h \frac{\partial \mu}{\partial t} \, dz \quad . \tag{8.17}$$

Since the derivation of (8.17) from (8.15) does not depend on the coincidence of the wave normal and ray direction (8.17) is correct including the effect of the earth's magnetic field.

The integral form for the Doppler shift as given in (8.14)(for propagation at any angle of incidence neglecting the effect of the earth's

magnetic field) or as given in (8.17) (for vertical propagation including the effect of the earth's magnetic field) is convenient since it can be used in a computer ray tracing program to calculate the Doppler shift by performing a sum approximating the integral along the path as the ray is traced.

9. Appendix II - Equivalence Theorem for Doppler Shifts

To show: $\Delta f(f, \phi_o) = \Delta f(f \cos\phi_o, 0)$,

where the first argument is the wave frequency and the second argument is the angle of incidence of the wave on the ionosphere.

Restrictions:

(1) The curvature of the ionosphere is neglected.

(2) The effect of the earth's magnetic field is neglected.

(3) The effect of collisions is neglected.

Proof:

The Doppler shift is given by (8.1) of Appendix I.

$$\Delta f = - \frac{f}{c} \int_{\text{path}} \frac{\partial \mu}{\partial t} \, ds \quad . \tag{9.1}$$

The refractive index is given by

$$\mu^2 = 1 - \frac{kN}{f^2} \quad . \tag{9.2}$$

Differentiating (9.2) with respect to t and dividing by 2μ,

$$\frac{\partial \mu}{\partial t} = - \frac{k}{2\mu f^2} \frac{\partial N}{\partial t} \quad . \tag{9.3}$$

Combining (9.1) and (9.3),

$$\Delta f = \frac{k}{2cf} \int \frac{\frac{\partial N}{\partial t}\, ds}{\mu} \quad . \tag{9.4}$$

Substituting $ds = dz/\cos\phi$ in (9.4),

$$\Delta f = \frac{k}{2cf} \int \frac{\frac{\partial N}{\partial t}\, dz}{\mu \cos\phi} \quad . \tag{9.5}$$

Operating on (9.5) with straightforward algebra, using a trigonometric substitution, and applying Snell's law, $\mu \sin\phi = \sin\phi_o$,

$$\Delta f = \Delta f(f, \phi_o) = \frac{k}{2cf \cos\phi_o} \int \frac{\frac{\partial N}{\partial t}\, dz}{\sqrt{1 - \frac{kN}{f^2 \cos^2 \phi_o}}} \quad . \tag{9.6}$$

Substituting into the function defined by (9.6), it can be seen that

$$\Delta f(f, \phi_o) = \Delta f(f\cos\phi_o, 0) \quad . \tag{9.7}$$

An interpretation of (9.7) is that Δf depends only on the equivalent vertical-incidence frequency, $f\cos\phi_o$.

10. Appendix III - Relationship Between Doppler Shift and Virtual Height

To show:

$$f\Delta f = \frac{k}{c}\frac{\partial N}{\partial t}(h' - h_o) \tag{10.1}$$

if $\partial N/\partial t$ is zero from the ground up to h_o and constant above h_o.

Restrictions:

(1) Only vertical propagation is considered.

(2) Collisions are neglected.

(3) Effect of the earth's magnetic field is neglected.

Proof:

The Doppler shift for vertical propagation is given by (8.2) of Appendix I.

$$\Delta f = -2\frac{f}{c}\int_o^h \frac{\partial \mu}{\partial t}\,dz \tag{10.2}$$

If the Doppler shift is entirely due to changes in electron density in the ionosphere, then from (10.2),

$$\Delta f = -2\frac{f}{c}\int_0^h \frac{\partial \mu}{\partial N}\frac{\partial N}{\partial t}\,dz \tag{10.3}$$

The index of refraction is given by

$$\mu^2 = 1 - \frac{kN}{f^2} \tag{10.4}$$

Differentiating (10.4) with respect to N and dividing by 2μ,

$$\frac{\partial \mu}{\partial N} = - \frac{k}{2\mu f^2} \tag{10.5}$$

Since $\mu = 1/\mu'$,

$$\frac{\partial \mu}{\partial N} = - \frac{k}{2f^2} \mu' \tag{10.6}$$

Substituting (10.6) into (10.3),

$$\Delta f = \frac{k}{fc} \int_o^h \mu' \frac{\partial N}{\partial t} \, dz \tag{10.7}$$

For the special case in which $\partial N/\partial t$ is zero from the ground up to a height h_o, and constant above h_o,

$$\Delta f = \frac{k}{fc} \frac{\partial N}{\partial t} \int_{h_o}^h \mu' \, dz \tag{10.8}$$

Since μ' is one below h_o for the special case that the region is nondeviative,

$$\Delta f = \frac{k}{fc} \frac{\partial N}{\partial t} \left[\int_o^h \mu' \, dz - \int_o^{h_o} dz \right] \tag{10.9}$$

Performing the indicated integrations in (10.9),

$$\Delta f = \frac{k}{fc} \frac{\partial N}{\partial t} (h' - h_o) \tag{10.10}$$

Multiplying (10.10) by f,

$$f\Delta f = \frac{k}{c}\frac{\partial N}{\partial t}(h' - h_o) \qquad (10.11)$$

which was to be proved.

A physical interpretation of (10.11) is that the product of the frequency and the Doppler shift for vertical propagation is proportional to the virtual height minus some constant height at all frequencies. Therefore, if $\partial N/\partial t$ is independent of height in the ionosphere, a plot of $f\Delta f$ versus f should look like the ionogram. This relation is approximately valid even if the magnetic field is included as shown by figure 10.1 for conditions at Boulder (dip = 70°, f_H = 1.47 Mc/s).

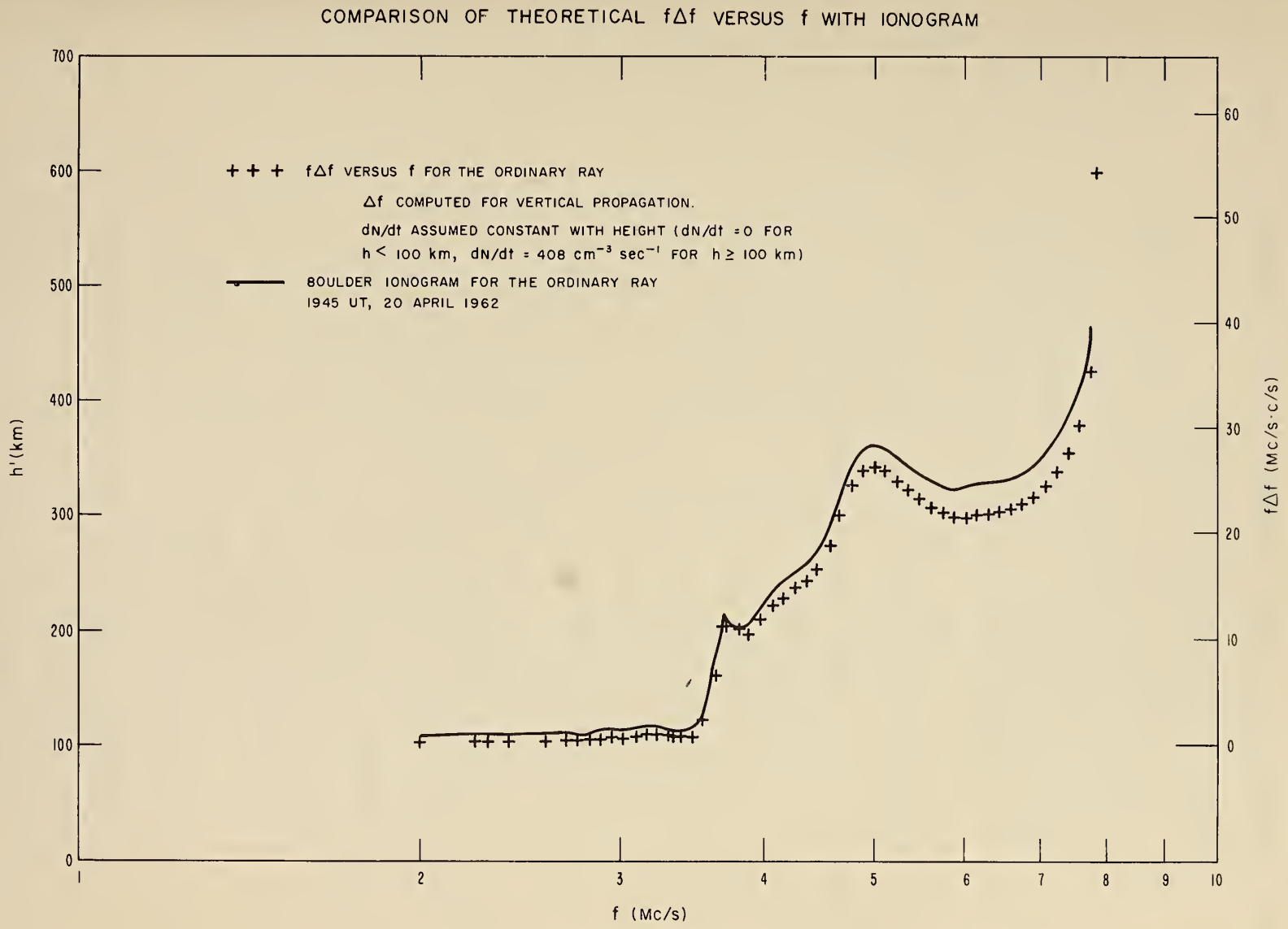
COMPARISON OF THEORETICAL fΔf VERSUS f WITH IONOGRAM
+ + + fΔf VERSUS f FOR THE ORDINARY RAY
Δf COMPUTED FOR VERTICAL PROPAGATION.
dN/dt ASSUMED CONSTANT WITH HEIGHT (dN/dt = 0 FOR
h < 100 km, dN/dt = 408 cm⁻³ sec⁻¹ FOR h ≥ 100 km)
BOULDER IONOGRAM FOR THE ORDINARY RAY
1945 UT, 20 APRIL 1962
h'(km)
fΔf (Mc/s·c/s)
f (Mc/s)
0
100
200
300
400
500
600
700
1
2
3
4
5
6
7
8
9
10
0
10
20
30
40
50
60

Figure 10.1

11. Appendix IV - Catalog of Sudden Frequency Deviations Observed From October 1, 1960 to December 31, 1962.

The following table lists the sudden frequency deviations observed for the various paths in operation from October 1, 1960, to December 31, 1962. This table also gives the solar flares and solar radio emissions as well as ionospheric effects which were reported to have occurred at the same time that a sudden frequency deviation was observed. Since the paths from WWV to Boulder and the near vertical-incidence paths at Boulder (Sunset to Boulder) were used for flare monitoring during this period, the table includes all SFD's observed on the Boulder records. Consequently there are some entries for which no flares were reported optically. The records for receiving sites other than Boulder have not been examined as closely as have the Boulder records, and only SFD's which could be attributed to reported optical flares have been included in the table for these paths. It should be emphasized that, although all the sudden frequency deviations listed have the characteristics of flare effects, some of the smaller effects, especially those which do not correspond to optically reported flares, may not be due to flare-induced ionization.

A brief description of the method of data reduction may be of assistance in evaluating the information contained in the catalog. The data is recorded on slowly moving magnetic tape (0.02 ips) in the form of the difference frequency between the received frequency and a stable local reference frequency offset from the transmitted frequency by a few cycles per second (typically 2-5 c/s). This magnetic tape is then played back at 30 ips into an audio spectrum analyzer to give a continuous visual

record of the recorded difference frequency versus time. Changes in the received frequency are indicated by the variations of the difference frequency. A sample of such a record is shown in figure 11.1a. Any events of interest can be examined in greater detail by expanding the time scale, as illustrated in figures 11.1b and 11.1c. The times and magnitudes of sudden frequency deviations are determined from the expanded records.

Figure 11.1 illustrates some of the difficulties often encountered in deciding whether an observed effect is, or is not, related to a solar flare. The effects at 1715, 1942, 2050, 2153, and 2240 UT are well defined sudden frequency deviations. The events at 1822, 1837, and 1928 are not as well defined. It is often questionable whether such effects are flare related or arise from some other type of ionospheric disturbance. The effect at 2333 UT, which begins with a negative frequency shift, is definitely not a sudden frequency deviation.

The table gives the times of sudden frequency deviations to the nearest minute with the symbols E (before) and D (later than) being used occasionally for further qualification. D or E used with a beginning or maximum time applies only between successive minutes, whereas a D used with an end time may mean that the end of the effect occurred some undeterminable number of minutes after the given time.

The frequency deviations, Δf, are given in cycles per second. The accuracy with which small frequency variations can be measured from the records is extremely limited so that the smaller events (NM or 0.1 to 0.2 c/s) have no quantitative usefulness. NR has been used to indicate

Sample Doppler record illustrating the range in magnitude of the sudden frequency deviations detected

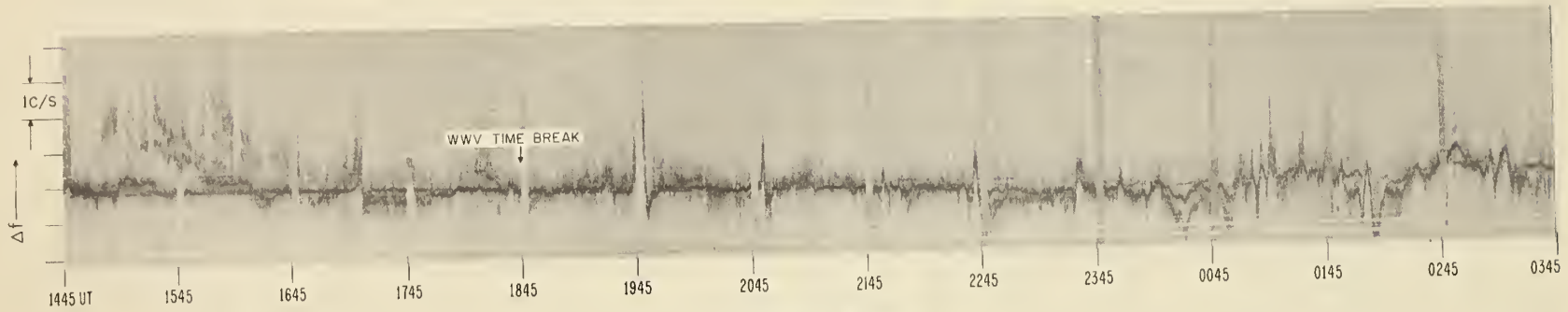

(a) NORMAL RECORD

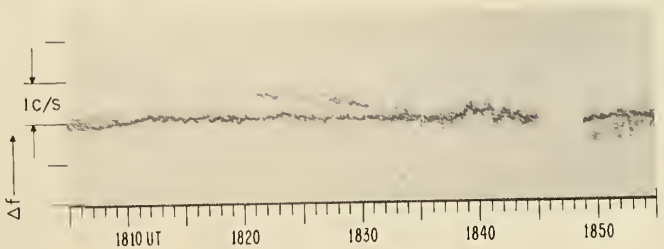

(b) EXPANDED TIME SCALE

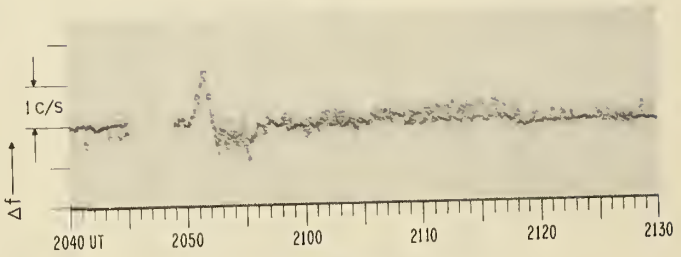

(c) EXPANDED TIME SCALE

15 - 16 APRIL, 1962

WWV - 10 MC/S TO BOULDER, COLORADO

Figure 11.1

that no record exists for the given path and frequency for a given event. The nonexistence of records designated by NR may be due to equipment malfunction or to propagation conditions. An NR has been used when the ground wave has over-powered the sky wave on the vertical-incidence paths. NM (not measurable) indicates that an effect probably exists but that the frequency deviation cannot be measured. This is used for effects too small to measure or for which the quality of the records is not good enough to permit unambiguous interpretation.

The format of the SFD section of the table is as follows:

Time: The times of the beginning, maximum positive frequency deviation, and end of the SFD are given in universal time. If more than one distinct peak exists for a given event, the times of the maxima are listed.

Path and Frequency: The path is given by designating the transmitting and receiving locations. The operating frequency, f, is given to the nearest Mc/s.

Frequency Deviation, Δf: The maximum positive frequency deviation, $\Delta f(+)$, is given in cycles per second. If more than one distinct peak exists the frequency deviation of each maximum is given. For those events which showed a measurable negative frequency deviation, the maximum negative frequency shift, $\Delta f(-)$, is also given.

Change in Absorption, ΔA: The maximum change in absorption, ΔA, is given in decibels for those events for which it was measurable. No signal strength records are available for those events which occurred before September 1961.

Phase Path Change, ΔP: The maximum change in phase path, ΔP, is given in kilometers for selected events. The phase path change is the time integral of the frequency deviation:

$$\Delta P = - \frac{c}{f} \int \Delta f \, dt.$$

The solar flare, solar radio emissions, and the ionospheric effects sections of the table are essentially the same as given in the CRPL-F Series, Solar-Geophysical Data; the descriptive text* for this publication should be consulted for a more complete description of the information contained therein. The order in which the beginning, maximum, and end times, or duration, are given has been changed to be consistent with the SFD section of the table. The radio bursts at 18 Mc/s given in the F-Series under ionospheric effects have been included in the table under solar-radio emissions. An attempt has been made to make the table as complete as space would allow in order that the SFD data available from October 1, 1960, to December 31, 1962, may be brought to the attention of other interested workers.

Abbreviations and Symbols Used

The following list defines the abbreviations used in the table of SFD's. For those portions of the table extracted from the CRPL-F Series, only the notation which differs from that of the F-Series is explained

---

* "Descriptive Text and Index for CRPL-F, Part B, Solar-Geophysical Data," U. S. Department of Commerce, National Bureau of Standards, Central Radio Propagation Laboratory, Boulder, Colorado, November 1961, 1962, 1963.

below. For a full explanation of notation used by the F-Series, reference should be made to the Descriptive Text of the CRPL-F Series, Part B, Solar-Geophysical Data.

Time:

D - greater than

d - duration

E - less than

U - uncertain

Path:

Transmitters	Receivers
MN - Monrovia, Liberia	AC - Accra, Ghana
PB - Point Barrow, Alaska	AN - Anchorage, Alaska
SS - Sunset, Colorado	BL - Boulder, Colorado
TR - Tripoli, Libya	FC - Fort Collins, Colorado
WWV - Beltsville, Maryland	MY - Midway Island, Pacific
WWVH - Maui, Hawaii	SY - Shickley, Nebraska
	WK - Wake Island, Pacific

Frequency Deviation, Δf:

NM - not measurable

NR - no record

Solar Flares:

NFR - no flare reported

NFP - no flare patrol

Solar Radio Emissions:

2800 Mc/s

1S1 - 1-Simple 1

2S2 - 2-Simple 2

3S3 - 3-Simple

4PI - 4-Post-burst increase

5 Abs - 5-Absorption

6C - 6-Complex

8G - 8-Group

9Pre - 9-Precursor

18 Mc/s

Bur - Burst

Table 11.1

Catalog of Sudden Frequency Deviations

Observed from October 1960 through December 1962

Date	SFD's							Solar Flares		Solar Radio Emissions				Ionospheric Effects		
	UT	Path	f	Δf, cps		ΔA	−ΔP	UT	Imp	UT	Type	Freq	Int or Peak Flux	UT	Type	Imp
1960	Beg - Max - End		Mc/s	(+)	(−)	db	km	Beg - Max - End		Beg - Max - End		Mc/s		Beg - Max - End		
10-05	2023- 2023D- 2024	WWV-BL	20	0.1				2022	S							
10-05	2038- 2038D- 2039	WWV-BL	20	0.1				2038	S							
10-08	1802- 1803 - 1805	WWV-BL	20	0.2				1802- 1812- 1830U	1							
10-09	2340- 2341- 2342	WWV-BL	20	0.1				2336	S							
10-11	1609- 1610- 1612	WWV-BL	20	0.1				NFR		1610.2-1610.7-1611.2	1S1	2800	4			
10-11	1759- 1800- 1802	WWV-BL	20	0.1				1746- 1810- 2007	2	1748 - 1815 - 1934	3S3A	2800	13	1800- 1850	S-SWF	1+
										1759.5-1804.7-1812	2S2f	2800	190	1803- 1830-	SEA	1+
										1803.4-1804.7-1807	8	108	3	1805- 1812- 1845	SCNA	1
															ABS	20
10-12	1724- 1726- 1731	WWV-BL	20	0.1				1722- 1728- 1820	1	1722 - -1847	3S3A	2800	8	1729-	SL-SWF	2-
										1725 -1726.5 -1731	6Cf	2800	29			
										1734 -1736.5 -1739	6C	2800	8			
										1725.0-1727.5-1730	8	108	2			
										1726 - -1730	Bur	18	1			
10-12	1743- 1744- 1745	WWV-BL	20	0.1				1742- 1750- 1852	1	1745.5-1748 - 1752.5	6Cf	2800	83	1744- 1810	S-SWF	
										1751.5-1753.0-1753.5	3	108	3	1747- 1755-1840D	SEA	1
										1756.8-1758.9-1801	8	108	3	1749- 1751-1815	SCNA	1
															ABS	20
10-12	1856- 1857- 1903	WWV-BL	20	0.1				1856	S							
10-13	1722- 1724- 1726	WWV-BL	20	0.3				1722- 1728- 1820	1							
10-15	1923- 1924D-1927	WWV-BL	20	0.3				1924- 1925- 1943	1	1924 -1924.5- 1926	2S2f	2800	12			
										1928- - 1932	Bur	18	2			
10-26	1836- 1838- 1841	WWV-BL	20	0.1				1834	S							
11-02	1941- 1943- 1945	WWV-BL	20	0.2				1942	S	1941 - 1942 - 1945	6C	2800	3			
11-03	1821- 1823- 1831	WWV-BL	20	0.5	0.1			1819E	S	1821.5-1824 - 1831.5	6Cf	2800	9			
11-05	1536- 1539E-1543	WWV-BL	20	0.3	0.1			NFR						1539- 1550-	SEA	1+
11-07	1919- 1919D-1921	WWV-BL	20	0.1				1920E	S							

Date 1960	SFD's							Solar Flares		Solar Radio Emissions				Ionospheric Effects		
	UT	Path	f	Δf, cps		ΔA	−ΔP	UT	Imp	UT	Type	Freq	Int or Peak Flux	UT	Type	Imp
	Beg - Max - End		Mc/s	(+)	(−)	db	km	Beg - Max - End		Beg - Max - End		Mc/s		Beg - Max - End		
11-10	2110- 2112D-2114	WWV-BL	20	0.2				2110	S							
11-11	1421E-1422 -1425	WWV-BL	20	0.1				1422E	S							
11-11	1508E-1508D-1509	WWV-BL	20	0.6				1510E-1510U-1558U	1	1508.5-1509 -1509.5	1S	2800	6			
11-11	1629 -1630 -1631	WWV-BL	20	0.2				1625E	S							
11-11	1709 -1710 -1717	WWV-BL	20	0.8	0.3			1704	S							
11-11	2054E-2054D-2056	WWV-BL	20	0.2				2052	S							
11-12	1324 -1328E-1339	WWV-BL	20	11.2	0.8			1315 -1330 -1425D	3+	1240E - -1320D	9Pre	2800	11	1325- 1350	SCNA	3
										1320 - 1345 -1920	Gt Bur	2800	5500	1325- 1345-1530	SEA	2+
										1347 - -2320	6	108	2	1326- -1600	S-SWF	3+
11-12	1657 -1658 -1659	WWV-BL	20	0.2				1657	S							
11-14	1551 -1552 -1554	WWV-BL	20	0.2				1554E- -1645D	1					1542- -1618	S-SWF	2
11-14	2037 -2038 -2040	WWV-BL	20	0.2				2036	S							
11-14	2117 -2119E-2122	WWV-BL	20	0.4				2114 -2120 -2154	2							
11-15	1656 -1657 -1659	WWV-BL	20	0.3				1657	S							
11-15	2101 -2102 -2104	WWV-BL	20	0.1				2100	S							
11-15	2122 -2122D-2124	WWV-BL	20	0.2				2120	S							
11-16	1810 -1811 -1814	WWV-BL	20	0.1				NFR								
11-17	1504 -1506E-	WWV-BL	20	0.2				1506 -1511 -1538	1	1504.5-1506 -1508.5	6C	2800	38			
	-1507D-1510	WWV-BL	20	0.2						d15	4PI	2800	5			
11-17	1751 -1755 -1757	WWV-BL	20	0.2				1754 -1756 -1806	1							
								1750	S							
11-17	1925 -1926 -1927	WWV-BL	20	0.1				1920	S							
11-18	1507 -1510 -1512	WWV-BL	20	0.2				1508	S							
11-18	1742E-1742 -1744	WWV-BL	20	0.2				NFR								

Date 1960	SFD's							Solar Flares		Solar Radio Emissions				Ionospheric Effects		
	UT	Path	f	Δf, cps		ΔA	−ΔP	UT	Imp	UT	Type	Freq	Int or Peak Flux	UT	Type	Imp
	Beg - Max - End		Mc/s	(+)	(−)	db	km	Beg - Max - End		Beg - Max - End		Mc/s		Beg - Max - End		
11-19	1549E- -1600	WWV-BL	20	NM	0.2			1543 -1551 -1649	2	1554 -1555 -1556	1S1	2800	4			
										1557.5-1557.5-1558.5	3	108	2			
11-19	2042 -2043 -2045D	WWV-BL	20	0.2				2026 -2045 -2053	1							
11-20	2023E-2023 -2024	WWV-BL	20	0.1				2017 -2020 -2024	1	1939 - -2023	9Pre	2800	14	2023- -2145	SL-SWF	3-
										2023 -2026.5-2110	6Cf	2800	400	2023-2041-2140	SEA	2+
														2028-2053-2340	SCNA	3
															ABS	80
11-21	2104 -2106E-2108	WWV-BL	20	0.2				2035 -2105 -2148	1							
11-26	1803 -1805 -1807	WWV-BL	20	0.1				1804	S							
12-02	1841 -1841D-1842	WWV-BL	20	0.1				1840	S							
12-02	1904 -1905 -1907	WWV-BL	20	0.1				1904	S							
12-03	1637 -1638 -1642	WWV-BL	20	0.2	0.1			1631	S							
12-03	1826 -1828 -1831	WWV-BL	20	0.1				1820	S							
12-06	1614 -1616 -1618	WWV-BL	20	0.5				1615	S	1616 -1616.5-1621	2S2	2800	17			
12-06	1917 -1919 -1920	WWV-BL	20	0.2				1918	S							
12-06	2027 -2029 -2031	WWV-BL	20	0.2				2025	S	2029.0-2030 -2032.4	8	108	3			
12-16	1523 -1524	WWV-BL	20	0.1				1517 -1532 -1630	2	1520 -1550 -1630	3S3A	2800	9	1530- -1605	SL-SWF	1+
	-1526 -1528	WWV-BL	20	0.1						1523 -1527 -1531	1S1	2800	6			
										1531 -1532.6-1535.5	8	108	3			
12-19	2336 -2337 -2338	WWV-BL	20	0.3				2334	S							
			10	0.2												
12-20	1856 -1858 -1904	WWV-BL	20	0.2				1852 - -1900D	1					1856-1902-1920	SEA	1+
			10	NR												
12-21	1843 -1844 -1845D	WWV-BL	20	0.1				1842E	S							
			10	NR												
12-26	1622 -1625 -1630	WWV-BL	20	0.4				1624	S							
			15	0.3												

Date 1960	SFD's							Solar Flares		Solar Radio Emissions				Ionospheric Effects		
	UT	Path	f	Δf, cps		ΔA	−ΔP	UT	Imp	UT	Type	Freq	Int or Peak Flux	UT	Type	Imp
	Beg - Max - End		Mc/s	(+)	(−)	db	km	Beg - Max - End		Beg - Max - End		Mc/s		Beg - Max - End		
12-27	1536 -1537D-1539	WWL-BL	20	NR				1536 -1539U-1544D	1							
			15	0.2												
12-27	2020 -2021 -2022	WWV-BL	20	NR				2021	S	2019.8-2020.1-2020.3	3	108	2			
			15	0.2												
12-27	2040 -2041 -2043	WWV-BL	20	NR				2037	S							
			15	0.2												
12-27	2057E-2057 -2059	WWV-BL	20	NR				2046	S							
			15	0.1	0.1											
12-30	0140 -0141 -0145D	WWVH-BL	15	0.6	0.2			0141 - -0148	1							
12-30	1700E-1700 -1702	WWV-BL	20	0.1				1659	S							
			15	0.1												
12-30	1730 -1730D-1732	WWV-BL	20	0.2				1726 -1740 -1757	1	1725 - -2312	7	108	2			
			15	0.4												
12-30	1739 -1740 -1742	WWV-BL	20	0.1				1740	S							
			15	0.2												
12-30	1806D-1807 -1809	WWV-BL	20	0.1				1806	S							
			15	0.2												
12-30	1826 -1831 -1834	WWV-BL	20	0.3				1826 -1833 -1851	1							
			15	0.4												
12-31	1413 -1414D-1416	WWV-BL	20	0.2				1407 - -1430	1+							
			15	0.2												
12-31	2009 -2009D-2010	WWV-BL	20	0.2				2008	S							
			15	0.2												
1961																
01-01	1538 -1539 -1541	WWV-BL	20	0.1				NFR								
			15	0.1												
01-01	1640 -1641 -1643	WWV-BL	20	0.1				NFR								
			15	0.2												
01-03	1518 -1520 -1524	WWV-BL	20	0.1				1520	S							
			15	0.1												

Date 1961	SFD's							Solar Flares		Solar Radio Emissions				Ionospheric Effects		
	UT	Path	f	Δf, cps		ΔA	−ΔP	UT	Imp	UT	Type	Freq	Int or	UT	Type	Imp
	Beg - Max - End		Mc/s	(+)	(−)	db	km	Beg - Max - End		Beg - Max - End		Mc/s	Peak Flux	Beg - Max - End		
01-03	1907 -1908 -1914	WWV-BL	20	0.7	0.2			1900	S					1910- -1925	SL-SWF	1-
			15	NR												
01-03	1952 -1953 -1954	WWV-BL	20	0.2				1952	S							
			15	NR												
01-04	0206 -0208 -0223	WWVH-BL	15	1.0	0.2			0206 -0208 -0220	2					0207- -0230	S-SWF	1
														0206-0210-0223	SCNA	1
															ABS	25
														0207-0225-0304	SEA	1+
01-04	1623 -1624 -1627	WWV-BL	20	0.3				1621	S							
			15	0.1												
01-04	1710E-1710D-1724	WWV-BL	20	0.6				1729E-1729E-1747U	1	1710 -1711 -1719	2S2f	2800	40	1712- -1755	SL-SWF	1+
			15	0.3						d2:10	4PI	2800	17	1707-1720-1803	SEA	2
														1713-1721-1800	SCNA	1
															ABS	20
01-08	1827 -1828 -1830	WWV-BL	20	0.1				1821	S							
			15	0.1												
01-18	1727 -1728 -1729	WWV-BL	20	0.1				NFR								
			15	NR												
01-27	1638E-1639E-1641	WWV-BL	20	0.2				1636	S							
			15	NR												
01-29	2133 -2134 -2136	WWV-BL	20	0.1				2133	S	2122.8- -2134.9	2	108	3			
			15	0.3												
01-29	2148E-2149E-2150D	WWVH-BL	15	1.2				2146	S							
01-30	1423E-1423D-1435	WWV-BL	20	1.8	0.2			1420 -1425 -1440	1	1423.8-1424.7-1430.8	2S2f	2800	160	1423- -1440	S-SWF	1
			15	1.8	0.3					1412E -1508 -2348D	6	108	2	1425- -1445	SEA	1
										1424.0-1425.5-1426.0	8	108	3			
										1426.0-1428.0-1429.5	9	108	3			
01-30	1856 -1858E-1859	WWV-BL	20	0.2				1842	S							
			10	NM												
01-30	2002 -2004 -2010D	WWV-BL	20	3.0	1.2			2000 -2004 -2013	1	2003 -2004.3-2006	2S2f	2800	70	2005-2011-2033	SEA	1
			10	6.6	NM					2004 - -2006	Bur	18	1	2006E-2009-2010D	SCNA	1
										2010 - -2011	Bur	18	1		ABS	10

Date 1961	SFD's							Solar Flares		Solar Radio Emissions				Ionospheric Effects		
	UT	Path	f	Δf, cps		ΔA	−ΔP	UT	Imp	UT	Type	Freq	Int or Peak Flux	UT	Type	Imp
	Beg - Max - End		Mc/s	(+)	(−)	db	km	Beg - Max - End		Beg - Max - End		Mc/s		Beg - Max - End		
01-31	1511 -1514 -1526	WWV-BL	20	1.0	0.4			1509 -1514 -1535	1	1511.5-1514.3-1516.5	2S2f	2800	350	1512- -1526	S-SWF	1
			10	2.4	0.7					d10	4PI	2800	2			
										1512.0-1513.2-1514.6	8	108	2			
										1517.0-1518.3-1518.9	3	108	3			
01-31	1724D-1726 -1727	WWV-BL	20	0.2				1717	S							
			10	NM												
01-31	2109 -2110 -2113	WWV-BL	20	0.2				2108	S	2109.5-2110.5-2113.5	1S1	2800	5			
			10	0.2												
01-31	2134E-2135E-2137	WWV-BL	20	0.5				2131 -2137 -2155	1	2133.5-2135 -2139	2S2	2800	14	2137-2140-2153	SCNA	1
			10	1.0						2131.0-2131.9-2132.5	3	108	2		ABS	5
										2133.0-2135.5-2136	8	108	3	2137-2145-2200	SEA	1
										2134 - -2137	Bur	18	1			
02-02	1432 -1433D-1435	WWV-BL	20	0.1				NFP								
			10	NM												
02-02	1852 -1854 -1856	WWV-BL	20	0.1				1851	S							
			10	0.1												
02-03	1853 -1854 -1856	WWV-BL	20	0.1				NFR								
			10	0.2												
02-03	1908 -1910D-1914	WWV-BL	20	0.2				1905	S							
			10	NM												
02-04	1702 -1703 -1705	WWV-BL	20	0.2				NFR								
			10	0.2												
02-06	1411 -1414 -1416	WWV-BL	20	NR				1410 -1416 -1425	1+							
			10	0.3												
02-12	1506 -1508D-1510	WWV-BL	20	0.1				NFP		1507 -1909 -1517	3S3f	2800	2			
			10	0.3												
02-14	1355 -1357 -1359	WWV-BL	20	NR				1356 -1358 -1406	1							
			10	0.2												
02-17	2203E-2205 -2210	WWV-BL	20	0.3				NFR								
		WWVH-BL	10	0.4												

Date 1961	SFD's							Solar Flares		Solar Radio Emissions				Ionospheric Effects		
	UT	Path	f	Δf, cps		ΔA	−ΔP	UT	Imp	UT	Type	Freq	Int or Peak	UT	Type	Imp
	Beg - Max - End		Mc/s	(+)	(−)	db	km	Beg - Max - End		Beg - Max - End		Mc/s	Flux	Beg - Max - End		
02-17	2213 -2214 -2216	WWV-BL	20	0.1				NFR								
		WWVH-BL	10	0.1												
02-25	0008 -0009 -0011	WWV-BL	20	0.1				0008	S							
			10	NR												
02-25	0025 -0025D-0028	WWV-BL	20	0.2				NFR								
			10	NR												
03-14	1728 -1728D-1730	WWV-BL	20	NR				1722	S							
			10	0.2												
03-14	2041 -2042 -2044	WWV-BL	20	NR				2040	S							
			10	0.1												
03-16	1641 -1643E-1644	WWV-BL	20	0.2				1640E- -1700D	1	1642.8-1643.6-1645	3	108	2			
			10	NM						1642 - -1644	IIIG	450-30	2			
03-18	1738 -1739D-1758	WWV-BL	20	0.5	0.2			1738 -1742 -1810	1+	1738.5-1741.5-1747	7 Irreg Act	2800	15	1740-1743-1755	SEA	1
			10	0.9	0.4					1739 - -1743	IIIG	420-25	3			
										1749 - -1754	II	115-70	1			
										1757 - -1800	II	80-25	2			
										1728 - -1748	Bur	18	1			
03-23	1300 -1304 -1314	WWV-BL	20	NR				1217E- -1236D	1	1315 -1618 -1825	7	108	3			
			10	0.4						1320 - -2040	I	400-25	1-3			
03-26	1831 -1832 -1843	WWV-BL	20	0.6	0.1			1830	S							
			10	0.2	0.2											
03-26	2215 -2217 -2220	WWV-BL	20	0.1				2215E	S	2220.0-2236.8-2242	2	108	1			
			10	0.2						2221 - -2223	IIIG	150-50	1			
03-27	1417 -1419 -1427	WWV-BL	20	0.1	0.3			1416E- 1450D	1	1428.4-1429.0-1429.6	3	108	2			
			10	0.3	NM											
03-27	1718 -1721 -1724	WWV-BL	20	0.2				1714	S							
			10	0.4												
03-28	1716 -1717 -1720	WWV-BL	20	0.1				1715	S							
			10	0.3												

Date 1961	SFD's							Solar Flares		Solar Radio Emissions				Ionospheric Effects		
	UT	Path	f	Δf, cps		ΔA	−ΔP	UT	Imp	UT	Type	Freq	Int or Peak Flux	UT	Type	Imp
	Beg - Max - End		Mc/s	(+)	(−)	db	km	Beg - Max - End		Beg - Max - End		Mc/s		Beg - Max - End		
03-28	1908 -1909 -1911	WWV-BL	20 10	0.1 0.1				1908	S							
03-28	2214 -2214D-2216	WWV-BL	20 10	NM 0.1				2214	S							
03-29	1643E-1643D-1645D	WWV-BL	20 10	0.2 NM				1641	S							
03-29	1832E-1833E-1835	WWV-BL	20 10	0.4 1.1				1831	S	1831.8-1832.2-1833	2S2	2800	9			
03-29	2253 -2256 -2259	WWV-BL	20 10	0.1 0.3				2253 -2259 -2323	1							
03-30	0028 -0029 -0031	WWV-BL	20 10	0.1 NM				0023	S							
03-30	1437 -1438 -1441	WWV-BL	20 10	0.1 0.3				NFR								
03-30	1902 -1903 -1906	WWV-BL	20 10	0.1 0.3				1848 -1910 -1930D	1	1902 -1903 -1906	2S2 4PI	2800 2800	13 2			
03-30	2135 -2136 -2138	WWV-BL	20 10	NM 0.3				2134	S							
04-03	1710 -1712E-1716	WWV-BL	20 10	NR 0.6				1711 - -1725D	1+	1711 -1711.8-1712.5	2S2f	2800	35			
04-04	1411 -1413 -1415	WWV-BL	20 10	NR 0.2				1411	S	1412.5- -1429 1412.5-1413.3-1415.5	8G(2) 2S2f	2800 2800	 14			
04-04	1920D-1923E-1926	WWV-BL	20 10	0.1 NM				1921	S							
04-04	2233 -2234D	WWV-BL	20 10	0.1 0.3				2233 -2240 -2306	1	2232.5-2237.7-2244 2234.5- -2320	6Cf IV	2800 580-90	25 2			
	-2237 -2239	WWV-BL	20 10	0.2 0.4						2239.8- -2245	Uncl	130-50	2			

Date 1961	SFD's							Solar Flares		Solar Radio Emissions				Ionospheric Effects		
	UT	Path	f	Δf, cps		ΔA	−ΔP	UT	Imp	UT	Type	Freq	Int or Peak Flux	UT	Type	Imp
	Beg - Max - End		Mc/s	(+)	(−)	db	km	Beg - Max - End		Beg - Max - End		Mc/s		Beg - Max - End		
04-05	1551 -1554	WWV-BL	20	NR				1545	S							
			10	0.4												
	-1555D-1558	WWV-BL	20	NR				1555 -1629 -1647	1+	1603.7-1604.2-1604.4	3	108	2			
			10	0.5												
04-05	1621 -1624 -1640D	WWV-BL	20	2.1	0.2			1555 -1629 -1647	1+	1623.5-1625.5-1627.5	6C	2800	14	1623- -1645	S-SWF	1+
			10	0.7	0.5			1556 -1625 -1635	1	1624	IIIg	975-600	1-	1623-1626-1641	SCNA	25
										1625	cont	540-950	1-	1624-1629-1717	SEA	
										1625 - -1628	IV	580-280	2			
04-05	1814 -1815 -1817	WWV-BL	20	0.1				1800	S	1815.2-1816 -1816.2	3	108	2			
			10	0.2												
04-05	2055 -2057E-2100	WWV-BL	20	0.2				2051 -2059 -2149	1	2056 -2141	3S3A	2800	3			
			10	0.3						2059.0-2059.9-2108	2	108	2			
										2056 - -2104	cont	540-950	3			
										2056.7- -2105	IV	3000-125	1-3			
04-06	1749E-1751 -1753	WWV-BL	20	0.2				1740	S	1747 -1753 -1927	3S3	2800	4	1745- -1820	SL-SWF	1
			10	0.3												
04-06	1835 -1836D-1838	WWV-BL	20	0.1				NFP								
			10	0.3												
04-06	2129 -2132 -2136	WWV-BL	20	0.1				2131 -2140 -2223	1	2130 - -2230	3S3A	2800	3			
			10	0.3						2132 -2132.7-2133.5	1S1	2800	4			
04-08	1557 -1559 -1601	WWV-BL	20	NR				NFR								
			10	0.2												
04-09	1533 -1534D-1537	WWV-BL	20	NR				1532 - -1541	1							
			10	0.7												
04-10	1828E-1830 -1833	WWV-BL	20	0.2				1827	S	1829 -1831 -1834	2S2f	2800	14			
			10	0.6						d15	4PI	2800	1.8			
04-10	1924 -1925D-1928	WWV-BL	20	0.2				1924	S	1925.5-1925.8-1926.5	1S1	2800	3			
			10	0.5						1925.1-1926.5-1926.6	3	108	3			
04-10	2232E-2233 -2235	WWV-BL	20	0.2				NFR								
			10	0.4												
04-11	1717 -1718D-1720	WWV-BL	20	NM				NFR		1720 - -1724	Bur	18	1			
			10	0.2												

Date 1961	SFD's							Solar Flares		Solar Radio Emissions				Ionospheric Effects		
	UT	Path	f	Δf, cps		ΔA	−ΔP	UT	Imp	UT	Type	Freq	Int or	UT	Type	Imp
	Beg - Max - End		Mc/s	(+)	(−)	db	km	Beg - Max - End		Beg - Max - End		Mc/s	Peak Flux	Beg - Max - End		
04-15	1616 -1617D-1619	WWV-BL	20 10	NR 0.3				1604	S							
04-18	2355E-2355D-2357	WWV-BL	20 10	0.1 0.2				2356	S							
04-19	1859 -1900D-1906	WWV-BL	20 10	NM 0.7				1900	S							
04-24	0042 -0043 -0045	WWV-BL	20 10	0.3 NM				0035 -0050 -0145	1							
04-25	2007 -2008D-2022	WWV-BL	20 10	0.1 0.6				2003 -2010 -2030	1	2007.3-2008.2-2009.7	2S2	2800	10.7			
04-26	1652 -1700E-1720D	WWV-BL	20 10	0.3 1.2				1648 -1718 -1945	3	1640 -Indet -2037 1656.8-1702 -1704.8 1647.5-1648 -1648.1	3S3A 6C 3	2800 2800 108	32 18.3 2	1650- -1843 1652-1707-1825	SL-SWF SCNA ABS	3 2 30
04-26	1730E-1730D-1734	WWV-BL	20 10	NM 0.5				1755E-1758 -1834D	2+							
04-26	2352 -2353 -2355	WWV-BL	20 10	NM 0.1				2353	S							
04-27	1611 -1613 -1615	WWV-BL	20 10	NM 0.2				1607E	S	1600 - -2010	7 Irreg Act	2800	5.1			
04-27	1617 -1618 -1620	WWV-BL	20 10	NM 0.2				1612	S	1600 - -2010	7 Irreg Act	2800	5.1			
04-27	1709 -1710 -1715	WWV-BL	20 10	0.2 0.3				1708	S							
04-27	1740 -1741 -1743	WWV-BL	20 10	NM 0.2				1738	S							
04-27	1835E-1836D-1840	WWV-BL	20 10	0.1 0.5				1836	S							
04-27	1933 -1936 -1940	WWV-BL	20 10	0.3 0.3				1933	S	1934.3-1934.7-1935.3	1S1	2800	3.8			
04-27	2205 -2207E-2211	WWV-BL	20 10	0.4 0.6				2202	S							

Date 1961	SFD's							Solar Flares		Solar Radio Emissions				Ionospheric Effects		
	UT	Path	f	Δf, cps		ΔA	−ΔP	UT	Imp	UT	Type	Freq	Int or	UT	Type	Imp
	Beg - Max - End		Mc/s	(+)	(−)	db	km	Beg - Max - End		Beg - Max - End		Mc/s	Peak Flux	Beg - Max - End		
04-28	1212 -1213 -1216	WWV-BL	20 10	NR 0.4				1201 - -1239D	1	1205 -Indet -1235 1211.7-1212.9-1214	3S3A 2S2	2800 2800	5.3 8.9			
04-28	1622 -1624 -1628	WWV-BL	20 10	NM 0.4				1622	S							
04-28	1904 -1904D-1905	WWV-BL	20 10	NR 0.1				1905	S							
04-28	1940 -1941 -1943	WWV-BL	20 10	NR 0.2				NFR								
04-28	2010 -2012 -2014	WWV-BL	20 10	NM 0.4				2011	S							
04-28	2049E-2051D-2054	WWV-BL	20 10	NM 0.3				2047	S							
04-29	1406 -1407 -1408	WWV-BL	20 10	NM 0.2				1406	S							
04-29	1451 -1451D-1455	WWV-BL	20 10	NM 0.1				1451	S							
04-29	1537 -1538 -1539	WWV-BL	20 10	NM 0.2				1540E	S							
05-03	1549E-1550 -1551	WWV-BL	20 10	0.1 NM				NFR								
05-03	2330 -2331 -2333	WWV-BL	20 10	0.1 0.3				NFR								
05-04	1309E-1310E-1313	WWV-BL	20 10	NM 0.6				1309 -1313 -1323	1	1309.5-1310.3-1312.5	1S1	2800	4			
05-04	1614 -1615D-1617	WWV-BL	20 10	0.2 NM				1615 -1617 -1637	1							

Date 1961	SFD's							Solar Flares		Solar Radio Emissions				Ionospheric Effects		
	UT	Path	f	Δf, cps		ΔA	−ΔP	UT	Imp	UT	Type	Freq	Int or Peak Flux	UT	Type	Imp
	Beg - Max - End		Mc/s	(+)	(−)	db	km	Beg - Max - End		Beg - Max - End		Mc/s		Beg - Max - End		
05-04	2204 -2207	WWV-BL	20	NR				2145 -2212 -2333D	3	2145 -Indet -2221	3S3A	2800	10	2205- -2245	SL-SWF	1+
			10	1.4						2205 -2208.8-2214	2S2f	2800	95	2203-2225-2308	SEA	2
	-2211 -2240	WWV-BL	20	NR						2207.5-2208.6-2210.5	3	108	2	2205-2220-2300U	SCNA	2
			10	2.2	0.4					2202 - -2205	Bur	18	2		ABS	50
										2209 - -2212	Bur	18	2			
										2207.5- -2210	IV	3900-2100	2			
05-05	1622 -1624 -1625	WWV-BL	20	NR				1609 - -1627D	1							
			10	0.2												
05-05	1725 -1726 -1728	WWV-BL	20	NR				1724 -1726 -1731	1							
			10	0.4												
05-05	1733 -1735 -1738	WWV-BL	20	NR				NFR								
			10	0.2												
05-05	1929 -1930 -	WWV-BL	20	NM				1928 -1933 -1949	1	1929 -1930 -1930	3	108	3			
			10	0.6				1928 -1945 -1949	1	1929 - -1930	IIIG	250-25	3			
	-1932 -	WWV-BL	20	NM												
			10	0.5	0.6											
	-1942E-1950	WWV-BL	20	NM												
			10	0.7												
05-05	2231 -2232 -2242	WWV-BL	20	NR				2231	S	2230.0-2232.0-2232.0	3	108	3	2236-2248-2335	SEA	2
			10	0.8						2230 - -2232	IIIG	300-25				
05-09	1543 -1544D-1545D	WWV-BL	20	1.6				1540 -1552 -1942	2	1540 -Indet -1830	3S3A	2800	6			
			10	2.4						1543 -1544.8-1546.3	2S2f	2800	9			
										1551 - -1621	Bur	18	4			
05-10	1858 -1859E-1902	WWV-BL	20	0.2	0.1			1858	S	1858.3-1859.6-1900.1	2	108	2			
			10	1.8	0.3											
05-11	1927 -1929 -1931	WWV-BL	20	NM				1927	S							
			10	0.3												
05-12	1355 -1356 -1357	WWV-BL	20	NR				1354	S	1250 -Indet -1515	3S3A	2800	5			
			10	0.6						1355.2-1355.8-1356.9	2S2	2800	12			
										1355.2-1356.8-1356.9	3	108	3			
05-12	1757 -1758D-1801	WWV-BL	20	NR				1758	S	1803.2-1803.8-1803.8	3	108	3			
			10	0.3												

Date 1961	SFD's							Solar Flares		Solar Radio Emissions				Ionospheric Effects		
	UT	Path	f	Δf, cps		ΔA	−ΔP	UT	Imp	UT	Type	Freq	Int or Peak Flux	UT	Type	Imp
	Beg - Max - End		Mc/s	(+)	(−)	db	km	Beg - Max - End		Beg - Max - End		Mc/s		Beg - Max - End		
05-12	1825 -1826D-1829	WWV-BL	20	NR				1825 -1828 -1838	1							
			10	0.2												
05-13	0000 -0000D-0001	WWV-BL	20	NR				0002E- -0006	1							
			10	0.4												
05-13	1131 -1131D-1132	WWV-BL	20	NR				NFR								
			10	0.1												
05-15	1940 -1940D-1942	WWV-BL	20	NM				1938	S							
			10	0.3												
05-24	2203 -2204 -2206	WWV-BL	20	NR				2200	S							
			10	0.1												
05-25	1553 -1555E-1559	WWV-BL	20	NM				1555E- -1606D	1							
		WWVH-BL	10	0.6												
05-28	1413 -1414 -1417	WWV-BL	20	0.1				1412	S							
			10	0.2												
05-28	1906 -1907E-1909	WWV-BL	20	0.4	0.2			1904	S							
			10	1.6	0.6											
05-28	2023 -2025 -	WWV-BL	20	0.1				2024	S							
			10	0.4												
	-2028 -2032	WWV-BL	20	0.1												
			10	0.3												
05-28	2341 -2342D-2344	WWV-BL	20	NM				2340	S							
			10	0.1												
05-29	1930 -1931 -1932	WWV-BL	20	NM				1928	S							
			10	0.2												
06-05	1521 -1525 -1536	WWV-BL	10	NM				1520 -1538 -1604	1	1520 -1528 -1532.5	6C	2800	15	1525- -1600	S-SWF	1+
		WWVH-BL	10	NM						dl:12	4PI	2800	4	1525-1535-1610	SPA	
										1523 - -1531	Uncl	580-125	1-			
06-06	2328 -2329 -2332	WWV-BL	10	NM				2328	S							
06-09	1436E-1436D-1445D	WWV-BL	10	0.4				1436 -1440 -1508	1					1438- -1452	S-SWF	1

Date 1961	SFD's							Solar Flares		Solar Radio Emissions				Ionospheric Effects		
	UT	Path	f	Δf, cps		ΔA	−ΔP	UT	Imp	UT	Type	Freq	Int or Peak Flux	UT	Type	Imp
	Beg - Max - End		Mc/s	(+)	(−)	db	km	Beg - Max - End		Beg - Max - End		Mc/s		Beg - Max - End		
06-09	1510 -1511 -1513	WWV-BL	10	NM				1511 - -1526	1	1510 -1511.1-1512.7	1S1	2800	4			
		WWVH-BL	10	NM												
06-09	1736 -1736D-1738	WWV-BL	10	0.5				NFR								
06-09	1751 -1751D-1753	WWV-BL	10	0.6				1750 -1752 -1756	1							
06-09	2103D-2104 -2107	WWV-BL	10	0.8				2100 -2103 -2110	1							
06-09	2249E- -2259	WWV-BL	10	NM				2248 -2254 -2306	2							
06-10	1516 -1517E-	WWV-BL	10	0.6				1509 -1514 -1526	1							
	-1518 -1522	WWV-BL	10	1.5	0.7											
06-11	1501 -1507 -1530	WWV-BL	10	NM				1502 -1518 -1612	2	1500 -1507 -1527	6Cf	2800	365	1503- -1600	S-SWF	2+
		WWVH-BL	10	NM						d1:21	4PI	2800	10	1505-1513-1520	SCNA	1+
										1505.0-1506.0-1509.5	9a	108	3		ABS	22
										1509.5-1513 -1529.5	9b	108	3	1505-1519-1600	SEA	1+
										1505 - -1511	Bur	18	2+			
										1515 - -1519	Bur	18	2			
06-14	1629E-1630 -1633	WWV-BL	10	NM	0.8			1618 -1631 -1650		1611 -Indet -1651	3S3A	2800	2	1625- -1650	SL-SWF	1+
										1612 -1614.5-1618	1S1f	2800	6			
										1627 -1629.5-1635	2S2f	2800	30			
										1618.8-1620.0-1620.8	3	108	3			
										1633.0-1634.2-1637.5	8	108	2			
										1629.5-	IIIg	880-850	1-			
										1629.5-	IIIb	780-750	1-			
06-15	1635 -1641 -1645D	WWV-BL	10	3.2				1622 -1636 -1705	1+	1630 -Indet -1725	3S3fA	2800	5	1640-1650-1705	SCNA	1
										1638 -1642 -1647	2S2f	2800	185		ABS	20
										1638.7-1640.5-1641.5	2	108	2	1640-1655-1710	SEA	1
										1643.0-1645.0-1646.5	8	108	3	1640- -1715	S-SWF	1+
										1651.7-1653.5-1656.0	9a	108	3			
										1700.0-1708.0-1849.0	9b	108	2			
										1635 - -1638	Bur	18	1+			
										1638 - -1643	Bur	18	2			
										1644 - -1653	Bur	18	1+			
06-15	1702 -1706 -1708	WWV-BL	10	0.6				1702 - -1730	1							
06-15	1718E-1718D-1723	WWV-BL	10	5.0	1.0			1718E-1720U-1728U	1	1717.5-1718.5-1723.5	2S2f	2800	95	1720- -1735	S-SWF	1-
										1717 - -1722	Bur	108	2			
06-15	1833 -1834 -1835	WWV-BL	10	0.2				1833	S							

Date 1961	SFD's							Solar Flares			Solar Radio Emissions				Ionospheric Effects		
	UT	Path	f	Δf, cps		ΔA	−ΔP	UT		Imp	UT	Type	Freq	Int or Peak Flux	UT	Type	Imp
	Beg - Max - End		Mc/s	(+)	(−)	db	km	Beg - Max - End			Beg - Max - End		Mc/s		Beg - Max - End		
06-15	1840 -1842 -1845D	WWV-BL	10	0.3				1840		S							
06-15	2203 -2204 -	WWV-BL	10	0.7				2200		S	2203.5-2203.7-2204	2S2	2800	95			
	-2206 -2210	WWV-BL	10	0.5				2202		S	2206.6-2208.0-2208.6	3	108	3			
											2210.0-2211.5-2211.5	3	108	3			
											2203 - -2206	Bur	18	2			
06-16	1754 -1755 -1757	WWV-BL	10	0.4				1755		S							
06-16	2009 -2010 -2015	WWV-BL	10	0.2				2009		S							
06-23	2319 -2320 -2331	WWV-BL	10	0.7	0.3			2318		S	2319.8-2320.4-2320.7	2S2f	2800	30			
06-24	1859 -1902 -1911	WWV-BL	10	0.6				1854E		S							
06-24	1927 -1928	WWV-BL	10	0.2					NFR								
	-1931 -1933	WWV-BL	10	0.3													
06-24	1950 -1951 -1953	WWV-BL	10	0.3					NFR								
06-25	1500 -1502 -1506	WWV-BL	10	0.3				1455		S							
06-25	1515 -1516 -1517	WWV-BL	10	0.3					NFR								
06-28	2053 -2054 -2059	WWV-BL	10	0.3	0.2			2051		S							
06-29	1917 -1918 -1928	WWV-BL	10	0.2				1917		S	1915 - -1917	Bur	18	1			
06-29	1953E-1953D-1956	WWV-BL	10	0.5	0.4			1947		S	1955 - -2030	Bur	18	1+			
06-29	2100 -2101 -	WWV-BL	10	0.4				2057		S					2050-2110-2150	SCNA	1+
	-2103 -	WWV-BL	10	0.3												ABS	25
	-2105 -	WWV-BL	10	0.2											2050-2117-2200	SEA	1+
	-2109 -2112	WWV-BL	10	1.8	0.4										2100-2108-2150	SPA	
															2102- -2125	SL-SWF	1-
07-01	2132 -2133 -2137	WWV-BL	10	1.2	0.4			2132		S							
07-02	1325 -1327D-1333	WWV-BL	10	0.4				1335E-	-1357	1							
07-05	2042 -2043 -2045D	WWV-BL	10	0.2				2042		S							
07-09	1507 -1507D-1509	WWV-BL	10	0.3				1506		S							

Date 1961	SFD's							Solar Flares		Solar Radio Emissions				Ionospheric Effects		
	UT	Path	f	Δf, cps		ΔA	−ΔP	UT	Imp	UT	Type	Freq	Int or	UT	Type	Imp
	Beg - Max - End		Mc/s	(+)	(−)	db	km	Beg - Max - End		Beg - Max - End		Mc/s	Peak Flux	Beg - Max - End		
07-10	1315 -1315D-1317	WWV-BL	10	3.1				1312 - -1450	1					1313- -1335	S-SWF	1+
07-10	1732 -1733D-1738	WWV-BL	10	1.6	0.6			NFR								
07-10	1743 -1743D-1745D	WWV-BL	10	0.4	0.4			1741 -1753 -1800	1							
07-10	1828 -1830 -1832	WWV-BL	10	0.4				NFR								
07-11	2313 -2313D-2315	WWV-BL	10	1.4				2313	S							
07-12	1934 -1935 -1937	WWV-BL	10	0.2				1940E	S							
07-12	1955 -1956 -1959	WWV-BL	10	0.4				1955	S							
07-12	2136 -2138 -2143	WWV-BL	10	0.8	0.5			2135	S					2130-2140-2220	SPA	
07-12	2249E- -2252	WWV-BL	10	NM	0.5			2248 -2254 -2318	1					2249-2252-2303	SCNA	1
															ABS	15
														2251-2257-2324	SEA	1
07-13	2212 -2214E-2216	WWV-BL	10	1.4	0.3			2211	S	2135 -2256 -2345	3S3fA	2800	10	2213-2221-2234	SEA	2
										2213 -2214 -2215.3	2S2	2800	11			
07-14	1216E-1216 -1217	WWV-BL	10	0.8				NFR								
07-14	1218 -1218D-1220	WWV-BL	10	1.0				NFR								
07-14	1225E-1225 -1225D	WWV-BL	10	1.0				1227	S							
07-14	1314 -1314D-1316	WWV-BL	10	0.4				1314	S							
07-14	1800 -1801 -1803	WWV-BL	10	0.4				NFR								
07-15	1510 -1512 -	WWVH-BL	10	4.2				1434 -1508 -1857U	3	1510.5-1512 -1517	6Cf	2800	76	1512-1517-1530	SCNA	1
	-1514 -	WWVH-BL	10	2.8				1508 -1512 -1530	2	1536 -1610 -1623	6Cf	2800	111		ABS	21
	-1520 -1530D	WWVH-BL	10	2.0						1505 -1616 -1845	9	108	3	1512- -1705	S-SWF	3
														1515- -1517	SEA	1-
07-16	1259 -1300 -1310	WWV-BL	10	3.0				1258 -1300 -1316	1					1300- -1340	SEA	1
07-16	1507 -1509 -1511	WWV-BL	10	0.2				1507E- -1525D	1							
07-16	1557 -1557D-	WWV-BL	10	1.3				1556	S	1557.3-1557.8-1606.8	2S2	2800	15			
	-1558D-1559	WWV-BL	10	0.6												

TOT

Date 1961	SFD's							Solar Flares		Solar Radio Emissions				Ionospheric Effects		
	UT	Path	f	Δf, cps		ΔA	−ΔP	UT	Imp	UT	Type	Freq	Int or	UT	Type	Imp
	Beg - Max - End		Mc/s	(+)	(−)	db	km	Beg - Max - End		Beg - Max - End		Mc/s	Peak Flux	Beg - Max - End		
07-16	1630 -1631 -1642	WWV-BL	10	1.4	0.8			1625	S	1620 -1628 -1650	3S3	2800	4			
07-16	1650E-1651 -1653	WWV-BL	10	0.8				1650	S							
07-16	1659 -1700 -1701	WWV-BL	10	0.6				NFR								
07-16	1856E-1856 -1857	WWV-BL	10	0.3				1856E	S							
07-16	1911E-1911D-1912	WWV-BL	10	0.5				1910	S							
07-16	1920 -1923E-1929	WWV-BL	10	1.0	0.8			1909 -1922 -1935	1							
07-16	1939 -1940D-1943	WWV-BL	10	1.2	0.3			1938 -1943 -2055	1+	1933 -1955 -2125	3S3A	2800	16	1942-2008-2040	SPA	
								1938 -2040 -2055	1	1950 -1952 -1955.3	2S2	2800	14			
	1957 -1958E-1959	WWV-BL	10	0.2												
	2001 -2001D-2003	WWV-BL	10	0.4												
	2009 -2009D-2011	WWV-BL	10	0.3												
	2019 -2020E-2022	WWV-BL	10	0.5												
	2030 -2031 -	WWV-BL	10	0.6												
	-2037 -2043D	WWV-BL	10	2.4	0.6											
07-16	2059 -2100 -2105	WWV-BL	10	0.6	0.4			2057	S							
07-17	1435 -1436D-1438	WWV-BL	10	1.0				NFR								
07-17	1610 -1611 -1613	WWV-BL	10	0.4				1610E- -1804D	1							
07-17	1649E-1649D-	WWV-BL	10	0.6				1645 -1657 -1711	1	1640 -1650 -1720	3S3fA	2800	4			
	-1653 -	WWV-BL	10	0.5						1657 -1657.5-1659	6C	2800	7			
	-1655 -	WWV-BL	10	0.6												
	-1658 -1700	WWV-BL	10	0.6												
07-17	1820 -1820D-1842	WWV-BL	10	0.8				1817	S	1830 -1850 -1915	3S3	2800	4			
07-17	1913 -1915E-	WWV-BL	10	3.4	1.0			1907 -1916 -1935	1							
	-1928 -1930	WWV-BL	10	0.6												
07-17	2034E-2034 -2036	WWV-BL	10	0.3				2033	S							
07-17	2132 -2133E-	WWV-BL	10	0.6				2125 -2138 -2255	1	2140 -2141.8-2202	6Cf	2800	54	2140-2147-2220	SCNA	2
	-2135D-			0.6						d1:17	4PI	2800	15		ABS	35
	-2138 -			0.6										2140- -2230	S-SWF	2+
	-2140 -			1.0										2140-2144-2300	SPA	
	-2141 -			1.6										2141-2152-2230	SEA	2+
	-2143D-2145D			1.1												

Date 1961	SFD's							Solar Flares		Solar Radio Emissions				Ionospheric Effects		
	UT	Path	f	Δf, cps		ΔA	−ΔP	UT	Imp	UT	Type	Freq	Int or Peak Flux	UT	Type	Imp
	Beg - Max - End		Mc/s	(+)	(−)	db	km	Beg - Max - End		Beg - Max - End		Mc/s		Beg - Max - End		
07-18	1441 -1441D-1443	WWV-BL	10	0.4				1436	S							
07-18	1917 -1917D- -1918D- -1919D-	WWV-BL	10	1.0 0.6 0.6				1916	S							
07-18	2051 -2052 -2057	WWV-BL	10	0.2				2046	S							
07-18	2103 -2104 -2106	WWV-BL	10	0.2				2102	S	2106 -2112 -2140	3S3	2800	4			
07-18	2257 -2259 -2301	WWV-BL	10	0.5				2258	S							
07-19	1501 -1502 -1504	WWV-BL	10	0.2				1501E- -1510D	1	1452 -1454 -1550	3S3A	2800	2			
07-19	1806 -1808 -1810	WWV-BL	10	0.3				1801	S							
07-19	1906 -1910 -1922	WWV-BL	10	0.8				1903 -1912 -1945	1							
07-19	2055 -2059D-2110D	WWV-BL	10	2.0	2.4			2051 -2102 -2120	1	2100 -Indet -2114	3S3A	2800	2	2055-2110-2200	SPA	
										2103.3-2105 -2109.3	6C	2800	13	2100- -2125	SL-SWF	1+
07-20	1551 -	WWV-BL	10	NM				1553	3	1552 -1553.5-	6Cf	2800	1200	1550- -2200	S-SWF	3+
		SS-BL	2.1	NM						-1621.3-1634	6Cf		1800	1551- -1600	SPA	
										d7:30	4PI	2800	80	1552- -1752	SEA	2+
										1557.0-1559.0-1604.2	9A	108	3	1552- -2140	SCNA	3
										1605.2-1608.0-1617.7	9B	108	3		ABS	88
										1557 - -2013	Bur	18	2			
07-21	1714 -1717 -1728	WWV-BL	10	2.6	1.4			1714 -1718 -1734	2	1655 -1827 -2330	3S3A	2800	10	1702- -1815	S-SWF	2+
										1701 -1703.5-1721	6Cf	2800	59	1702-1710-1900	SPA	
														1703-1708-	SCNA	1
															ABS	20
														1703-1710-	SEA	2
07-22	1634 -1634D-1635	WWV-BL	10	0.3				1636	S	1635 -Indet -1750	3S3	2800	5			
07-23	1835 -1836D-1839	WWV-BL	10	0.7				1835	S							
07-23	2130 -2131 -2133	WWV-BL	10	0.4				2130	S							
07-23	2227 -2228 -2233	WWV-BL	10	0.3				2227	S	2227 - -2231	Bur	18	2			
07-24	1813 -1814 -1820	WWV-BL	10	0.6				1722 -1827U-2214	2+	1730 -1802 -2330D	3S3f	2800	16	1748-1810-1900	SPA	
										1816 - -1820	Bur	18	1	1755- -1930	SL-SWF	2+

Date 1961	SFD's							Solar Flares		Solar Radio Emissions				Ionospheric Effects		
	UT	Path	f	Δf, cps		ΔA	−ΔP	UT	Imp	UT	Type	Freq	Int or	UT	Type	Imp
	Beg - Max - End		Mc/s	(+)	(−)	db	km	Beg - Max - End		Beg - Max - End		Mc/s	Peak Flux	Beg - Max - End		
07-24	1830 -1831 -1833	WWV-BL	10	0.3				NFR								
07-25	1219 -1220 -1223	WWV-BL	10	0.3				1219	S	1224 -1224.8-1228 1220 -1226 -1231	6C Bur	2800 18	7 1+			
07-25	1356 -1357D-1403	WWV-BL	10	0.8				1354	S	1335 -1357.5-1407	3S3f	2800	5			
07-25	1441 -1442 -1443	WWV-BL	10	0.9				1441	S							
07-25	2241 -2241D-2245	WWV-BL	10	0.6				2242E-2244 -2316	1	2239.5-2241.5-2243.5 d20	2S2f 4PI	2800 2800	13 5			
07-26	1940 -1941 -1942	WWV-BL	10	0.4				1940	S							
07-26	1946D-1947D- -1948D-1949D	? -BL ? -BL	10 10	4.0 1.0				1947	S	1947 -1947.8-1952	2S2	2800	45	1948-1955-2030	SPA	
07-28	1956 -1957E-1959	WWV-BL	10	0.4	0.4			1954	S							
07-28	2223 -2224 -2227	WWV-BL	10	0.3	0.4			2222	S	2223 -2223.5-2224	1S1	2800	5			
07-28	2338E-2339 -2341	WWV-BL	10	0.4				2338	S							
08-10	1438 -1439 -1441	WWV-BL	10	0.6				1436 -1440 -1448	1	1438.3-1439.2-1441.8 1432 - -1443	1S1 Bur	2800 18	3.5 2	1435-1445-1500	SEA	1
08-10	1505E-1505 -1506	WWV-BL	10	0.5				1502 - -1510D	1	1505.2-1505.5-1506 1505 - -1510	1S1 Bur	2800 18	6 2			
08-10	2314 -2318 -2323	WWV-BL SS-BL	10 4	0.5 0.6				2309 -2320 -2353	1	2315.5-2316.8-2318	2S2	2800	22	2321-2328-2346	SEA	1
08-11	1705 -1709 -1716	WWV-BL	10	0.5				1708	S					1718-1732-1805	SEA	2
08-12	1614 -1615 -1617	WWV-BL	10	0.2				1614 -1618 -1635D	1	1611 -Indet -1656 1613.5-1616 -1618 1614 - -1635	3S3A 1S1 Bur	2800 2800 18	2 7 1	1615-1630-1645	SEA	1+
08-12	1628 -1629 - -1633 -1636	WWV-BL WWV-BL	10 10	0.5 0.5				1628	S	1629 -1630.3-1633 1620.5-1622.5-1625	2S2f 8	2800 108	12 3			
08-12	1711 -1713 -1717	WWV-BL SS-BL	10 5	1.0 NM	0.6			1705 -1714 -1736	1	1712.5-1713.2-1713.5 1711.2-1714.0-1716.7 1711 - -1717	1S1 8 Bur	2800 108 18	3 3 2			

Date 1961	SFD's							Solar Flares		Solar Radio Emissions				Ionospheric Effects		
	UT	Path	f	Δf, cps		ΔA	−ΔP	UT	Imp	UT	Type	Freq	Int or	UT	Type	Imp
	Beg - Max - End		Mc/s	(+)	(−)	db	km	Beg - Max - End		Beg - Max - End		Mc/s	Peak Flux	Beg - Max - End		
08-12	2048 -2049 -	WWV-BL	10	2.2				2050 -2052 -2115	1	2048.5-2051.3-2052.5	6Cf	2800	60	2052- -2105	S-SWF	1-
		SS-BL	5	1.4						d10	4PI	2800	4			
	-2050 -	WWV-BL	10	1.4						2048.9-2049.0-2053.9	8	108	3			
		SS-BL	5	0.8												
	-2051 -2054	WWV-BL	10	2.4	1.0											
		SS-BL	5	NM	NM											
08-13	1906 -1908 -1914	WWV-BL	10	2.2	0.3			1906 -1910 -1931	1	1907.5-1909 -1919.5	2S2	2800	10	1907-		
										1907.0-1907.5-1913	2	108	2			
										1907 - -1914	Bur	18	2			
08-14	2214E-2214 -2216	WWV-BL	10	0.2				2213	S							
08-15	1646 -1647 -1648D	? -BL	10	2.8				1640 -1647 -1710	1	1645 -1705 -1735	3S3A	2800	3	1643-1652-1720	SPA	
										1646.5-1648.3-1651.5	6Cf	2800	13	1647-1655-1708	SEA	1+
08-18	2038 -2041D-	WWV-BL	10	0.6				2038 -2048 -2103	2	2036 -2052 -2115	3S3A	2800	12	2040- -2120	S-SWF	1+
	-2054 -	WWV-BL	10	0.2						2039 -2044 -2050	2S2f	2800	43	2040-2055-2220	SPA	
	-2056 -2100	WWV-BL	10	0.3						2054.2-2056.3-2058	6C	2800	28	2045-2107-2135	SEA	3
										2047.5-2049.3-2054	8	108	3	2049E- -2200U	SCNA	
										2036 - -2050	Bur	18	3			
08-25	1608 -1611 -1612	WWV-BL	10	0.2				1608	S							
08-25	1624 -1625 -1629	WWV-BL	10	0.3				1625E	S							
08-25	2007 -2008 -2010	WWV-BL	10	0.6				2006	S							
08-25	2356 -2356D-2357	WWV-BL	10	NM				2357	S							
		SS-BL	4	0.1												
08-25	2358 -2358D-2400	WWV-BL	10	NM				2359 - -0018	1							
		SS-BL	4	0.3												
08-26	1617 -1618 -1621	WWV-BL	10	0.2				1616E- -1630D	1							
08-29	1714 -1715 -1718	WWV-BL	10	0.3				1715	S							
08-29	1849E-1851 -1855	WWV-BL	10	0.5				1846	S							
08-29	2020 -2021 -2024	WWV-BL	10	0.2				2021	S	2020.0-2023.0-2023.8	2	108	3			
08-30	1618 -1621 -1624	WWV-BL	10	0.3				1617 -1623 -1634	1							
08-31	1459 -1502 -1506	WWV-BL	10	0.4				1458 -1506 -1520	1							

Date 1961	SFD's							Solar Flares		Solar Radio Emissions				Ionospheric Effects		
	UT	Path	f	Δf, cps		ΔA	−ΔP	UT	Imp	UT	Type	Freq	Int or Peak	UT	Type	Imp
	Beg - Max - End		Mc/s	(+)	(−)	db	km	Beg - Max - End		Beg - Max - End		Mc/s	Flux	Beg - Max - End		
08-31	1512 -1513 -1516	WWV-BL	10	0.3				NFR								
08-31	1758 -1759 -1802	WWV-BL	10	0.1				1756	S	1747 -Indet -1825	3S3A	2800	2			
										1758.3-1800.5-1803	1S1	2800	6			
08-31	2109 -2110 -2111	WWV-Bl	10	0.2				2110	S							
08-31	2121D-2122 -2123	WWV-BL	10	0.1				NFR								
09-01	1413 -1414 -1417	WWV-BL	10	NM				1427E- -1512D	1	1308E - -1540	cont	20-41	1			
		WWV-SY	10	0.7												
		SS-BL	5	0.7												
			4	0.6												
09-01	1423 -1423D-1425	WWV-BL	10	NM				1420 -	S	1308E - -1540	cont	20-41	1			
		WWV-SY	10	0.3												
		SS-BL	5	NM												
			4	NM												
09-02	0320 -0322 -0324	WWVH-SY	10	3.5				0321 -0324 -0346	1					0323-0325-0405	SCNA	1
															ABS	15
														0324-0340-0402	SEA	1
09-02	1413 -1417 -1419	WWV-BL	10	0.4				1348 -1413 -1439D	1	1412 - -1415	Bur	18	1			
		WWV-SY	10	0.2						1416 - -1419	Bur	18	1-			
		SS-BL	5	NM												
			4	NM												
09-02	1431 -1432 -1436	WWV-BL	10	1.3				1432 -	S	1431.45- -1435.30	III	11-41	2+	1347-1358-1445	SEA	1
		WWV-SY	10	1.4						1431.9-1432.6-1434.7	3	108	3			
		SS-BL	5	0.4						1433 - -1437	BUR	18	1+			
			4	0.4												
09-02	1509 -1510 -1512	WWV-BL	10	0.3				NFR								
		WWV-SY	10	NM												
		SS-BL	5	NM												
			4	0.2												
09-02	1645D-1646 -1649	WWVH-SY	10	1.4				1638U-1650 -1700	1					1638-1647-1715U	SEA	
		SS-BL	4	0.3										1646-1651-1658	SCNA	1
															ABS	10

Date 1961	SFD's							Solar Flares		Solar Radio Emissions				Ionospheric Effects		
	UT	Path	f	Δf, cps		ΔA	−ΔP	UT	Imp	UT	Type	Freq	Int or	UT	Type	Imp
	Beg - Max - End		Mc/s	(+)	(−)	db	km	Beg - Max - End		Beg - Max - End		Mc/s	Peak Flux	Beg - Max - End		
09-02	2235 -2238 -2240D	WWV-BL	10	0.4				2230 -2250 -2350	1+	2238 - -2241	BUR	18	1			
		WWV-SY	10	0.2												
		SS-BL	5	NM												
			4	NM												
09-02	2319 -2320 -2324	WWV-BL	10	0.3												
		WWV-SY	10	NM												
		SS-BL	5	NM												
			4	0.2												
09-02	2333 -2334 -2336	WWV-BL	10	0.3				2335 - -2346D	1							
		WWV-SY	10	0.2												
		SS-BL	5	NM												
			4	0.2												
09-03	1625 -1626 -1628	WWV-BL	10	0.1				1626	S							
		WWV-SY	10	NM												
		SS-BL	5	NR												
			4	NM												
09-03	1834 -1835 -1839	WWV-BL	10	0.2				NFR								
		WWV-SY	10	NM												
		SS-BL	5	NR												
			4	NM												
09-03	2019 -2024 -2030	WWV-BL	10	0.4				2015 -2026U-2100U	1	2016 - -2025	cont	28-41	1			
		WWV-SY	10	NM						2020 - -2022.15	III	21-41	2			
		SS-BL	5	NM						2021 - -2026	BUR	18	1			
			4	NM						2024 - -2024.15	III	20-41	1			
09-03	2040 -2045D-2100	WWV-BL	10	NM	NM			2040 -2047 -2125	1	2042 -2045.5-2052	2S2f	2800	270	2043- -2115	S-SWF	1+
		WWV-SY	10	NM	NM					d1:58	4PI	2800	8	2044-2051-2103	SCNA	2
		SS-BL	5	4.2	1.0					2042 - -2042.30	III	24-35	1-		ABS	35
			4	1.2	NM					2050.0-2050.7-2052	3	108	2	2044-2050-2140	SPA	51
										2053.30- -2113.30	II	30-41	1+	2045-2053-	SEA	2+
09-04	1430 -1432 -1434	WWV-BL	10	12	2.4	8		1425 -1435 -1512	1	1425 - -2105	3S3A	2800	6	1429-1439-1510U	SPA	26
		WWV-SY	10	NM						1431.5-1432.3-1433.5	2S2f	2800	46	1430- -1500	S-SWF	1+
		SS-BL	5	NM						d14.5	4PI	2800	7	1433-1437-1449	SCNA	1
			4	6	0.8					1435.15- -1437.15	III	16-41	1+		ABS	10
										1446.15- -1446.30	III	22-40	1	1433- -1458	SEA	1

Date 1961	SFD's							Solar Flares		Solar Radio Emissions				Ionospheric Effects		
	UT Beg - Max - End	Path	f Mc/s	Δf, cps (+)	Δf, cps (−)	ΔA db	−ΔP km	UT Beg - Max - End	Imp	UT Beg - Max - End	Type	Freq Mc/s	Int or Peak Flux	UT Beg - Max - End	Type	Imp
09-04	1513E-1513D-	WWV-BL	10	6.0				1512 -1520 -1540U	1	1513.7 -1514 -1516.2	2S2f	2800	85	1510-1518-1600	SPA	39
		WWV-SY	10	4.0						d42.8	4PI	2800	4	1512-1518-1542	SCNA	1+
		SS-BL	5	1.8											ABS	30
			4	1.6										1514- -1534	SEA	1
														1515- -1540	S-SWF	1+
	-1514 -1516	WWV-BL	10	3.0	0.8											
		WWV-SY	10	2.0	0.6											
		SS-BL	5	0.9	0.2											
			4	0.8	0.4											
09-04	1530 -1532 -1540	WWV-BL	10	0.3				1538E	S							
		WWV-SY	10	0.3												
		SS-BL	5	NM												
			4	0.3												
09-04	1807 -1808 -1810	WWV-BL	10	1.0	0.4			1807	S							
		WWV-SY	10	0.6	NM											
		SS-BL	5	NM	NM											
			4	0.2	NM											
09-04	1834 -1835 -1837	WWV-BL	10	1.1	0.4			1834 -1846 -2010	1+	1842.45- -1843.15	III	21-32	1	1833-1840-1910U	SPA	26
		WWV-SY	10	0.8	0.4											
		SS-BL	5	NM	NM											
			4	NM	NM											
09-04	1853 -1854 -1855	WWV-BL	10	0.4				NFR								
		WWV-SY	10	0.2												
		SS-BL	5	NM												
			4	0.1												
09-04	1902 -1903D-	WWV-BL	10	2.6				1902 -1905 -1919U	1	1902.8 -1903.2-1905.0	2S2f	2800	16			
		WWV-SY	10	1.8												
		SS-BL	5	1.0												
			4	0.5												
	-1905 -1909	WWV-BL	10	1.0	0.8									1910-1915-2040	SPA	58
		WWV-SY	10	0.8	0.5											
		SS-BL	5	0.5	0.4											
			4	0.7	NM											
09-04	1911 -1915 -1920	WWV-BL	10	6.6	3.0			1911 -1924U-2018	2	1911 -1914.8 -1919	6Cf	2800	143	1913- -1940	S-SWF	1+
		WWV-SY	10	4.6	1.8					d31	4PI	2800	8	1914-1919-1950	SCNA	2
		SS-BL	5	3.0	1.1										ABS	30
			4	NM	NM											

Date 1961	SFD's							Solar Flares		Solar Radio Emissions				Ionospheric Effects		
	UT	Path	f	Δf, cps		ΔA	−ΔP	UT	Imp	UT	Type	Freq	Int or Peak Flux	UT	Type	Imp
	Beg - Max - End		Mc/s	(+)	(−)	db	km	Beg - Max - End		Beg - Max - End		Mc/s		Beg - Max - End		
09-05	1415 -1418 -1420	WWV-BL	10	1.5				1415 - -1510D	1	1415 - -2155	3S3A	2800	12	1418-1441-1600	SEA	1
		WWV-SY	10	NM						1415.5-1417.2-1422.5	6cf	2800	88			
		SS-BL	5	NR												
			4	NR												
09-05	1427 -1431 -1435	WWV-BL	10	0.8				1428E- -1514D	1+	1428.3- 1432 - 1439	6Cf	2800	50	1430- -1450	S-SWF	1
		WWV-SY	10	NM												
		SS-BL	5	NR												
			4	NR												
09-05	1514 -1515 -1518	WWV-BL	10	1.0				1514 - -1544D	1	1509.9-1510.3-1512	1S1	2800	6			
		WWV-SY	10	NM												
		SS-BL	5	0.3												
			4	NR												
09-05	1649E-1652 -1655	WWV-BL	10	0.5				1644 -1658 -1734	1	1647 - 1652 - 1655	2S2	2800	20	1640- -1730	SL-SWF	2+
		WWV-SY	10	0.6						dl:03	4PI	2800	8	1649-1650-	SPA	32
		SS-BL	5	0.4										1653-1702-1730	SEA	2
			4	NR												
09-05	1811 -1816 -	WWV-BL	10	0.3				1812	S							
		WWV-SY	10	NM												
		SS-BL	5	NR												
			4	NR												
09-05	1822 -1825 -1829	WWV-BL	10	0.3				1817	S							
		WWV-SY	10	0.3												
		SS-BL	5	NR												
			4	NR												
09-08	1330 -1331 -1334	WWV-BL	20	NR				1331 -1335 -1350	1							
			10	NM												
		WWV-SY	10	NM												
		SS-BL	5	NR												
			4	0.2												
09-08	1628 -1629 -1632	WWV-BL	20	NR				1628	S	1430 - - 2115	3S3A	2800	9	1552-1614-1640	SEA	2
			10	0.7						1601.45- - 1630	II	11-41	3	1552- -1705	SL-SWF	2+
		WWV-SY	10	0.4						1606.30- - 1730	IV	20-41	2	1553- -1633	SPA	X
		SS-BL	5	0.2						1621.8-1623.2- 1627	2S2f	2800	10	1558-1605-1624	SCNA	2
			4	0.2						1641 - 1647.2- 1657	6C	2800	9		ABS	30

Date 1961	SFD's							Solar Flares		Solar Radio Emissions				Ionospheric Effects		
	UT	Path	f	Δf, cps		ΔA	−ΔP	UT	Imp	UT	Type	Freq	Int or	UT	Type	Imp
	Beg - Max - End		Mc/s	(+)	(−)	db	km	Beg - Max - End		Beg - Max - End		Mc/s	Peak Flux	Beg - Max - End		
09-08	1754 -1755 - 1757	WWV-BL	20	NR				NFP		1754.3-1755.3-1758.5	2S2	2800	25			
			10	NR												
		WWV-SY	10	0.4												
		SS-BL	5	NR												
			4	NR												
09-10	1950 -	WWV-BL	20	NM				1950 - 2010 - 2052	1	1927.30- - 1930	III	8-34	1-	1940-2003-2125U	SEA	2
			10	NM						1930 - 2001 - 2031	6Cf	2800	880	1942- -2123	SL-SWF	3
		WWV-SY	10	NM						d2:00	4PI	2800	44	1943-1959-2115	SCNA	2
		SS-BL	5	NM						1931.15- -1932.15	III	8-39	1-		ABS	59
			4	NM						1933.15- - 1935	III	8-41	1-			
										1934 -1939.3 - 2014	7	108	2			
										1935.15- - 2038	II	7.6-41	2			
										1951 - - 2025	BUR	18	3			
										2013 - - 2154	IV	21-41	1+			
09-13	1020	TR-AC	20	.33				1020E- - 1045D	1							
09-13	1120 -	TR-AC	20	.2				1119 -1129 -1131	1							
	1125 -	TR-AC	20	.33												
09-14	1929 -1930 -1933	WWV-BL	10	0.3				1932E	S							
		WWV-SY	10	0.2												
		SS-BL	5	NM												
			4	NR												
09-14	1937 -1937D-1940	WWV-BL	20	0.2				1936	S							
			10	0.6												
		WWV-SY	10	0.5												
		SS-BL	5	NM												
			4	NR												
09-15	0735 -	TR-AC	20	.25				0735E-0744U-0757D	1							
09-16	1058 -	TR-AC	20	3				1057 -1105 -1258D	2+					1102- -1152	S-SWF	2
09-17	0920 -	TR-AC	20	1				0919E- -0948D	1							
09-17	1306 -	TR-AC	20	.33				1304 - -1328	1	1305 - 1330 - 1513	3S3f	2800	4			
09-17	1726 -1727 -1735	TR-AC	20	0.8				1726 -1734 -1744	1	1730.5-1731.5-1732	1S1	2800	4			
		WWV-BL	20	0.2												
			10	0.4												
		WWV-SY	10	0.4												
		SS-BL	5	NM												
			4	NM												

Date 1961	SFD's							Solar Flares		Solar Radio Emissions				Ionospheric Effects		
	UT	Path	f	Δf, cps		ΔA	−ΔP	UT	Imp	UT	Type	Freq	Int or Peak Flux	UT	Type	Imp
	Beg - Max - End		Mc/s	(+)	(−)	db	km	Beg - Max - End		Beg - Max - End		Mc/s		Beg - Max - End		
09-17	1749 -1752 -1756	WWV-BL	20	0.2				1748 -1756 -1808	1	1741.5-1742.5-1742.6	3	108	2			
			10	0.7						1750.2-1752.4-1757.9	2S2f	2800	18			
		WWV-SY	10	0.4						d47	4PI	2800	2			
		SS-BL	5	0.2												
			4	NM												
09-18	2041 -2044 -2045D	WWV-BL	20	0.2				2042	S							
			10	0.3												
		WWV-SY	10	0.3												
		SS-BL	5	0.1												
			4	NM												
09-20	1021 -	TR-AC	20	2.5				1021 -1022 -1026	1							
09-22	2050 -2051D-2054	WWV-BL	20	0.1				2052	S							
			10	0.2												
		WWV-SY	10	0.2												
		SS-BL	5	NR												
			4	NM												
09-23	1103 -	TR-AC	20	.25				1101E- -1113D	1							
09-23	1323 -	TR-AC	20	.25				1323 - -1407	1							
09-24	0705 -	TR-AC	20	.25				0700E- -0900D	1							
								0708E- -0850	1							
09-24	1352 -	TR-AC	20	.67				1350 - - 1431D	1							
09-25	0640 -	TR-AC	20	.5				0641 - - 0720	1							
09-25	1015 -	TR-AC	20	1.33				1016 - - 1030D	1							
09-25	1838 -1839D-1843	WWV-BL	20	NR				1838 -	S	1839.5-1840.3-1841.5	2S2	2800	12			
			10	0.7												
		WWV-SY	10	0.5												
		SS-BL	5	NR												
			4	0.2												
09-26	0620 -	TR-AC	20	.25				0620E- - 0903D	2							
09-26	0911 -	TR-AC	20	.25				0909E-	1							
09-26	1015 -	TR-AC	20	.25				1016E- - 1108D	2							

Date 1961	SFD's							Solar Flares		Solar Radio Emissions				Ionospheric Effects		
	UT	Path	f	Δf, cps		ΔA	−ΔP	UT	Imp	UT	Type	Freq	Int or	UT	Type	Imp
	Beg - Max - End		Mc/s	(+)	(−)	db	km	Beg - Max - End		Beg - Max - End		Mc/s	Peak Flux	Beg - Max - End		
09-26	1518 -	TR-AC	20	.33				1518E- - 1547D	1							
09-27	1107 -	TR-AC	20	4.5				1107 -1110- 1121	1							
09-27	1448	TR-AC	20	.5				1445 -1451- 1506	1							
09-27	1952 -1954E -2000	WWV-BL	20	NR				1950 -1958- 2007	1	1952.45- -1956.15	III	7.6-41	2	1950- -2045	SEA	2
			10	4.0	1.0					1952.5-1952.7-1954.5	6C	2800	13	1955- -2015	S-SWF	1
		WWV-SY	10	2.8	0.8					1952.5-1953.4-2004.5	2	108	2			
		SS-BL	5	1.9	0.3					1959.15- -1959.30	III	7.6-41	1-			
			4	1.4	NM					2001.30- - 2015	II	25-41	1+			
09-28	0910 -	TR-AC	20	0.7				0907E-0911-0922	1							
	0917 -	TR-AC	20	0.8				0915 -0917-0921	1							
09-28	1022 -	TR-AC	20	.5				1018E- -1034D	1							
								1022E- -1050D	1							
09-28	1527 -1530E-1535	TR-AC	20	0.3				1520E-1530-1536	1	1432 - -2214.30	cont	21-41	1-			
		WWV-BL	20	NR						1528.5- 1529 -1530.5	1S1	2800	6			
			10	0.5	NM											
		WWV-SY	10	0.8	0.3											
		SS-BL	5	0.6	0.3											
			4	0.4	0.2											
09-28	2212 -2216D-2223	WWV-BL	20	2.8	0.4			2202 - 2224 - 2530	3	2211 - 2218 - 2241D	2S2f	2800	800	2211-2228-2300D	SPA	30
			10	5.6	1.4					2212 - -2212.30	III	16-41	2	2216-2224-2258	SEA	2
		WWV-SY	10	4.2	1.0					2213 - 2217 - 2222	9A	108	3	2218- -2320	S-SWF	2
		SS-BL	5	3.0	0.8					2214 - - 2308	BUR	18	3			
			4	3.0	0.8					2214.30- - 2358	IV	14-41	2+			
										2217 - - 2249	II	15-41	3+			
										2222 - 2347 - 2404	9B	108	3			
09-29	1051 -	TR-AC	20	2				1052E- - 1111D	1							
09-29	1150 -	TR-AC	20	.3				1148E- - 1216D	1+							
10-03	0720 -	TR-AC	20	.33				0720 - - 0732	1							
10-03	2305 -2307 -2315	WWV-BL	20	NR				2305 - 2308 - 2318	1+					2305-2307-2318	SCNA	1
			10	0.8	0.5										ABS	25
		WWV-SY	10	0.4	NM									2313-2322	SEA	1
		SS-BL	5	0.4	0.2											
			4	0.4	0.4											

Date 1961	SFD's							Solar Flares		Solar Radio Emissions				Ionospheric Effects		
	UT	Path	f	Δf, cps		ΔA	−ΔP	UT	Imp	UT	Type	Freq	Int or	UT	Type	Imp
	Beg - Max - End		Mc/s	(+)	(−)	db	km	Beg - Max - End		Beg - Max - End		Mc/s	Peak Flux	Beg - Max - End		
10-04	0632 -	TR-AC	20	.2				0632E- - 0705	1+							
10-05	0722 -	TR-AC	20	.2				0720E- - 0735	1							
10-09	0945 -	TR-AC	20	.33				0940 - - 1017	2							
10-12	1042 -	TR-AC	20	.33				1041E- - 1045D	1							
10-13	1238 -	TR-AC	20	.5				1225 - - 1309D	1							
10-14	1442 -	TR-AC	20	.33				1440E- - 1454D	1							
11-06	1849 -1852 -1857	WWV-BL	20	0.1	0.2			NFP		1845 - 1850 - 1913	3S3	2800	3			
			10	0.3	0.2											
		WWV-SY	10	0.5	0.3											
		SS-BL	5	0.1	NM											
			4	NM	NM											
11-09	1333 -1335 -1339	WWV-BL	20	NR				1335E- -1346D	1							
			10	0.2												
		WWV-SY	10	0.1												
		SS-BL	5	NM												
			4	0.1												
11-09	1700 -1704 -1710	WWV-BL	20	NR				1702	S	1700.15- -1700.30	III	25-41	1-			
			10	0.3												
		WWV-SY	10	0.2												
		SS-BL	5	NM												
			4	NM												
11-10	1436 -1438 -1441	WWV-BL	20	NM				1434 - 1444 - 1452	1+	1404 - - 1432	1	108	1	1432-1445-1730	SPA	60
			10	0.1						1428 - 1444 - 1506	6Cf	2800	124	1433-	SCNA	1+
		WWV-SY	10	0.1						d2:50	4PI	2800	8	1435-1456-	SEA	2
		SS-BL	5	NM						1432.0-1435 - 1437	9A	108	3	1436- -1534	SL-SWF	2+
			4	0.1						1433.45- - 1509	II	21-41	3			
										1438.0-1441 - 1501	9B	108	3			
										1440 - - 1543	IV	21-41	3			
										1445 - - 1516	BUR	18	2			

Date 1961	SFD's							Solar Flares		Solar Radio Emissions				Ionospheric Effects		
	UT	Path	f	Δf, cps		ΔA	−ΔP	UT	Imp	UT	Type	Freq	Int or	UT	Type	Imp
	Beg - Max - End		Mc/s	(+)	(−)	db	km	Beg - Max - End		Beg - Max - End		Mc/s	Peak Flux	Beg - Max - End		
11-10	1526 -1528 -1534	WWV-BL	20	0.2				1510E- -1530D	1	1440 - -1543	IV	21-41	3			
			10	0.4												
		WWV-SY	10	0.3												
		SS-BL	5	NM												
			4	0.1												
11-11	1541 -1543 -1545D	WWV-BL	20	0.2				1540	S	1541.5-1542.5-1544.3	8	108	3			
			10	0.4						1542 - -1543.45	III	23-41	1+			
		WWV-SY	10	NR												
		SS-BL	5	NM												
			4	NM												
11-11	1915 -1918 -1922	WWV-BL	20	0.1				NFR								
			10	0.2												
		WWV-SY	10	NM												
		SS-BL	5	0.1												
			4	0.1												
11-19	1608 -1612 -1617	WWV-BL	20	0.1				1615E	S							
			10	0.2												
		WWV-SY	10	NM												
		SS-BL	5	NM												
			4	NM												
11-21	1819 -1821 -1825	WWV-BL	20	NM				1818	S							
			10	0.1												
		WWV-SY	10	NR												
		SS-BL	5	NM												
			4	NM												
11-22	2014 -2016 -2024	WWV-BL	20	0.6	NM	10	0.09	2012 -2016 -2044	2					2015-2018-2045	SCNA	1
			10	1.6	0.4	10	0.57								ABS	25
		WWV-SY	10	0.9	NM									2016-2025-2115	SEA	1+
		SS-BL	5	0.7	0.4											
			4	0.8	0.3											
11-24	1852 -1854 -1857	WWV-BL	20	NM				1853E	S							
			10	0.1												
		WWV-SY	10	NR												
		SS-BL	5	NM												
			4	NM												

Date 1961	SFD's							Solar Flares		Solar Radio Emissions				Ionospheric Effects		
	UT	Path	f	Δf, cps		ΔA	−ΔP	UT	Imp	UT	Type	Freq	Int or Peak Flux	UT	Type	Imp
	Beg - Max - End		Mc/s	(+)	(−)	db	km	Beg - Max - End		Beg - Max - End		Mc/s		Beg - Max - End		
12-01	1633 -1634D-1637	WWV-BL	20	NR				NFR								
			10	0.4												
		WWV-SY	10	0.3												
		SS-BL	5	NM												
			4	NR												
12-01	1817 -1818 -1820	WWV-BL	20	NR				1816 -1817- 1840	1	1817 -1817.5 - 1818.5	2S2	2800	8			
			10	0.5						d23.5	4PI	2800	2			
		WWV-SY	10	0.5												
		SS-BL	5	0.6												
			4	0.6												
12-01	1910 -1911D-1915	WWV-BL	20	NR				NFR								
			10	0.5												
		WWV-SY	10	0.4												
		SS-SY	5	0.4												
			4	0.3												
12-01	2132 -2133 -2137	WWV-BL	20	NR				NFR								
			10	0.5												
		WWV-SY	10	0.4												
		SS-BL	5	NM												
			4	0.2												
12-02	1920 -1922 -1926	WWV-BL	20	0.3				1920 - 1925 - 1942D	1	1920.5- 1924 - 1932	2S2f	2800	26	1820-1903-2020	SCNA	2
			10	1.0		10				d45	4PI	2800	6		ABS	55
		WWV-SY	10	0.8						1921.6-1922.3-1927.4	8	108	3	1928- -1952	SL-SWF	1+
		SS-BL	5	0.5						1922 - - 1925	BUR	18	1			
			4	0.6						1922 - - 1925	III	16-41	1+			
										1922 - - 1925	IIIG	25-400	3+			
										1925.30- -1927.45	III	16-41	1			
										1926 - - 1929	IIIG	25-240	3			
12-05	1357 -1359 -1402	WWV-BL	20	NR				NFR								
			10	NR												
		WWV-SY	10	1.5												
		SS-BL	5	NR												
			4	NR												
12-06	1758 -1801 -1805	WWV-BL	20	0.2				1755	S							
			10	0.2												
		WWV-SY	10	NR												
		SS-BL	5	NM												
			4	NM												

Date 1961	SFD's							Solar Flares		Solar Radio Emissions				Ionospheric Effects		
	UT	Path	f	Δf, cps		ΔA	−ΔP	UT	Imp	UT	Type	Freq	Int or	UT	Type	Imp
	Beg - Max - End		Mc/s	(+)	(−)	db	km	Beg - Max - End		Beg - Max - End		Mc/s	Peak Flux	Beg - Max - End		
12-21	1820 -1821D-1824	WWV-BL	20	0.1				1820	S							
			10	0.2												
		WWV-SY	10	NM												
		SS-BL	5	NR												
			4	NM												
12-27	1657 -1701 -1706	WWV-BL	20	NM				1656 -1703 -1838	1	1657 -1702 -1800	3S3	2800	5			
			10	0.2												
		WWV-SY	10	0.2												
		SS-BL	5	NR												
			4	NM												
12-28	2134 -2135 -2137	WWV-BL	20	0.2				2130	S							
			10	0.3												
		WWV-SY	10	NM												
		SS-BL	5	NR												
			4	NM												

Date 1962	SFD's							Solar Flares		Solar Radio Emissions				Ionospheric Effects		
	UT	Path	f	Δf, cps		ΔA	−ΔP	UT	Imp	UT	Type	Freq	Int or	UT	Type	Imp
	Beg - Max - End		Mc/s	(+)	(−)	db	km	Beg - Max - End		Beg - Max - End		Mc/s	Peak Flux	Beg - Max - End		
01-26	1841 -1842 -1845D	WWV-BL	15	NM				1841	S							
		WW	10	0.2												
		WWV-SY	10	0.1												
		SS-BL	5	0.1												
			4	0.1												
01-27	1613D-1614E-1615	WWV-BL	15	0.3				1613 - 1614 - 1618	1-	1618 - - 1618.3	III	22-41	1			
			10	0.4												
		WWV-SY	10	NM												
		SS-BL	5	NM												
			4	NM												
01-28	1930E-1932 -1935	WWV-BL	15	0.25				1920U-1936U-1945U	1	1915 - indet - 1959	3S3A	2800	1.3			
			10	0.6						1929 - 1932.2 - 1937	6C	2800	6			
		WWV-SY	10	0.3												
		SS-BL	5	0.15												
			4	0.3												
01-31	1441 -1441D-1444	WWV-BL	15	0.35				1441 - 1443 - 1454D	1	1441.3-1442 - 1444.1	1S1f	2800	4			
			10	0.65						1447 - 1447.7-1450.5	1S1	2800	3			
		WWV-SY	10	0.45												
		SS-BL	5	NM												
			4	0.15												
01-31	1537 -1538D-1541	WWV-BL	15	0.2				1533 - 1539 - 1551	1							
			10	0.35												
		WWV-SY	10	0.40												
		SS-BL	5	NM												
			4	NM												
01-31	1903E-1904 -1906	WWV-BL	15	NM				1902 - 1906 - 1940	1	1902 - 1904 - 1908	1S1	2800	6			
			10	0.5						d35	4PI		2			
		WWV-SY	10	0.4												
		SS-BL	5	0.1												
			4	0.15												
01-31	2111 -2112 -2114	WWV-BL	15	0.15				2110	1-							
			10	0.3												
		WWV-SY	10	NM												
		SS-BL	5	0.1												
			4	0.15												

Date 1962	SFD's							Solar Flares		Solar Radio Emissions				Ionospheric Effects		
	UT	Path	f	Δf, cps		ΔA	−ΔP	UT	Imp	UT	Type	Freq	Int or Peak	UT	Type	Imp
	Beg - Max - End		Mc/s	(+)	(−)	db	km	Beg - Max - End		Beg - Max - End		Mc/s	Flux	Beg - Max - End		
02-01	1509 -1509 -1511	WWV-BL	15	0.1				1508 - 1510 - 1518	1-	1414E - 1509 - 0003D	6	108	2			
			10	0.1						1410 - - 2320	cont	21-41	1-			
		WWV-SY	10	NM												
		SS-BL	5	NM												
			4	NM												
02-01	1551 -1552 -1554	WWV-BL	15	0.2				1552 - 1555 - 1622	1	1550 - 1554 - 1610	3S3A	2800	3			
			10	0.2					1-	1552 - 1552.3-1553	1S1	2800	1.5			
		WWV-SY	10	NM						1410 - - 2320	cont	21-41	1-			
		SS-BL	5	NM												
			4	NM												
02-01	1635E-1635 -1636	WWV-BL	15	0.2				1635 - 1644 - 1738	1					1634-1642-1735U	SEA	2
			10	0.3												
		WWV-SY	10	0.3												
		SS-BL	5	0.2												
			4	NM												
02-01	1639 -1640E -1643	WWV-BL	15	0.9				1636 - 1640 - 1653	1	1636 - 1640 - 1641	2S2	2800	8	1640-	S-SWF	1
			10	1.5												
		WWV-SY	10	1.4												
		SS-BL	5	0.7												
			4	0.4												
02-01	1654 -1656 -1659	WWV-BL	15	0.5				1655 - 1659 - 1706	1	1654 - 1723 - 1744	3S3A	2800	3	1656-1704-1738	SEA	1+
			10	0.8						1654 - 1657 - 1705	2S2f	2800	7	1657- -1720	S-SWF	1+
		WWV-SY	10	0.7												
		SS-BL	5	0.3												
			4	0.3												
02-01	1818D-1819 -1822	WWV-BL	15	0.2				1818 - 1824 - 1832	1-	1829 - - 1829.3	III	19-41	1+	1815-1830U-1850U	SEA	2
			10	NM												
		WWV-SY	10	0.8												
		SS-BL	5	NM												
			4	0.4												
02-02	2215D-2217D -2222	WWV-BL	15	0.2				2215 - 2220 - 2300	2							
			10	0.4												
		WWV-SY	10	0.3												
		SS-BL	5	0.3												
			4	0.3												
		SS-FC	4	NR												

Date 1962	SFD's							Solar Flares		Solar Radio Emissions				Ionospheric Effects		
	UT	Path	f	Δf, cps		ΔA	−ΔP	UT	Imp	UT	Type	Freq	Int or	UT	Type	Imp
	Beg - Max - End		Mc/s	(+)	(−)	db	km	Beg - Max - End		Beg - Max - End		Mc/s	Peak Flux	Beg - Max - End		
02-04	1730 -1731D-1735	WWV-BL	15	0.1				1726- 1732- 1746	1-	1400 - 1550 - 1845	3S3f	2800	8	1728-1733-1810	SPA	9
			10	0.2												
		WWV-SY	10	0.1												
		SS-BL	5	NR												
			4	NR												
		SS-FC	4	NM												
02-06	1624 -1625 -1629	WWV-BL	15	0.1				1624- 1628- 1634	1-							
			10	0.3												
		WWV-SY	10	NM												
		SS-BL	5	NM												
			4	0.2												
		SS-FC	4	NM												
02-06	1837 -1839 -1842	WWV-BL	15	0.1				NFR		1833.45 - - 1834.30	III	21-32	1+			
			10	0.1												
		WWV-SY	10	NM												
		SS-BL	5	NM												
			4	NM												
02-07	0426D-0427D-0430	WWVH-BL	10	1.5				NFR								
02-07	2127 -2128 -2130	WWV-BL	15	0.1				NFR								
			10	0.3												
		WWV-SY	10	0.2												
		SS-BL	5	NM												
			4	NM												
		SS-FC	4	NM												
02-10	2124 -2125E-2126	WWV-BL	15	0.1				2124 - 2128 - 2154	1							
			10	0.1												
		WWV-SY	10	NR												
		SS-BL	5	NM												
			4	NM												
		SS-FC	4	NM												
02-15	2054 -2055D-2058	WWV-BL	15	0.1				NFR								
			10	0.2												
		WWV-SY	10	0.3												
		SS-BL	5	NR												
			4	NM												
		SS-FC	4	NM												

Date 1962	SFD's							Solar Flares		Solar Radio Emissions				Ionospheric Effects		
	UT	Path	f	Δf, cps		ΔA	−ΔP	UT	Imp	UT	Type	Freq	Int or Peak	UT	Type	Imp
	Beg - Max - End		Mc/s	(+)	(−)	db	km	Beg - Max - End		Beg - Max - End		Mc/s	Flux	Beg - Max - End		
02-16	0142 -0142D-0145	WWV-BL	15	NM	NM			NFR								
			10	0.3	0.2											
		WWV-SY	10	NR	NR											
		SS-BL	5	0.2	0.2											
			4	NM	NM											
		SS-FC	4	NM	NM											
02-19	2134 -2136 -2146	WWV-BL	15	0.3				2134E-2144 - 2202	2	1230E - 1319 - 2025D	rec	2800	39			
			10	0.5							inc					
		WWV-SY	10	0.3												
		SS-BL	5	0.5												
			4	0.4												
		SS-FC	4	NR												
02-21	1829 -1830 -1833	WWV-BL	15	1.3				1835E-1835U-1855	1-	1805 - 1841.5 - 1928	3S3Af	2800	3			
			10	2.3						1831.8-1833.2 -1835.1	1S1f	2800	3			
		WWV-SY	10	1.6						1832 - - 1834	III	16-41	1+			
		SS-BL	5	1.4												
			4	0.6												
		SS-FC	4	NR												
02-21	2033 -2034 -2036	WWV-BL	15	0.2				NFR		2048 - - 2048.3	III	21-41	1+			
			10	0.4						2040 - - 2300	cont	24-41	1-			
		WWV-SY	10	0.3												
		SS-BL	5	0.1												
			4	0.1												
		SS-FC	4	NR												
02-22	2014 -2015E-2018	WWV-BL	15	0.7				2013 - 2015 - 2033	1-	2000 - 2030 - 2055	3S3	2800	4			
			10	1.3						2002 - - 2003.3	III	23-41	1			
		WWV-SY	10	1.0												
		SS-BL	5	0.4												
			4	0.5												
		SS-FC	4	0.5												
02-23	1416 -1417E-1420	WWV-BL	15	0.1				1416 - - 1419	1-	1348E - 1424 - 1614	6	108	1			
			10	0.2												
		WWV-SY	10	0.2												
		SS-BL	5	NM												
			4	NM												
		SS-FC	4	NM												

Date 1962	SFD's							Solar Flares		Solar Radio Emissions				Ionospheric Effects		
	UT Beg - Max - End	Path	f Mc/s	Δf, cps (+)	Δf, cps (−)	ΔA db	−ΔP km	UT Beg - Max - End	Imp	UT Beg - Max - End	Type	Freq Mc/s	Int or Peak Flux	UT Beg - Max - End	Type	Imp
02-23	1655 -1656 -1659	WWV-BL	15	0.8				1654 - 1656 - 1700U	1-	1657 - - 1659.2	III	21-41	1-			
			10	1.8												
		WWV-SY	10	1.1												
		SS-BL	5	0.5												
			4	0.5												
		SS-FC	4	0.5												
02-23	1828 -1830 -1832	WWV-BL	15	0.4				1823 - 1848 - 1902	1+	1750 - 1913 - 2200	3S3Af	2800	28			
			10	0.5												
		WWV-SY	10	0.4												
		SS-BL	5	0.3												
			4	0.2												
		SS-FC	4	0.3												
02-23	1841 -1843D-1848	WWV-BL	15	1.3				NFR								
			10	2.8												
		WWV-SY	10	1.5												
		SS-BL	5	1.0												
			4	0.8												
		SS-FC	4	0.9												
02-23	1900 -1901 -1903	WWV-BL	15	0.7				NFR								
			10	1.2												
		WWV-SY	10	0.8												
		SS-BL	5	0.2												
			4	0.2												
		SS-FC	4	0.3												
02-23	1950D-1951 -1955	WWV-BL	15	NM				NFR		1949 - - 0029	9	108	3			
			10	NM												
		WWV-SY	10	NM												
		SS-BL	5	0.3												
			4	0.2												
		SS-FC	4	0.2												
02-23	2155D-2156D-2157	WWV-BL	15	0.7				2202 - 2205 - 2209U	1-	2105 - - 2435	cont	22-41	2			
			10	0.8												
		WWV-SY	10	0.6												
		SS-BL	5	0.5												
			4	0.5												
		SS-FC	4	0.7												

Date 1962	SFD's							Solar Flares		Solar Radio Emissions				Ionospheric Effects		
	UT Beg - Max - End	Path	f Mc/s	Δf, cps (+)	Δf, cps (−)	ΔA db	−ΔP km	UT Beg - Max - End	Imp	UT Beg - Max - End	Type	Freq Mc/s	Int or Peak Flux	UT Beg - Max - End	Type	Imp
02-24	1341 -1342 -1345D	WWV-BL	15	0.1				1341 -1342 - 1349	1-	1346E - - 0030	6	108	3			
			10	0.3						1400E - - 1800	cont	22-41	1-			
		WWV-SY	10	0.2												
		SS-BL	5	NR												
			4	0.1												
		SS-FC	4	NR												
02-24	1442E-1443 -1444	WWV-BL	15	0.4				1430E - - 1506D	1+	1400E - - 1800	cont	22-41	1-			
			10	0.5												
		WWV-SY	10	0.5												
		SS-BL	5	0.2												
			4	0.1												
		SS-FC	4	0.1												
02-24	1450 -1453 -1500	WWV-BL	15	1.0	0.3			1452E-1454 - 1456	1							
			10	1.4	0.4											
		WWV-SY	10	1.0												
		SS-BL	5	0.3	NM											
			4	0.2	NM											
		SS-FC	4	0.2												
02-24	1621 -1623 -1625	WWV-BL	15	0.3				1620 - 1625 -1635	1-	1631 - 1632 - 1640	3S3	2800	2			
			10	NM						1626.3 - - 1627.2	III	16-41	1+			
		WWV-SY	10	0.4												
		SS-BL	5	NM												
			4	0.1												
		SS-FC	4	0.15												
02-25	1612 -1614 -1620D	WWV-BL	15	0.1				1612 - 1614 - 1620	1-	1415 - 1513 - 2030	3S3Af	2800	5			
			10	NM						1345E - - 0031	6	108	3			
		WWV-SY	10	0.2						1400E - 2400	cont	21-41	1-			
		SS-BL	5	NM												
			4	NM												
		SS-FC	4	NM												
02-25	1815E-1815 -1817	WWV-BL	15	0.3				1814 - 1817 - 1831	1-							
			10	NM												
		WWV-SY	10	0.2												
		SS-BL	5	0.2												
			4	NM												
		SS-FC	4	0.2												

Date 1962	SFD's							Solar Flares		Solar Radio Emissions				Ionospheric Effects		
	UT	Path	f	Δf, cps		ΔA	−ΔP	UT	Imp	UT	Type	Freq	Int or Peak Flux	UT	Type	Imp
	Beg - Max - End		Mc/s	(+)	(−)	db	km	Beg - Max - End		Beg - Max - End		Mc/s		Beg - Max - End		
02-25	1823 -1824 -1825	WWV-BL	15	0.3				1814 - 1824 - 1831	1-							
			10	NM												
		WWV-SY	10	0.4												
		SS-BL	5	0.2												
			4	0.2												
		SS-FC	4	0.2												
02-25	1835 -1837E -1839	WWV-BL	15	0.2				1825 - 1828 - 1836	1-							
			10	NM												
		WWV-SY	10	0.3												
		SS-BL	5	NM												
			4	NM												
02-25	1912 -1912D -1915	WWV-BL	15	0.1				1912 - 1920 - 1935	1-	1918 - 1918.5 - 1920.3	1S1f	2800	3			
			10	NM						1911 - -1914.15	III	16-41	2			
		WWV-SY	10	0.1												
		SS-BL	5	NM												
			4	NM												
		SS-FC	4	0.2												
02-25	1941 -1942 -1944	WWV-BL	15	0.5				1940 - 1943 - 1955	1-	1942.2 - - 1943	III	21-41	1+			
			10	0.8												
		WWV-SY	10	0.5												
		SS-BL	5	0.3												
			4	0.3												
		SS-FC	4	0.3												
02-26	1440 -1441D-1444	WWV-BL	15	0.5				NFP		1343E - - 1835	6	108	2			
			10	0.7						1450E - - 2400D	cont	23-41	1-			
		WWV-SY	10	0.4												
		SS-BL	5	0.3												
			4	0.2												
		SS-FC	4	0.2												
02-27	1359 -1402 -1405	WWV-BL	15	NR				1358 - - 1402	1-	1342E - 1552 - 2108D	6	108	2			
			10	0.2						1356E - - 2400	cont	23-41	1-			
		WWV-SY	10	0.1												
		SS-BL	5	NM												
			4	NM												
		SS-FC	4	NM												

Date 1962	SFD's							Solar Flares		Solar Radio Emissions				Ionospheric Effects		
	UT	Path	f	Δf, cps		ΔA	−ΔP	UT	Imp	UT	Type	Freq	Int or Peak Flux	UT	Type	Imp
	Beg - Max - End		Mc/s	(+)	(−)	db	km	Beg - Max - End		Beg - Max - End		Mc/s		Beg - Max - End		
02-27	1420 -1421D -1424	WWV-BL	15	NR				1422E - - 1435D	1-	1426 - 1434.2 - 1442	3S3	2800	2			
			10	0.2												
		WWV-SY	10	NM												
		SS-BL	5	NM												
			4	0.1												
		SS-FC	4	NM												
02-27	1732 -1733D-1735	WWV-BL	15	NR				1715 - 1735 - 1750	1-	1517 - 1625 - 1917	3S3Af	2800	8			
			10	NM				1731 - 1734 - 1740	1-							
		WWV-SY	10	0.5												
		SS-BL	5	0.3												
			4	0.2												
		SS-FC	4	0.3												
02-27	2048 -2051D-2059	WWV-BL	15	NR				2050 - 2055 - 2120	1	2050 - 2058 - 2200	3S3A	2800	8			
			10	0.8						2050 - 2051.8-2053	2S2	2800	14			
		WWV-SY	10	0.5												
		SS-BL	5	0.6												
			4	0.4												
		SS-FC	4	0.6												
02-28	1806 -1808 -1813	WWV-BL	15	NR				1806 - 1812 - 1930	1	1804 - 1815 - 1825	6Cf	2800	29			
			10	0.8						d34	4PI	2800	5			
		WWV-SY	10	0.7						1810.1 - - 1811.6	3	108	2			
		SS-BL	5	0.4												
			4	0.5												
		SS-FC	4	0.3												
02-28	1936 -1938E -1946	WWV-BL	15	NR				1934 - 1941 - 2028	1	1937 - 1938.5 - 1940	2S2	2800	10			
			10	2.5						d18	4PI	2800	8			
		WWV-SY	10	1.6						1855 - - 2000	cont	24-41	1			
		SS-BL	5	1.0												
			4	0.7												
		SS-FC	4	0.7												

Date 1962	SFD's							Solar Flares		Solar Radio Emissions				Ionospheric Effects		
	UT Beg - Max - End	Path	f Mc/s	Δf, cps (+)	Δf, cps (−)	ΔA db	−ΔP km	UT Beg - Max - End	Imp	UT Beg - Max - End	Type	Freq Mc/s	Int or Peak Flux	UT Beg - Max - End	Type	Imp
03-01	1636 -1637	WWV-BL	15	NR				1635- 1643 - 1723	2	1634.3 - - 1635	III	24-41	1	1634- -1720	S-SWF	2+
			10	7.0						1635 - 1642.5 - 1657	6Cf	2800	425	1636-1648-1730	SPA	83
		WWV-SY	10	4.8						d28	4PI	2800	8	1638-1644-1720	SCNA	2
		SS-BL	5	1.4						1636.5-1645U -1648.5	9a	108	3		ABS	50
			4	1.4						1637.2D- - 1705	II	21-41	3+	1641- -1734	SEA	2
		SS-FC	4	1.4						1639 - - 1640	BUR	18	1			
										1645 - - 1647	BUR	18	1			
	- 1638 -	WWV-BL	15	NR						1648.5 - - 1740.5	96	108	1			
			10	7.0						1654 - - 1656	BUR	18	1			
		WWV-SY	10	4.2												
		SS-BL	5	1.6												
			4	1.4												
		SS-FC	4	1.4												
	- 1640D -	WWV-BL	15	NR												
			10	7.0												
		WWV-SY	10	NM												
		SS-BL	5	2.0												
			4	1.8												
		SS-FC	4	1.8												
	- 1641D-1705	WWV-BL	15	NR												
			10	NM												
		WWV-SY	10	NM												
		SS-BL	5	2.8												
			4	2.8												
		SS-FC	4	2.8												
03-01	1842 -1844D-1845D	WWV-BL	15	NR				1842 - 1844 - 1849	1-	1844 - 1844.3 - 1844.9	1S1	2800	1			
			10	1.2						1845.2-1845.5-1846.1	1S1	2800	3			
		WWV-SY	10	0.6												
		SS-BL	5	0.3												
			4	0.2												
03-13	1449E-1450	WWV-BL	15	4.7	0.6			1448 - 1451 - 1640D	2+	1447.5-1450.5-1507	6Cf	2800	470	1445-1505-1640	SPA	99
			10	7.6	1.2	35				d6:23	4PI	2800	12	1448- -1622	S-SWF	3
		WWV-SY	10	NR										1450-1500-1545	SCNA	1
		SS-BL	5	1.8	0.4										ABS	20
			4	2.4	0.2									1450- -1555	SEA	2

Date 1962	SFD's							Solar Flares		Solar Radio Emissions				Ionospheric Effects		
	UT	Path	f	Δf, cps		ΔA	−ΔP	UT	Imp	UT	Type	Freq	Int or	UT	Type	Imp
	Beg - Max - End		Mc/s	(+)	(−)	db	km	Beg - Max - End		Beg - Max - End		Mc/s	Peak Flux	Beg - Max - End		
03-13	-1452D-1500	WWV-BL	15	1.4						1450 - 1452.3 - 1512	8	108	2			
			10	1.8						1517.3-1520 - 1521.2	6Cf	2800	3			
		WWV-SY	10	NR												
		SS-BL	5	0.4												
			4	0.6												
03-17	1938 -1940E-1943	WWV-BL	15	1.4				1934 - 1941 - 1959	1	1939 - 2000 - 2120	3S3A	2800	2	1933-1944-1953	SEA	1
			10	NR		15				1939-1940.2 - 1942	1S1	2800	6	1940- -2010	S-SWF	1
		WWV-SY	10	1.6						1940 - 1949 - 2155	BUR	18	2	1940-1944-2015	SCNA	1
		SS-BL	5	0.9											ABS	20
			4	NR												
03-19	0100 -0101 -0105	WWV-BL	15	NR				0100 - 0107 - 0125D	1							
			10	0.6												
		WWV-SY	10	0.4												
		SS-BL	5	NR												
			4	NM												
03-19	2119 -2120 -2122	WWV-BL	15	NR				NFP		1338 -	RiseA	2800	13			
			10	0.9						2120 - 2120.7 - 2121	2S2	2800	20			
		WWV-SY	10	0.6												
		SS-BL	5	NR												
			4	0.4												
03-19	2126D-2127 -2129	WWV-BL	15	NR				NFR								
			10	0.4												
		WWV-SY	10	0.3												
		SS-BL	5	NR												
			4	0.2												
03-22	1558 -1600 -1603	WWV-BL	15	0.3				1558 - 1602 - 1610	1	1505E - - 2445	cont	24-41	1-			
			10	0.4						1559.6-1600.5-1600.6	3	108	2			
		WWV-SY	10	0.3						1605.0-1605.0-1606.0	3	108	3			
		SS-BL	5	0.1												
			4	0.1												
03-22	2136 -2137D-2140	WWV-BL	15	0.3				2136 - 2140 - 2154U	1-	2132 - 2145 - 2158	3S3A	2800	6			
			10	NR						2136 - 2138 - 2143	2S2	2800	18			
		WWV-SY	10	0.3												
		SS-BL	5	0.1												
			4	NR												

Date 1962	SFD's							Solar Flares		Solar Radio Emissions				Ionospheric Effects		
	UT	Path	f	Δf, cps		ΔA	−ΔP	UT	Imp	UT	Type	Freq	Int or Peak	UT	Type	Imp
	Beg - Max - End		Mc/s	(+)	(−)	db	km	Beg - Max - End		Beg - Max - End		Mc/s	Flux	Beg - Max - End		
03-22	2227 -2230 -2234	WWV-BL	15	NM				2220U-2241-2310U	3	2214 - 2230 - 2250D	rec	2800	35			
			10	NR							inc					
		WWV-SY	10	0.3												
		SS-BL	5	0.1												
			4	NR												
03-24	1354 -1355 -1357	WWV-BL	15	0.2				NFR		1353 - 1354 - 1409	3S3	2800	4			
			10	0.3												
		WWV-SY	10	0.3												
		SS-BL	5	0.1												
			4	0.1												
03-25	1234 -1236 -1238	WWV-BL	15	NR				1254E- -1325D	1	1208E- 1425 - 1648D	3S3Af	2800	16	1237- -1327	SPA	2
			10	1.1						1208E-1209.5- 1212D	2S2	2800	9	1238- -1306	S-SWF	2
		WWV-SY	10	1.0						1223 - 1224 - 1227	1S	2800	4	1238-1242-1334	SEA	1+
		SS-BL	5	NR						1234 - 1237 - 1246	2S2	2800	90			
			4	0.1												
03-25	1358 -1359 -1401	WWV-BL	15	0.2				1405E-1436 -1506	1+	1357 - 1358.5 - 1402	1S1f	2800	5			
			10	0.4												
		WWV-SY	10	0.2												
		SS-BL	5	0.1												
			4	0.1												
03-25	1904 -1905 -1909	WWV-BL	15	0.4				1902 -1908 -1924	1-	1901 - 1907 - 1930	3S3f	2800	3			
			10	0.6				1903 -1909 -1940	1-	1906.1-1906.2-1907.9	3	108	2			
		WWV-SY	10	0.4						1902.3- -1904.3	III	8.5-41	2			
		SS-BL	5	0.4						1905.15- -1909.45	III	7.6-41	2+			
			4	0.3												
03-27	2107 -2107D-2110	WWV-BL	15	NM				2107 -2108 -2117	1-							
			10	NM												
		WWV-SY	10	0.1												
		SS-BL	5	NM												
			4	NM												
03-30	1436 -1437 -1439	WWV-BL	15	0.2				1431 -1438 -1446	1-							
			10	0.6												
		WWV-SY	10	0.4												
		SS-BL	5	NM												
			4	NM												

Date 1962	SFD's							Solar Flares		Solar Radio Emissions				Ionospheric Effects		
	UT	Path	f	Δf, cps		ΔA	−ΔP	UT	Imp	UT	Type	Freq	Int or	UT	Type	Imp
	Beg - Max - End		Mc/s	(+)	(−)	db	km	Beg - Max - End		Beg - Max - End		Mc/s	Peak Flux	Beg - Max - End		
03-30	1459 -1500 -1503	WWV-BL	15	0.2				1458 - 1505 - 1516	1-							
			10	0.3												
		WWV-SY	10	0.2												
		SS-BL	5	NM												
			4	NM												
03-31	1900 -1903 -1912	WWV-BL	15	0.7				1858 - 1905 - 1954	1+							
			10	1.4												
		WWV-SY	10	0.9												
		SS-BL	5	0.5												
			4	0.3												
03-31	2135 -2138 -2143	WWV-BL	15	0.3	0.2			2130 - 2139 - 2152	1							
			10	0.8	0.4											
		WWV-SY	10	0.5												
		SS-BL	5	0.3	0.2											
			4	0.2	0.3											
04-07	1732 -1733D-1736	WWV-BL	15	NR				NFR								
			10	0.6												
		WWV-SY	10	0.3												
		SS-BL	5	NR												
			4	0.7												
04-07	1818 -1820D-1823	WWV-BL	15	NR				1819E-1822 - 1906	1+							
			10	0.3												
		WWV-SY	10	0.2												
		SS-BL	5	NR												
			4	NM												
04-12	2149E-2150 -2152	WWV-BL	15	0.4			0.41	2149 - 2213 - 2244	1-	2134 - - 2216	BUR	18	3	2134- -2216	BUR	3
			10	0.6			0.73			2147.8-2150.9-2158.9	9a	108	3	2212- -2400	G-SWF	1+
		WWV-SY	10	0.4						2148 - 2212 - 2221	6Cf	2800	150	2215-2218-2227	SEA	1
		SS-BL	5	0.2			1.35			2148.15- - 2156	cont	8.5-41	2+			
			4	0.2			1.03									

Date 1962	SFD's							Solar Flares		Solar Radio Emissions				Ionospheric Effects		
	UT	Path	f	Δf, cps		ΔA	−ΔP	UT	Imp	UT	Type	Freq	Int or Peak	UT	Type	Imp
	Beg - Max - End		Mc/s	(+)	(−)	db	km	Beg - Max - End		Beg - Max - End		Mc/s	Flux	Beg - Max - End		
04-13	2117 -2118D-2121	WWV-BL	15	0.2			0.23	2117 - 2121 - 2130	1-							
			10	0.6			1.50									
		WWV-SY	10	0.2												
		SS-BL	5	0.2			1.79									
			4	0.2			1.46									
04-13	2254 -2256D	WWV-BL	15	0.4			0.61	2253 - 2302 - 2320	1-	2301.3 - - 2304.3	III	20-41	1+			
			10	0.7			1.29									
		WWV-SY	10	0.4												
		SS-BL	5	0.2			1.05									
			4	0.3			2.23									
04-13	-2300 -2302	WWV-BL	15	0.2			0.1									
			10	0.4			0.4									
		WWV-SY	10	0.2												
		SS-BL	5	0.2			0.8									
			4	0.3			1.9									
04-14	1301 -1302 -1303	WWV-BL	15	0.8			0.52	1300E-1302 - 1320	1-							
			10	1.1			1.28									
		WWV-SY	10	0.7												
		SS-BL	5	0.3			1.07									
			4	0.2			1.13									
04-14	1304 -1306D-1309	WWV-BL	15	0.4			0.6	1300E-1307- 1320	1-							
			10	0.7			1.21									
		WWV-SY	10	0.4												
		SS-BL	5	0.2			0.94									
			4	0.1			0.98									
04-14	1311 -1313 -1315	WWV-BL	15	0.1												
			10	0.3												
		WWV-SY	10	0.2												
		SS-BL	5	0.1												
			4	0.1												

Date 1962	SFD's							Solar Flares		Solar Radio Emissions				Ionospheric Effects		
	UT	Path	f	Δf, cps		ΔA	−ΔP	UT	Imp	UT	Type	Freq	Int or Peak Flux	UT	Type	Imp
	Beg - Max - End		Mc/s	(+)	(−)	db	km	Beg - Max - End		Beg - Max - End		Mc/s		Beg - Max - End		
04-14	1915 -1918 -1920	WWV-BL	15	0.8		12	0.16	1910E-1924 - 2005	1	1902 - 1933 - 2050	3S3A	2800	7	1903-1930-2030	SPA	75
			10	2.1		25	0.42			1913 - 1919 - 1930	2S2f	2800	59	1917-1924-2100U	SEA	2
		WWV-SY	10	1.5						1917 - - 1920	BUR	18	2	1918- -2027	S-SWF	2+
		SS-BL	5	1.1						1917.5- - 1921	III	7.6-41	2+	1920-1926-2030	SCNA	2
			4	0.9											ABS	30
04-15	1715 -1718 -1725	WWV-BL	15	0.3		3		1715 - 1720 - 1731	1-	1640 - - 1810	cont	18-41	1-	1715-1720-1800	SPA	12
			10	1.1		8				1716.5-1719.3-1732.5	6Cf	2800	10	1715-1721-1800	SEA	1+
		WWV-SY	10	0.5										1720- -1755	S-SWF	1-
		SS-BL	5	0.3												
			4	0.3												
04-15	1837 -1840 -1845D	WWV-BL	15	0.2				1835 -1845 - 1854	1-	1810 - - 2500	cont	21-41	1			
			10	0.2												
		WWV-SY	10	NM												
		SS-BL	5	0.1												
			4	0.1												
04-15	1928 -1930D-1933	WWV-BL	15	0.4				1929 - 1951 - 2007	1							
			10	0.6												
		WWV-SY	10	0.4												
		SS-BL	5	0.4												
			4	0.4												
04-15	1942 -1949D-1955	WWV-BL	15	1.3	NM			1942 - 1950 - 1956D	1-	1943 - 1944.3 - 1947	1S1	2800	5			
			10	2.2	0.6											
		WWV-SY	10	1.5												
		SS-BL	5	0.9	0.2											
			4	0.5	0.2											
04-15	2050 -2052E-2058	WWV-BL	15	0.6	0.2		0.93	2051 -2053 - 2058	1-							
			10	1.1	0.4		2.12									
		WWV-SY	10	0.8												
		SS-BL	5	1.0	NM		6.73									
			4	0.4	NM		2.54									
04-15	2153 -2154 -2158	WWV-BL	15	0.2			0.25	2153 - 2155 - 2158	1-							
			10	0.4			0.63									
		WWV-SY	10	0.3												
		SS-BL	5	0.2			0.98									
			4	0.2			1.09									

Date 1962	SFD's							Solar Flares		Solar Radio Emissions				Ionospheric Effects		
	UT	Path	f	Δf, cps		ΔA	−ΔP	UT	Imp	UT	Type	Freq	Int or Peak Flux	UT	Type	Imp
	Beg - Max - End		Mc/s	(+)	(−)	db	km	Beg - Max - End		Beg - Max - End		Mc/s		Beg - Max - End		
04-15	2240 -2242 -2249	WWV-BL	15	0.6			1.30	2241 - 2245 - 2252	1	2241 - 2243.8 - 2246	1S1f	2800	4			
			10	1.1			3.69									
		WWV-SY	10	0.8												
		SS-BL	5	0.5			3.80									
			4	0.5			5.75									
04-16	0234 -0235 -0244	FB-AN	10	0.3				0233 - 0236 - 0249	1-							
04-16	2146E-2156D-2148	WWV-BL	15	NR				2145 - 2147 - 2153	1-	1500E - - 2524	6	108	2			
			10	NR												
		WWV-SY	10	NR												
		SS-BL	5	0.4												
			4	NR												
04-17	0100 -0102 -0105	WWV-BL	15	0.3				NFR								
			10	0.7												
		WWV-SY	10	0.4												
		SS-BL	5	NM												
			4	NM												
04-17	1444 - 1445D-1447	WWV-BL	15	NR				1444 - 1446 - 1513	1	1438E - - 0125	1	108	2	1445-1450-1510	SEA	1-
			10	NR						1444.7-1445.9-1447.3	2S2	2800	10			
		WWV-SY	10	NR						1459E - -2525D	cont	7.6-41	3			
		SS-BL	5	0.2												
			4	0.2												
04-17	2252 -2253D-2256	WWV-BL	15	1.0			0.65	2252 - 2256 - 2313	1-	2252.5-2253.2-2300	2S2	2800	55			
			10	1.9			2.14									
		WWV-SY	10	1.0												
		SS-BL	5	1.1			2.10									
			4	1.1			2.89									
04-18	1801 -1803 -1805	WWV-BL	15	0.3				1734 -1804- 2129	3	1223E - 1630 - 2526	6	108	3	1750-	SCNA	2
			10	0.5						1734 - 1845 - 2229	3S3Af	2800	25	1752- -1940	G-SWF	3
		WWV-SY	10	NM						1800 -1803.5-1811	2S2	2800	20			
		SS-BL	5	NR												
			4	NR												

Date 1962	SFD's							Solar Flares		Solar Radio Emissions				Ionospheric Effects		
	UT	Path	f	Δf, cps		ΔA	−ΔP	UT	Imp	UT	Type	Freq	Int or Peak	UT	Type	Imp
	Beg - Max - End		Mc/s	(+)	(−)	db	km	Beg - Max - End		Beg - Max - End		Mc/s	Flux	Beg - Max - End		
04-19	1736 -1738 -1740	WWV-BL	15	0.2				1734 - 1743 - 1818	1-	1710 - 1746 - 1818	3S3A	2800	3			
			10	0.3						1735.15 - -1736.45	III	7.6-41	2			
		SS-BL	5	NM												
			4	NM												
04-19	1741 -1742D-1744	WWV-BL	15	0.8						1742.3-1742.7-1744	1S1	2800	5			
			10	1.4						1743.1-1743.7-1744.6	3	108	2			
		SS-BL	5	NM												
			4	NM												
04-19	1935 -1935D -1938D	WWV-BL	15	18	3.2	15	7	1935 - 1937 - 2031	2	1935 - 1936.3 - 1943	2S2	2800	165	1934-1937-2040	SEA	1+
			10	43+	7.2	24	34			d2:32	4PI	2800	5	1935-1938-1950	SCNA	1
		PB-AN	10	0.3											ABS	20
		SS-BL	5	32	5.6	11	32							1935- -2010	S-SWF	1+
			4	19	NM	18	14							1935-2010-2040	SPA	60
04-19	1954E-1955D-1957	WWV-BL	15	1.2				1942 - 1947 - 2000	2	1955 - 1955.3 - 1957	1S1	2800	3			
			10	1.6												
		SS-BL	5	1.0												
			4	0.6												
04-19	2035 -2037E-2040	WWV-BL	15	0.4	0.1			2035E-2038U-2053	1-							
			10	0.9	0.2			2036 -2039 -2042	1							
		SS-BL	5	0.4	0.2											
			4	0.3	0.2											
04-20	1322 -1323 -1325	WWV-BL	15	0.6				1314 - 1332 - 1432	1	1220E - - 0128	6	108	2			
			10	1.0						1328 - 1335 - 1344	3S3	2800	2			
		SS-BL	5	NM												
			4	NM												
04-20	1534 -1535 -1538	WWV-BL	15	NM				1536E- - 1547	1-	1220E - - 0128	6	108	2			
			10	0.3						1534.45 - - 1535.15	III	23-41	1+			
		SS-BL	5	NM												
			4	NM												
04-20	1626 -1628 -1633	WWV-BL	15	0.1				1625 - - 1629D	1-	1220E - - 0128	6	108	2			
			10	0.2												
		SS-BL	5	0.1												
			4	NM												

Date 1962	SFD's							Solar Flares		Solar Radio Emissions				Ionospheric Effects		
	UT	Path	f	Δf, cps		ΔA	−ΔP	UT	Imp	UT	Type	Freq	Int or Peak Flux	UT	Type	Imp
	Beg - Max - End		Mc/s	(+)	(−)	db	km	Beg - Max - End		Beg - Max - End		Mc/s		Beg - Max - End		
04-20	1734 -1736 -1740	WWV-BL	15	0.2				NFR		1220E - - 0128	6	108	2			
			10	0.3												
		SS-BL	5	0.1												
			4	NM												
04-20	1959 -2001E-2010D	WWV-BL	15	3.8		25	6.3	1958 -2002 -2038	2	1957.3 - 1959 - 2009	2S2f	2800	72	2000- -2030	S-SWF	2
			10	9.0		50	22			2000 - - 2004	III	7.6-41	2+	2000-2004-2035	SCNA	2
		SS-BL	5	6.0		15	26			2000 - - 2003	BUR	18	2		ABS	30
			4	3.4		10	15.4							2000-2007-2050	SPA	92
														2001- -2050	SEA	2
04-21	1316 -1317 -1319	WWV-BL	15	0.2				1307 -1321 -1353	1	1219E - - 0129	6	108	2			
			10	0.6												
		SS-BL	5	NM												
			4	0.2												
04-21	1450 -1451 -1455	WWV-BL	15	0.3				1450 -1453 -1457	1-							
			10	NM												
		SS-BL	5	0.9												
			4	0.6												
04-21	1920 -1920D-1932	WWV-BL	15	0.9				1918 -1922 -1932	1-	1920 - - 1926	BUR	18	1	1920-1925-2045	SEA	1+
			10	1.4						1920.0-1920.1-1926.0	8	108	2			
		SS-BL	5	0.6						1920 - - 1923	III	7.6-41	2+			
			4	0.4						1924 - - 1924.5	III	16-41	1+			
										1925 - - 1926.3	III	7.6-41	2			
04-26	0536 -0538 -0542	PB-AN	10	1.2				0532E- -0538D	1-							
04-26	1833 -1835 -1837	WWV-BL	15	NM				1828 -1838 -1840	1-							
			10	NM												
		SS-BL	5	NR												
			4	NR												
04-27	1410 -1412D-1425	WWV-BL	15	6	1.2	30	5.04	1350 -1413 -1440	2	1344 - 1356 - 1451	3S3Af	2800	4	1410-1426-1520	SPA	85
			10	10	4.4	30	10.8			1405 - 1413 - 1429	2S2f	2800	175	1410-1420-1526	SEA	2
		SS-BL	5	NR						1412.15- - 1415	III	11-41	2+	1413- -1433	S-SWF	1+
			4	NR						1412.3- - 1503	9	108	3	1414-1417-1430	SCNA	2
										1415.15- -1416.3	III	11-41	2+		ABS	30
										1418 - - 1426	II	16-41	2			
										1420 - - 1635	IV	22-41	2			

Date 1962	SFD's							Solar Flares		Solar Radio Emissions				Ionospheric Effects		
	UT	Path	f	Δf, cps		ΔA	−ΔP	UT	Imp	UT	Type	Freq	Int or	UT	Type	Imp
	Beg - Max - End		Mc/s	(+)	(−)	db	km	Beg - Max - End		Beg - Max - End		Mc/s	Peak Flux	Beg - Max - End		
04-27	2300 -2302E-2306	WWV-BL	15	0.2				2300 -2305 -2315	1-	2300 - - 2305	BUR	18	3			
			10	0.4						2300.3 - -2305.5	III	12-41	2			
		SS-BL	5	NR						2300.5-2304.3-2306.6	2	108	2			
			4	NR												
04-28	1718 -1719D-1721	WWV-BL	15	0.3				NFR		1556.5-1557.1-1758.5	4	108	2			
			10	0.6												
		SS-BL	5	NR												
			4	NR												
04-28	2025 -2027 -2029	WWV-BL	15	0.5				2023 -2029 -2041	1-	2021 - 2030 - 2044	3S3Af	2800	3			
			10	0.6						2023 - - 2032	BUR	18	1			
		SS-BL	5	NR						2023.45- - 2028	III	7.6-41	2			
			4	NR						2023.5-2027.2-2031	2	108	2			
										2026.8-2027.3-2027.8	1S1f	2800	7			
										2028 - - 2029	III	21-41	1+			
04-29	1800 -1801 -1804	WWV-BL	15	0.1				1801 - 1803 - 1806	1-							
			10	0.2												
		SS-BL	5	NR												
			4	NR												
05-01	1835 -1839E-1842	WWV-BL	15	0.3	0.1			NFR								
			10	0.7	0.2											
		SS-BL	5	NR												
			4	NR												
05-01	1914 -1916 -1927	WWV-BL	15	1.5	0.5	15		1915 - 1920 - 1928	1	1915 - 1920.5 - 2105	Irreg Act	2800	60	1916-	SCNA	X
			10	2.0	0.6	15								1916-1924-1940	SPA	36
		PB-AN	10	0.3						1918.3- -1921.3	III	7.6-41	3	1916- -1942	S-SWF	1+
		SS-BL	5	NR						1918.5-1922.5-1936.5	9	108	3	1916-1924-2000	SEA	2
			4	NR						1919 - - 1955	BUR	18	3			
05-01	2024 -2026 -2028	WWV-BL	15	0.2				NFR		1935 - - 2130	IV	23-41	1			
			10	0.2												
		SS-BL	5	NR												
			4	NR												
05-02	1927 -1928 -1930	WWV-BL	15	0.3				1927 - 1930 - 1952	1-	1927.3-1928.4-1931.0	2S2f	2800	12	1919-1927-1945	SEA	2
			10	0.4						d50	4PI	2800	1			
		SS-BL	5	NR												
			4	NR												

Date 1962	SFD's							Solar Flares		Solar Radio Emissions				Ionospheric Effects		
	UT	Path	f	Δf, cps		ΔA	−ΔP	UT	Imp	UT	Type	Freq	Int or Peak Flux	UT	Type	Imp
	Beg - Max - End		Mc/s	(+)	(−)	db	km	Beg - Max - End		Beg - Max - End		Mc/s		Beg - Max - End		
05-04	1616 -1617D-1619	WWV-BL	15	0.1				1617 - 1619 - 1621	1-	1619.15- -1620.4	III	20-41	1			
			10	NM												
		SS-BL	5	NR												
			4	NR												
05-09	2117 -2118D-2119	WWV-BL	15	0.2				NFR								
			10	0.2												
		SS-BL	5	0.1												
			4	NR												
05-10	1807 -1809 -1811	WWV-BL	15	0.4				1733 - 1738 - 1815	1-							
			10	0.6												
		SS-BL	5	NM												
			4	NM												
05-10	1906 -1908 -1913	WWV-BL	15	0.4				1905 - 1909 - 1929	1							
			10	0.6												
		SS-BL	5	NM												
			4	NM												
05-11	1332 -1333 -1335	WWV-BL	15	0.2				1334 - 1338 - 1344	1-							
			10	0.4												
		SS-BL	5	0.2												
			4	0.1												
05-11	1618 -1619 -1622	WWV-BL	15	0.3				1615 - 1622 - 1640	1-	1612 - - 1625	BUR	18	1			
			10	0.4						1620 - 1621.8- 1622.3	3	108	2			
		SS-BL	5	NM												
			4	NM												
05-11	2101 -2102 -2104	WWV-BL	15	0.1				2100 - 2103 - 2114	1-	2103 - - 2104	BUR	18	1			
			10	0.3												
		SS-BL	5	NR												
			4	0.1												
05-12	1352 -1354 -1357	WWV-BL	15	0.3				1351 - 1356 - 1403	1-	1325 - 1337 - 1530	3S3	2800	5			
			10	0.6												
		SS-BL	5	0.2												
			4	0.3												
05-13	2117 -2121 -2123	WWV-BL	15	0.2				2112 - 2123 - 2234	1	2121-2123.3 - 2124	1S1	2800	15	2120-2140-2200	SCNA	1
			10	NM						2129.7-2130.8-2136.3	6Cf	2800	8		ABS	15
		SS-BL	5	NM						2140 - 2202 - 2230	7	108	1	2120- -2200	G-SWF	1+
			4	NM										2120-2140-2230	SPA	24
														2122-2138-2205	SEA	1+

Date 1962	SFD's							Solar Flares		Solar Radio Emissions				Ionospheric Effects		
	UT Beg - Max - End	Path	f Mc/s	Δf, cps (+)	Δf, cps (−)	ΔA db	−ΔP km	UT Beg - Max - End	Imp	UT Beg - Max - End	Type	Freq Mc/s	Int or Peak Flux	UT Beg - Max - End	Type	Imp
05-18	1530 -1531D -	WWV-BL	15	0.7				1530 - 1534 - 1546	1	1531 - - 1535	BUR	18	1			
			10	1.1						1531.5 -1535-1541.5	8	108	3			
		SS-BL	5	NM						1531.7-1532.4-1536.7	2S2f	2800	56			
			4	NM												
	-1533D-1536	WWV-BL	15	0.9												
			10	1.5												
		SS-BL	5	NM												
			4	NM												
05-18	2002 -2004 -2007	WWV-BL	15	0.4				1958 - 2005 - 2015	1-							
			10	0.5												
		SS-BL	5	NR												
			4	NM												
05-20	2033 -2035 -2038	WWV-BL	15	0.1				2035 - 2040 - 2048	1-							
			10	0.3												
		SS-BL	5	NM												
			4	NM												
05-23	1753 -1754 -	WWV-BL	15	0.4				NFR								
			10	1.1												
		SS-BL	5	0.1												
			4	NM												
05-25	1158 -1200 -1204	WWV-BL	15	0.1				NFR		1142E - - 0156	6	108	2			
			10	0.2												
		SS-BL	5	0.2												
			4	0.1												
05-27	1516 -1516D	WWV-BL	15	1.3	0.3			1511 -1518 -1522	1-	1516 - 1516.5-1519.5	3	108	3			
			10	1.7	NM					1516.45- - 1520	III	7.6-41	2			
		SS-BL	5	0.7	NM					1517 - 1517.2 - 1520	2S2	2800	11			
			4	NM						1517 - - 1520	BUR	18	1			
05-27	-1517D-1521	WWV-BL	15	0.5												
			10	0.9												
		SS-BL	5	NM												
			4	NR												
05-29	1759 -1800D-1804	WWV-BL	15	0.2				1759 -1804 - 1830	1	1800 - 1802 - 1803	1S1	2800	5			
			10	1.0						- 1822	4PI	2800	2			
		SS-BL	5	0.3												
			4	0.2												

Date 1962	SFD's							Solar Flares		Solar Radio Emissions				Ionospheric Effects		
	UT	Path	f	Δf, cps		ΔA	−ΔP	UT	Imp	UT	Type	Freq	Int or	UT	Type	Imp
	Beg - Max - End		Mc/s	(+)	(−)	db	km	Beg - Max - End		Beg - Max - End		Mc/s	Peak Flux	Beg - Max - End		
05-30	1359 -1359D-1401E	WWV-BL	15	0.8				1358E- -1408D	1-	1359 - - 1400	III	16-41	1-			
			10	1.8						1359.15- - 1400	III	16-41	1-			
		SS-BL	5	NM												
			4	NM												
05-30	1636 -1637 -1639	WWV-BL	15	0.2				1627 - 1632 - 1645	1-	1633.45- -1634.2	III	27-41	1+			
			10	0.3						1635.5 - -1639.2	III	7.6-41	2			
		SS-BL	5	NM						1637 - - 1640	BUR	18	1			
			4	NM												
05-30	1657 -1658D-1700	WWV-BL	15	0.2				NFR								
			10	0.4												
		SS-BL	5	NM												
			4	NM												
05-31	0028 -0030 -0033	WWV-BL	15	NM				0030E - - 0050D	1							
			10	0.2												
		SS-BL	5	0.1												
			4	0.2												
06-01	1204 -1205D-1207	WWV-BL	15	NR				1203 - 1213 - 1238	1	1204.6-1205.3-1206.2	3	108	3			
			10	0.5						1205.15- -1206.3	III	17-41	1+			
		SS-BL	5	NR												
			4	0.1												
06-01	1955 -1956 -2000	WWV-BL	15	0.4				1954 - 1958 - 2010	1-	1950 - 2013 - 2110	3S3	2800	6			
			10	0.6						1956 - - 1957	III	21-41	1			
		SS-BL	5	NR												
			4	NM												
06-01	2006 - □ - □	WWV-BL	15	NM				2006 - 2019 - 2043	2	2005 - - 2015	II	19-41	2			
			10	NM						2008.3- - 2010	III	19-41	2-			
		SS-BL	5	NM						2009 - - 2015	BUR	18	1			
			4	NM												
06-19	2254 -2256 -2300D	WWVH-AN	15	0.5				2250 - 2301 - 2320	1-							
		PB-AN	10	0.2												
06-27	2039 -2041D-2045D	WWV-BL	15	NR				2035 - 2042 - 2049	1-							
			10	0.7												
		SS-BL	5	NR												
			4	0.2												

Date 1962	SFD's							Solar Flares		Solar Radio Emissions				Ionospheric Effects		
	UT Beg - Max - End	Path	f Mc/s	Δf, cps (+)	Δf, cps (−)	ΔA db	−ΔP km	UT Beg - Max - End	Imp	UT Beg - Max - End	Type	Freq Mc/s	Int or Peak Flux	UT Beg - Max - End	Type	Imp
07-05	1715 -1719 -1725	WWV-BL	15	0.3				1716 - 1722 - 1728	1-	1711 - 1714 - 1744	3S3f	2800	1.4	1708-1716-1745	SEA	3
			10	0.8										1715-1720-1730	SPA	22
		SS-BL	5	NM										1716-1721-1726	SCNA	1
			4	NM											ABS	10
														1716-1725-1800	SEA	2
														1717- -1728	S-SWF	1
07-05	1936 -1939E	WWV-BL	15	1.3				1935 - 1942 - 1957	1+	1934 - 1941 - 1954	3S3f	2800	3	1930-1940-1955	SEA	3+
			10	2.1	0.3					1954 - - 2034	5Abs	2800	-2	1935- -2001	SL-SWF	1
		WWVH-AN	15	2.3										1935-1944-2030	SPA	35
		-MY	15	0.9										1938-1943-2000	SCNA	1
			10	1.7											ABS	20
			5	7.+										1939-1947-2005	SEA	2+
		-WK	10	2.2										1940- -2000	S-SWF	1
		PB-AN	10	0.8												
		SS-BL	5	0.5												
			4	NM												
	-1940E-1945D	WWV-BL	15	1.3												
			10	2.1												
		WWVH-AN	15	2.0												
		-MY	15	NM												
			10	1.2												
			5	5+												
		-WK	10	2.0												
		PB-AN	10	0.8												
		SS-BL	5	0.5												
			4	0.4												
08-13	2038 -2039D-2044	WWVH-AN	15	1.6				2037- 2045- 2118	1-	2035.15- - 2046	cont	12-41	1	2040-2046-2110	SPA	5
		WWV-BL	15	1.3	0.2					2039.5- 2041- 2042.1	2S2f	2800	23	2040- -2140	SL-SWF	1
			10	2.0	0.3					d30	4PI	2800	2	2045-2050-2130U	SEA	3
		PB-AN	10	0.5						2039.5-2040.3-2041	3	108	2			
		SS-BL	5	1.2						2040 - - 2041	III	7.6-41	2			
			4	NM						2047 - - 2050	BUR	18	1			
08-13	2307 -2308 -2313	WWVH-AN	15	0.7				2304 - 2322 - 2344	1-	2304 - - 2307	BUR	18	1			
										2305.5- -2310.5	8G	2800				
										2305.5- 2306 - 2307	2S2	2800	22			
										2307.5-2308.5-2310.5	6C	2800	9			
08-14	0226 -0227 -0230	WWVH-AN	15	0.7				0226 - 0235 - 0300	1							

Date 1962	SFD's							Solar Flares		Solar Radio Emissions				Ionospheric Effects		
	UT	Path	f	Δf, cps		ΔA	−ΔP	UT	Imp	UT	Type	Freq	Int or Peak Flux	UT	Type	Imp
	Beg - Max - End		Mc/s	(+)	(−)	db	km	Beg - Max - End		Beg - Max - End		Mc/s		Beg - Max - End		
08-14	0244 -0246 -0251	WWVH-AN	15	0.4				0244 -0247 - 0310	1	0246 - - 0252	BUR	18	2	0245- -0300	S-SWF	1+
		PB-AN	10	0.3										0247-	SCNA	2
08-14	1836 -1837D-1842	WWVH-AN	15	0.4				1829 - 1839 - 1912	1-							
		WWV-BL	15	0.2												
			10	0.5												
		SS-BL	5	NM												
			4	NM												
08-14	2259 -2300D-2302	WWVH-AN	15	2.1				2256 - 2302 - 2337	1-							
		WWV-BL	15	0.5												
			10	NM												
		PB-AN	10	0.6												
		SS-BL	5	NR												
			4	NM												
08-15	2306 -2309 -2315	WWVH-AN	15	0.8				2606 - 2309 - 2313	1-	2305 - - 2310	BUR	18	1	2305- -2310	BUR	1
		WWV-BL	15	0.5						2305.3 - - 2310	III	7.6-41	2			
			10	NM						2305.5 - - 2310.5	8G(2)	2800				
		SS-BL	5	0.1						2305.5- 2306- 2307	2S2	2800	22			
			4	NM						2307.5-2308.5-2310.5	6C	2800	9			
08-16	1450 -1451 -1454	PB-AN	10	1.6				1440 - 1446 - 1452	1-							
08-18	2048 -2050 -2055	WWVH-AN	15	0.4				2048 - 2051 - 2101	1-	2049 - - 2055	BUR	18	1			
08-21	1714 -1715 -1717	WWV-BL	15	NM				1718 - 1720 - 1726	1-	1716.15- -1718.45	III	7.6-35	1			
			10	0.5						1718.30- -1720.45	III	7.6-41	1+			
		SS-BL	5	NM												
			4	NM												
08-24	2139 -2140D-2144	WWVH-AN	15	0.9				2128 - 2140 - 2158	1-	2136.45- -2137.30	III	12-41	1+			
		WWV-BL	15	0.2												
			10	0.4												
		SS-BL	5	NM												
			4	0.1												
08-24	2232 -2235 -2240	WWVH-AN	15	0.8				2225 - 2234 - 2247	1-							
		WWV-BL	15	0.1												
			10	0.3												
		SS-BL	5	NM												
			4	NM												

Date 1962	SFD's							Solar Flares		Solar Radio Emissions				Ionospheric Effects		
	UT Beg - Max - End	Path	f Mc/s	Δf, cps (+)	Δf, cps (−)	ΔA db	−ΔP km	UT Beg - Max - End	Imp	UT Beg - Max - End	Type	Freq Mc/s	Int or Peak Flux	UT Beg - Max - End	Type	Imp
09-01	1200 -1201 -1205	WWV-BL	15	NR				1155E- -1210	1-							
			10	NM												
		SS-BL	5	NR												
			4	NR												
09-01	1341 -1342D-1344	WWV-BL	15	NR				1341 - 1346 - 1353	1							
			10	0.3												
		SS-BI	5	NR												
			4	NM												
09-01	2040 -2041 -2044	WWV-BL	15	0.2				2040 -2043 -2048	1-	2039.15- -2039.3	III	23-37	1-			
			10	0.4												
		SS-BL	5	0.1												
			4	0.2												
09-01	2142 -2144E-2147	WWV-BL	15	0.2				2142 -2146 -2157	1-	2143 - 2144 - 2148	1S1	2800	4			
			10	0.3												
		SS-BL	5	0.3												
			4	0.2												
09-01	2236 -2237 -2240	WWV-BL	15	0.1				NFR								
			10	0.1												
		SS-BL	5	0.1												
			4	0.1												
09-02	1436 -1437D-1442	WWV-BL	15	0.1				1435E-1443 -1515	1-							
			10	0.3												
		SS-BL	5	NR												
			4	NM												
09-02	1620 -1622E-1625	WWV-BL	15	0.3				1619 -1624 -1730	1	1618 - 1637 - 1728	3S3	2800	5	1624-1633-1700	SPA	13
			10	0.6		5										
		SS-BL	5	NR												
			4	NM												
09-03	1828 -1830 -1836	WWV-BL	15	0.7	0.2			1830 -1837 -1921	1,2	1825 - 1846 - 2030	3S3f	2800	8			
			10	0.9	0.3					1829 - 1831 - 1836	8	108	3			
		SS-BL	5	0.7						1829 - - 1925	cont	7.6-41	3			
			4	0.4						1829 - - 1835	BUR	18	2			
09-04	1237 -1239 -1241	WWV-BL	15	NR				1237 -1243 -1306	1-	1235E-2324 - 0110	6	108	2			
			10	0.2						1239 - 1240 - 1244	2S2	2800	19			
		SS-BL	5	NR						dl:45	4PI	2800	2			
			4	NR						1357E- - 2000	cont	7.6-41	2			

Date 1962	SFD's							Solar Flares		Solar Radio Emissions				Ionospheric Effects		
	UT	Path	f	Δf, cps		ΔA	−ΔP	UT	Imp	UT	Type	Freq	Int or	UT	Type	Imp
	Beg - Max - End		Mc/s	(+)	(−)	db	km	Beg - Max - End		Beg - Max - End		Mc/s	Peak Flux	Beg - Max - End		
09-04	1709 -1711D-1716	WWV-BL	15	0				1711 -1715 -1724	1-	1705 - 1808 - 2045	3S3A	2800	4			
			10	0.4						1716.1-1716.9-1719.1	2	108	2			
		SS-BL	5	0.1												
			4	0.1												
09-04	2151 -2152 -2155	WWV-BL	15	0.1				2136 - -2142D	1-	2000 - - 2400	cont	15-41	1			
			10	0.2												
		SS-BL	5	0.1												
			4	0.1												
09-06	1709 -1711 -1714	WWV-BL	15	0.2				1706 -1712 -1724	1-							
			10	0.4												
		SS-BL	5	0.3												
			4	NM												
09-07	2154 -2155D-2200	WWV-BL	15	0.3				2152 -2157 -2223	1-	2149 - - 2300D	3S3A	2800	6			
			10	0.5						2155.2- 2156 -2158.9	2S2f	2800	8			
		SS-BL	5	NR						2155.45- -2156.45	III	12-41	1+			
			4	0.2												
09-09	1912 -1913 -1915	WWV-BL	15	0.4				1913 -1914 -1922	1-	1912.7-1913.4-1914.7	1S1	2800	3.5			
			10	0.6												
		SS-BL	5	NR												
			4	0.2												
09-10	2313 -2315 -2319	WWV-BL	15	0.2				2312 -2321 -2406	1-	2318.15- - 2320	III	22-41	1			
			10	0.4												
		SS-BL	5	NR												
			4	0.4												
09-11	1954 -1955D-1957	WWV-BL	15	NM				NFR								
			10	0.2												
		SS-BL	5	NR												
			4	0.1												
09-13	1229 -1230D-1237	WWV-BL	15	NR				1213 - -1235D	1-							
			10	0.6												
		SS-BL	5	NR												
			4	NM												
09-13	1730 -1732 -1736	WWV-BL	15	0				1729 -1733 -1739	1-							
			10	0.4												
		SS-BL	5	NR												
			4	NR												

Date 1962	SFD's							Solar Flares		Solar Radio Emissions				Ionospheric Effects		
	UT	Path	f	Δf, cps		ΔA	−ΔP	UT	Imp	UT	Type	Freq	Int or Peak Flux	UT	Type	Imp
	Beg - Max - End		Mc/s	(+)	(−)	db	km	Beg - Max - End		Beg - Max - End		Mc/s		Beg - Max - End		
09-14	1739 -1741 -1743	WWV-BL	15	NM				1721 -1728 -1739	1-							
			10	0.1												
		SS-BL	5	NR												
			4	0.1												
09-14	1825 -1826D-1829	WWV-BL	15	0.1				NFR								
			10	0.1												
		SS-BL	5	NR												
			4	NM												
09-14	1857 -1858 -1904	WWV-BL	15	NM				1858 -1858 -1912	1-							
			10	0.2												
		SS-BL	5	NR												
			4	0.1												
09-14	2010 -2011 -2014	WWV-BL	15	0.1				2006 -2010 -2015	1-							
			10	0.2												
		SS-BL	5	NR												
			4	0.1												
09-15	1249 -1250 -1254	WWV-BL	15	NR				1248 -1302 -1346	1-	1257 - 1259 - 1300 d10	1S1	2800	6			
			10	NM							4PI	2800	3			
		SS-BL	5	NR												
			4	NR												
09-15	1432 -1433D-1437	WWV-BL	15	0.1				1432E-1434 -1528D	1-							
			10	0.5												
		SS-BL	5	NR												
			4	NR												
09-15	1501 -1503 -1508	WWV-BL	15	0.4				1442E-1504 -1545D	1-							
			10	NM												
		SS-BL	5	NR												
			4	NR												
09-16	1428 -1429D -1431	WWV-BL	15	0.3				1429 -1430 -1440	1-	1407E - - 2425D	cont	20-41	1+			
			10	0.5												
		SS-BL	5	NR												
			4	NM												
09-16	1437 -1439 -1442	WWV-BL	15	0.2				1438 -1440 -1442	1-	1407E - - 2425E	cont	20-41	1+			
			10	0.3												
		SS-BL	5	NR												
			4	0.1												

Date 1962	SFD's							Solar Flares		Solar Radio Emissions				Ionospheric Effects		
	UT	Path	f	Δf, cps		ΔA	−ΔP	UT	Imp	UT	Type	Freq	Int or Peak Flux	UT	Type	Imp
	Beg - Max - End		Mc/s	(+)	(−)	db	km	Beg - Max - End		Beg - Max - End		Mc/s		Beg - Max - End		
09-16	1701 -1702 -1704	WWV-BL	15	0.2				NFR		1407E - - 2425D	cont	20-41	1+			
			10	0.4												
		SS-BL	5	NR												
			4	NR												
09-20	1808 -1809D-1813	WWV-BL	15	0.8				1809 -1811 -1825	1-	1809.5-1810.3-1812 d15	1S1	2800	7			
			10	1.0							4PI	2800	2			
		SS-BL	5	NR												
			4	0.3												
09-21	1314 -1315D-1318	WWV-BL	15	0.2				1314 -1314 -1321	1-							
			10	0.3												
		SS-BL	5	NR												
			4	NR												
09-22	2057 -2059 -2101	WWVH-AN	15	1.0				2055 -2101 -2117	1							
		WWV-BL	15	0.3												
			10	0.5												
		SS-BL	5	NR												
			4	0.3												
09-24	1531 -1532D-1536	WWV-BL	15	NR				1522 -1532 -1545	1-							
			10	0.1												
		SS-BL	5	NR												
			4	NR												
09-26	1628 -1631 -1635	WWV-BL	15	NR				NFR		1414E - - 2100	cont	22-41	1-			
			10	0.7												
		SS-BL	5	NR												
			4	0.5												
09-26	1721 -1722 -1725	WWV-BL	15	NR				1722 -1723 -1727	1-	1414E - - 2100	cont	22-41	1-			
			10	0.3												
		SS-BL	5	NR												
			4	0.2												
09-29	1625 -1628D-1635	WWV-BL	15	NM				1620 -1626 -1638	1-							
			10	0.2												
		SS-BL	5	NR												
			4	NR												

Date 1962	SFD's							Solar Flares		Solar Radio Emissions				Ionospheric Effects		
	UT	Path	f	Δf, cps		ΔA	−ΔP	UT	Imp	UT	Type	Freq	Int or Peak Flux	UT	Type	Imp
	Beg - Max - End		Mc/s	(+)	(−)	db	km	Beg - Max - End		Beg - Max - End		Mc/s		Beg - Max - End		
09-29	1753 -1755 -1758	WWV-BL	15	0.5				1753 -1757 -1810	1-							
			10	0.9												
		SS-BL	5	NR												
			4	NR												
09-30	1816 -1818 -1821	WWV-BL	15	0.1				1815 -1820 -1829	1-							
			10	0.2												
		SS-BL	5	NR												
			4	NR												
09-30	1925 -1926E-1929	WWV-BL	15	0.1				1924 -1930 -2037	1-							
			10	0.1												
		SS-BL	5	NR												
			4	NR												
09-30	2006 -2008 -2013	WWV-BL	15	0.2				2002 -2011 -2019	1-							
			10	0.4												
		SS-BL	5	NR												
			4	NR												
10-02	1252 -1253 -1256	WWV-BL	15	0.2				1313E- -1342D	1							
			10	0.3												
		SS-BL	5	NR												
			4	NR												
10-07	2342 -2343 -2345D	WWV-BL	15	0.1				NFR								
			10	0.4												
		SS-BL	5	NR												
			4	0.1												
10-08	1658 -1701E-1704	WWV-BL	15	0.3				NFR								
			10	0.4												
		SS-BL	5	NR												
			4	0.3												
10-09	2127 -2128D-2131	WWV-BL	15	0.2				2128 -2132 -2155	1-							
			10	0.3												
		SS-BL	5	NM												
			4	NM												
10-10	1320 -1325 -1330	WWV-BL	15	0.2				NFR								
			10	0.3												
		SS-BL	5	NM												
			4	NM												

Date 1962	SFD's							Solar Flares		Solar Radio Emissions				Ionospheric Effects		
	UT	Path	f	Δf, cps		ΔA	−ΔP	UT	Imp	UT	Type	Freq	Int or Peak Flux	UT	Type	Imp
	Beg - Max - End		Mc/s	(+)	(−)	db	km	Beg - Max - End		Beg - Max - End		Mc/s		Beg - Max - End		
10-12	2300 -2301D-2304	WWV-BL	15	0.2				2300 -2303 -2317	1-	2251 - - 2252	III	22-36	1-			
			10	0.3						2251.9-2252.1-2253	3	108	3			
		SS-BL	5	0.3						2300 - - 2304	III	19-41	3			
			4	0.3						2304.15- - 2305	III	22-41	1			
										2304.2-2305.3-2309.2	8	108	3			
10-13	1440 -1441D-1445D	WWV-BL	15	NM				NFR		1437.15- -1438.15	III	23-41	1+			
			10	0.1												
		SS-BL	5	NM												
			4	0.1												
10-13	1750E-1750D-1751	WWV-BL	15	1.0				1750 -1754 -1803	1-	1748.3- -1748.45	III	22-38	1-			
			10	1.3						1741 - - 1743	BUR	18	1			
		SS-BL	5	1.2												
			4	NM												
10-13	1805 -1806E-1808	WWV-BL	15	8.4	1.6			1805 -1808 -1825	1-	1808.3 - -1808.45	III	23-41	1			
			10	10.0	1.8					1809.15- -1811.30	III	10-41	2-			
		SS-BL	5	3.2	0.3					1808 - - 1810	BUR	18	1			
			4	3.6	0.4											
10-13	2033 -2034D-2037	WWVH-AN	15	0.4				2033 -2035 -2038	1-	2029.45- -2033.3	III	22-41	1-			
		WWV-BL	15	0.2						2033.3 - -2034.15	III	13-41	2			
			10	0.3						2034.45- -2037.15	III	13-41	2			
		SS-BL	5	NM						2038.9 -2039-2039.9	3	108	2			
			4	NM						2031 - - 2034	BUR	18	1			
10-16	2030 -2032D-2037	WWV-BL	15	NM				2032E-2034 -2042D	1-	2028.30- -2029.30	III	22-41	1			
			10	0.2						2029.45- -2030.3	III	20-41	1+			
		SS-BL	5	NM						2030.30- -2033.15	III	16-41	1+			
			4	NM						2034 - -2034.15	III	21-41	1			
										2031 - - 2034	BUR	18	1			
10-17	1803 -1804D-1807	WWV-BL	15	NM				1803 -1806 -1815	1-	1758 - -1758.3	III	26-39	1-			
			10	0.2												
		SS-BL	5	NR												
			4	0.1												
10-18	1705 -1706D-1709	WWV-BL	15	1.1				1706- -1800	1-	1706 - 1707 - 1711	2S2	2800	22			
			10	NR						d40	4PI	2800	3			
		SS-BL	5	0.8												
			4	0.6												

Date 1962	SFD's							Solar Flares		Solar Radio Emissions				Ionospheric Effects		
	UT	Path	f	Δf, cps		ΔA	−ΔP	UT	Imp	UT	Type	Freq	Int or	UT	Type	Imp
	Beg - Max - End		Mc/s	(+)	(−)	db	km	Beg - Max - End		Beg - Max - End		Mc/s	Peak Flux	Beg - Max - End		
10-18	2123 -2125D-2130	WWVH-AN	15	2.1				2111E-2135U-2155	1-	2005 - - 2125	9Pre	2800	2			
		WWV-BL	15	0.5						2125 - 2127 - 2130D	2S2	2800	14			
			10	NR												
		SS-BL	5	0.3												
			4	0.4												
10-20	1955 -1956E-1959	WWV-BL	15	0.6	0.1			1951 -1959 -2011	1-							
			10	NR												
		SS-BL	5	0.4	0.1											
			4	0.4	0.2											
10-20	2117 -2119 -2127	WWV-BL	15	0.3				NFR								
			10	NR												
		SS-BL	5	0.3												
			4	0.2												
10-25	1941 -1943 -1945	WWV-BL	15	0.2				1942 -1944 -1946	1-	1938.45- - 1939	III	26-41	1-			
			10	0.2												
		SS-BL	5	0.1												
			4	NM												
10-27	1840 -1841 -1843	WWV-BL	15	0.4				1836 -1843 -1901	1-	1838.15- -1839.15	III	16-41	1+			
			10	0.6						1841 -1841.5- 1843	2S2	2800	11			
		SS-BL	5	NM						1841.3 - -1842.15	III	16-41	1			
			4	NM						1845.15- - 1846	III	22-41	1-			
11-07	1411 -1411D	MN-AC	10	1.0				NFR								
	-1413 -1415	MN-AC	10	1.0												
11-14	1840 -1841D-1845D	WWV-BL	15	0.6				NFR								
			10	0.4												
		SS-BL	5	0.3												
			4	0.2												
11-16	1629 -1631E-1633	WWV-BL	15	0.6				NFR								
			10	1.3												
		SS-BL	5	NM												
			4	0.4												
11-16	2214 -2215 -2217	WWV-BL	15	0.5				NFR								
			10	0.7												
		SS-BL	5	NM												
			4	NM												

Date 1962	SFD's							Solar Flares		Solar Radio Emissions				Ionospheric Effects		
	UT	Path	f	Δf, cps		ΔA	−ΔP	UT	Imp	UT	Type	Freq	Int or	UT	Type	Imp
	Beg - Max - End		Mc/s	(+)	(−)	db	km	Beg - Max - End		Beg - Max - End		Mc/s	Peak Flux	Beg - Max - End		
11-24	2219 -2221 -2226	WWVH-AN	15	1.5				2218 -2222 -2230D	1-	2222 - - 2223	III	19-41	2			
		WWV-BL	15	0.2												
			10	NM												
		SS-BL	5	0.3												
			4	0.5												
11-30	1641 -1643 -1645D	WWV-BL	15	NR				1644 -1648 -1652	1-							
			10	0.3												
		SS-BL	5	0.2												
			4	0.3												
11-30	1928 -1930 -1933	WWV-BL	15	NM				1927 -1932 -1937	1	1830 - 1918 - 2028	3S3	2800	3			
			10	0.8												
		SS-BL	5	NM												
			4	0.3												
12-17	1629 -1630 -1640	WWV-BL	15	0.8				1630 -1633 -1640	1-	1625.5-1630.5-1632	2S2	2800	40			
			10	1.4						d3l	4PI	2800	2			
		MN-NA	20	12.0												
			10	3.5												
		MN-AC	10	0.6												
		SS-BL	5	0.3												
			4	0.3												
12-17	1732 -1733 -1735	WWV-BL	15	0.1				NFP								
			10	0.2												
		SS-BL	5	NM												
			4	0.2												
12-18	1654 -1656 -1657	WWV-BL	15	NM				1654 -1656 -1711	1-							
			10	0.3												
		SS-BL	5	NM												
			4	NM												
12-20	0827-0828D-0832	MN-NA	20	0.5				0815 - -0830	1							
			10	0.8												
		MN-AC	10	0.6												
12-22	0918-0919-0923	MN-NA	20	0.2				0918D-	1-							
			10	0.5												
		MN-AC	10	0.2												

GPO 849-173

DEPARTMENT OF COMMERCE
NATIONAL BUREAU OF STANDARDS